Simulation and experimental setup of a vehicle thermal management demonstrator

Auteur : Feron, Guillaume
Promoteur(s) : Lemort, Vincent
Faculté : Faculté des Sciences appliquées
Diplôme : Master en ingénieur civil électromécanicien, à finalité approfondie
Année académique : 2015-2016
URI/URL : http://hdl.handle.net/2268.2/2017

FACULTÉ DES SCIENCES APPLIQUÉES

AVL

Master's thesis :

Simulation and Experimental Setup of a Vehicle Thermal Management Demonstrator

produced in order to obtain the graduation for
the **Master in Electromechanical Engineering**

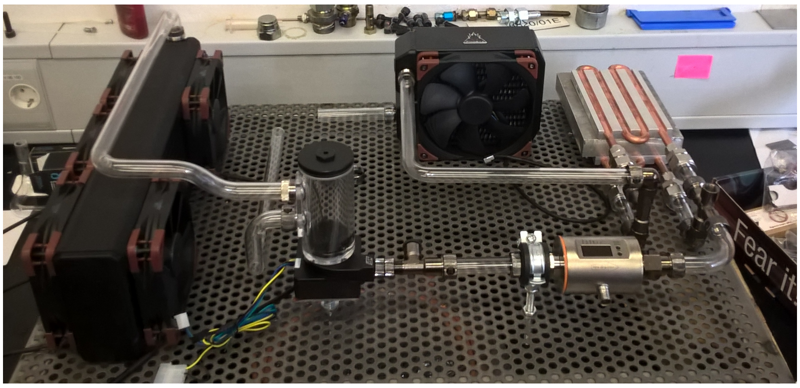

Author :
Guillaume FERON

Supervisor :
Vincent LEMORT

Committee :
Pierre DUYSINX, Sylvain QUOILIN, Armin TRAUSSNIG

Academic year 2015-2016

Simulation and Experimental Setup of a Vehicle Thermal Management Demonstrator

Guillaume Feron

Acknowledgements

Firstly, I would like to thank everybody that made the realisation of this master's thesis possible.

I want to thank first of all Armin Traußnig, who supervised me throughout the whole development of this thesis. I appreciate his assistance and his advices from the first day I arrived in the company. This thesis wouldn't have been possible without his guidance and his previous research and development of TheLib.

I would also like to thank Heinz Petutschnig, for his recommendations, and his supervision of my work and of my internship in AVL.

I want to thank Vincent Lemort, my academy advisor, for the organisation and his global supervision of the thesis.

A particular thank also to Sepp Steiner, my closest colleague in the office, for his insights about TheLib, AVL, and the countless times he helped me to debug the model.

Thanks to Erwin Starchl and Oliver Peter Reinisch for providing the tools to build the demonstrator and their help in the assembly.

I am also grateful to Maximilian Jauk, for his Catia skills, that he put at disposal for the development of the demonstrator CAD model, to be able to visualise the place of every component.

Thanks to Andreas Ennemoser, the DAC office manager, who welcomed me in his team.

And I would also like to thank Tinkara Kristovic, Arnaud Crater and all the other colleagues of the AVL's DAC office, who helped me directly or indirectly in this thesis, and for the warm welcome among them.

I thank in advance the committee members Pierre Duysinx, Sylvain Quoilin, and a second time Armin Traußnig and Vincent Lemort, for their interest and the time they will spent to read this master's thesis.

Thanks also to Dominik Gößler, to take over the development of the demonstrator.

I am very grateful as well to the ULg to have made the erasmus internship possible.

I want to thank AVL, for the possibility of this internship inside the company.

And finally, I must express my very profound gratitude to my family, my parents Corinne Voituron and Olivier Feron, my brother Jonas Feron, my grand-parents, and others members, who got interested in the thesis, for their patience and for their corrections in the re-reading of this thesis. They also provided me with great support and encouragements throughout my years of study and in this thesis.

Table of contents

Introduction

The thermal management of a vehicle internal combustion engine has always been a key to its good functioning. Without it, an engine would quickly overheat, and damage the structure.

Operating the engine at an optimal temperature also allows a better combustion efficiency and a better oil lubrification, which decrease fuel consumption, and pollutant emissions in the same time. The warm-up of the engine is thus a critical phase as well.

For a long time, the actuators (a bypass valve/thermostat, a pump and a fan) were mechanically and thermally driven, with poor capabilities of control. Nowadays, the recent integration of a wide variety of components under the hood (air conditioning, hybridisation of vehicle, other auxiliaries) has called for a more complex thermal management.

The electrification of these actuators addresses this issue : it allows a full control, with an accompanied potential reduction of the vehicle fuel consumption. However, the results are highly dependant of the control methodology put in place.

In this context, AVL elaborates personalised solutions of vehicle thermal management, as an integral part of more global powertrain projects for vehicle manufacturers and subcontractors. The goal of the internship, which I took part in this company, is incorporated within the framework of a progressive transition to a seamless development of thermal systems and related control functionality for future projects :

Within the scope of testing different control strategies, the development of a demonstrator platform allows to give a proof of feasibility and applicability of thermal management control in a real hardware device, and can also be used for customer presentations and exhibitions.

This thesis explains the development of this thermal management controller demonstrator and revolves around 5 chapters :

The first chapter concerns the basic principles of vehicle thermal management and summaries the scientific literature over the different possible strategies.

The second chapter broaches the concept of the demonstrator and the general properties of its components.

The third chapter details the adopted hardware devices inside the water circuit and their connected model.

The fourth chapter is assigned to the descriptions of electrical signals and control. It makes the link between the virtual world and the reality.

Finally, the sixth chapter presents some results to show the general behaviour of the demonstrator.

Remark : For a presentation of the company AVL, the reader is invited to read the related internship report.

Chapter 1

State of the art

1.1 Basic principles

Nowadays, even if electric and hybrid vehicles are spreading among the users, the internal combustion engine (ICE) is still used to propel a majority of vehicles.

Those engines burn fuel, and the resulting high pressure and high temperature of the gases in the combustion chamber exerts a force on a piston inside a cylinder. An assembly of cylinders and a right ignition sequence allows to move a crankshaft which in turn will rotate the wheels of the vehicle. A part of the power transferred to the shaft can also be redirected to power some auxiliaries (air conditioning compressor, pumps, alternator for the battery, etc.).

1.1.1 Engine thermal management

The useful power transferred to the wheels and to the auxiliaries is also stated as the nominal power of the engine. For a standard car, it is usually situated in a range between 45 and $200kW$ [1]. The temperature of the gases inside the cylinder can reach $2250°C$ [2].

The material used for the cylinder and the engine block which contains them needs to be cooled down to withstand such conditions. The cooling also preserves the lubrication of the moving parts of the engine. Removing heat from the system means that the energy released from the fuel won't be used entirely to move the vehicle but some losses will appear.

As in every plant, when it comes to develop a new engine, the main objective aimed is the highest efficiency, which is equivalent to decrease the losses. To get an approximation of the different proportions of those losses, if the fuel burned equals to 100% of the power, around 25% is a useful power [1], 40% are lost through the exhaust gases, 30% through the coolant, and 5% through friction between the mechanical components [3]. (Those proportions are very variable and another usual quick approximation for example is one third of the fuel power goes to the crankshaft, one third to the exhaust gases and the last third is lost through the coolant system, the friction being neglected.)

1. depending on the technology of the engine, the user profile, the external conditions, etc

The cooling liquid is a water based fluid, mixed with ethylene glycol or propylene glycol. The resulting fluid has the characteristic to not freeze in cold regions and to have a higher boiling point than water, which allows to use it around $100°C$.

As the fuel can release a lot of heat (especially under a heavy load), one of the main challenge in the functioning of the engine is therefore the regulation of the temperature of the engine.

Indeed, for a maximal efficiency of the engine, it needs to be kept within a reduced range of temperature :

— If the temperature is too low, *e.g.*when the engine starts, the viscosity of the oil is too high (which increases the frictional losses), the combustion is not complete (as the fuel is not fully vaporized in the combustion chamber and due to quenching effect on the cylinder wall), and the overall consumption and the pollutant emissions are higher (CO + HC - Carbon Oxide and Hydrocarbons). This is why the engine needs to warm-up quickly after cold start.

— On the other hand, if the temperature inside the engine is too high, it compromises the lubricating effect and the integrity of the structure, and it increases some other emissions (NOx - Oxides of Nitrogen).

As in practical, it is complicated to know if the temperature constraints is met in every point of the engine, only the coolant temperature at the outlet of the engine is measured and kept within a small interval. According to different sources, the optimal coolant temperature range at the engine outlet is situated between $80°C$ and $110°C$. The optimal point also depends on the load of the engine, in order to keep the best conditions in the combustion chamber.

Note : As this temperature is the main regulation objective, in the rest of this paper, the (coolant) temperature mentioned will always be the coolant temperature at the engine outlet if not specified otherwise.

The coolant circuit is composed of 4 main components : the engine itself (cylinders, engine block), the bypass valve, the radiator and the pump. The fluid flows from one component to the next one through hoses. A simplified layout is shown on Figure 1.1

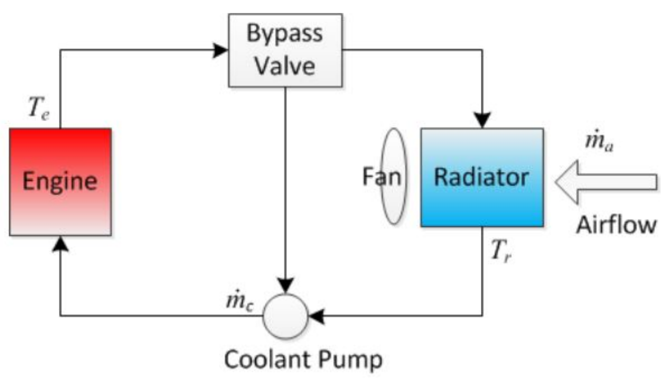

Figure 1.1 – Schematic of a simplified cooling system [4]

In the combustion chamber, as the combustion process is highly exothermic, a part of the heat contained in the burned fuel is transferred to the walls of the cylinder, to the piston and to the **engine block** in general, so that the temperature of the metal increases. The heat of the burned gases is not fully given to the structure and the rest of it goes out of the cylinder with the exhaust gases. This step is represented on Figure 1.2.

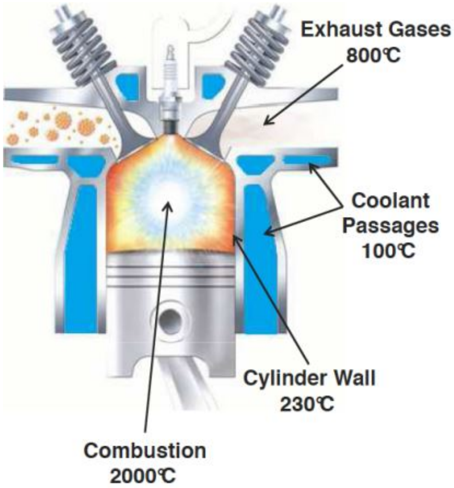

Figure 1.2 – Coolant circuit around the cylinder, in the engine [3]

Then, the coolant, flowing in channels around the cylinder, evacuates the heat of the metal out of the engine through a convective heat transfer. Thus, the fluid is hotter at the engine outlet - temperature T_e on the Figure 1.1 - and needs in turn to be cooled down to keep a good heat transfer and maintain the engine in its temperature range. At the end of the cooling process, the coolant will go back in the engine and the cycle goes on.

Note : As the engine structure temperature and the engine outlet coolant temperature are directly correlated (with heat transfer relations), the control of the engine temperature or of the coolant temperature may sometimes be used indistinctly in the rest of this paper.

From the engine outlet, the coolant goes to the **bypass valve**.

— In normal mode, when the engine is hot, the coolant is directed towards the **radiator** to evacuate the heat carried by the coolant.
This radiator, in front of the vehicle, is a crossflow heat exchanger. The coolant flows through small tubes (mounted in parallel), which transfers the heat to the airflow passing through the radiator. The heat transfer is improved with fins between the coolant tubes. The configuration is shown on Figure 1.3 and 1.4. The airflow $\dot{m}_a$, at the ambient air temperature, is created with the velocity of the vehicle or, when it is insufficient, with a fan (see Figure 1.1).
The **cooling fan** is placed on the engine side of the radiator and suck the air through it. It is often linked mechanically to the engine crankshaft, sometimes with an intermediary viscous-drive clutch which serves to engage or disengage the fan, eventually partially, depending on the coolant temperature, the ambient air temperature or on other factors like oil temperature.

— However, when the engine has just started, it is still cold and the coolant temperature T_e is under its lowest limit for an optimal coolant temperature. To improve the

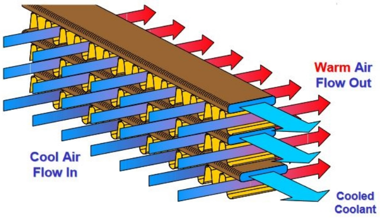

Figure 1.3 – Air and coolant flow in a radiator [5]

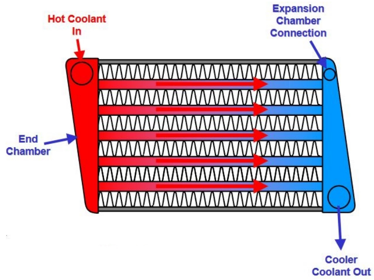

Figure 1.4 – Coolant flow in radiator tubes [5]

warm-up, the valve is closed and the fluid avoids circulating through the radiator. This allows to heat faster the engine because no heat is removed from the system, and the coolant temperature is the same at the engine inlet than it is at its outlet (neglecting the losses from the tubes to the ambiance).
Traditionally, the bypass valve was a wax thermostat, placed at the coolant engine outlet : as the combustion process goes on, the coolant temperatures increases through time, which in turn heats up the wax container of the thermostat. When the wax reaches the nominal opening temperature, it liquefies, and this process is accompanied by a large increase in volume. The wax compartment then compresses a spring, pushes a piston, which in turn opens progressively the branch for the coolant to the radiator, while the flow decreases in the bypass. The spring is used to pull the thermostat back as the temperature falls and the wax contracts.
The different parts of a wax thermostat are shown on Figure 1.5 and the different positions of the valve are visible on the Figure 1.6.

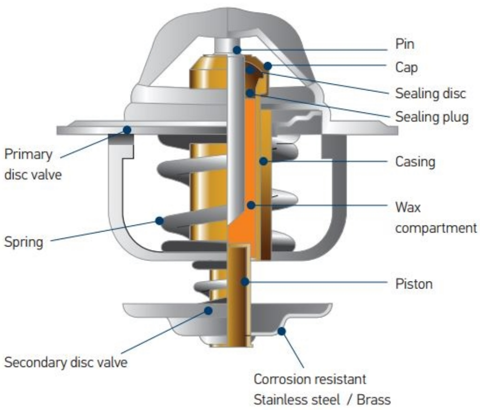

Figure 1.5 – Thermostat parts [6]

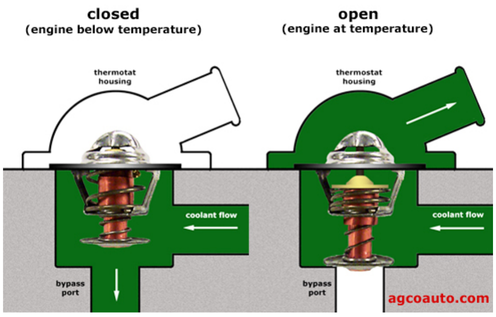

Figure 1.6 – Thermostat open or closed [7]

The opening of the valve is highly dependant of the temperature of the wax (and thus of the coolant). In normal operation, once the optimal temperature is reached, the thermostat is not fully open. This way, it can compensate any external imbalance (engine heat output, vehicle speed, or outside ambient temperature change) by opening or closing the passage to the radiator.
The manufacturer determines the characteristic curve of the thermostat (stage of opening, slope in function of the temperature) by modifying the composition of the wax. An example of a characteristic curve is shown on Figure 1.7.

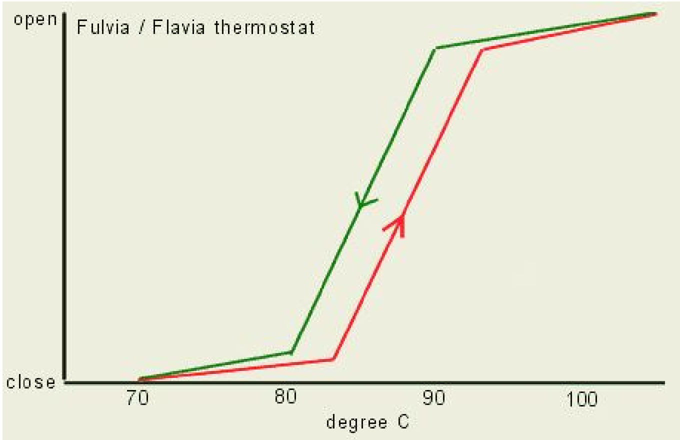

Figure 1.7 – Example of a characteristic curve of a wax thermostat [8]

It is worth mentioning that, in some recent designs, during warm-up, only the cylinder-head is cooled down, to ensure the structure integrity as it is the part exposed to the highest temperature. But as the heat spreads to every part of the engine, in normal operation, the full engine block is cooled additionally.

After the radiator or the bypass, the coolant goes into a centrifugal **pump**. This pump, also driven by the crankshaft via a pulley and a belt, serves to move the coolant inside the tube and overcome the pressure drop along the whole trajectory.

It is important to ensure a minimum coolant flow rate to avoid hot spots inside the engine and detect a temperature change at the outlet, where the thermostat is placed. The hot spots are those places where the coolant (almost) boils. This phenomenon decreases the heat transfer to the fluid. If the metal becomes hotter, it can warp or melt, which is very harmful for the engine.

An other phenomenon that can appear due to bad cooling method is a non uniform thermal expansion. This increases highly the internal stresses inside the engine block, which will then crack in the worst case scenarios.

An **expansion tank** is also inserted in the circuit to allow the coolant to change volume according to the temperature variation. Indeed its volumetric weight is not the same at $20°C$ or at $95°C$.

The lubricating oil, by its effect on the piston, also cools down the engine. This oil transfers then its thermal energy to the coolant or directly to the air through an **oil cooler** (positioned in front of the main radiator in the second case).

Another component that appears in the cooling circuit is the **cabin heater**. A part of the coolant flow is routed to this heat exchanger, which is used the same way than the main radiator. The hot air resulting is then blown (by an additional fan in front of the heater core) in the cabin, as required by the user.

The whole cooling system, with each previously described component, is represented at the Figure 1.8.

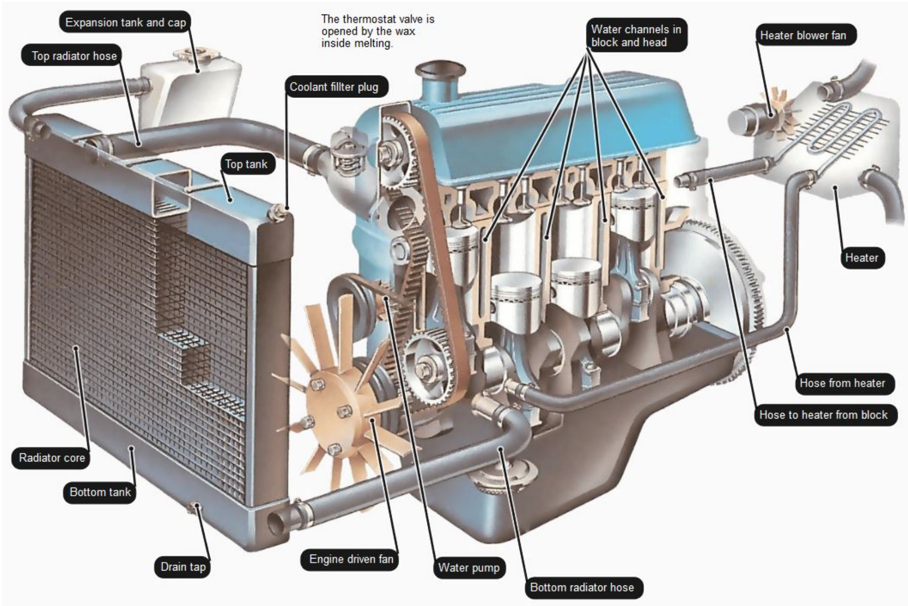

Figure 1.8 – Whole cooling system of a car engine [9]

1.1.2 Recent improvements

The engine and the cooling system are not alone under the car hood. Some improvements and other options requires also some extra components.

Specifically, the air conditioning and the charge air cooling system (CAC) need each one of them an additional heat exchanger in front of the main radiator. In hybrid vehicles, there is even an another heat exchanger at the same place to cool the high voltage components. All of these exchangers are usually placed in front of the main radiator and doesn't use the same working fluid nor are at the same level of temperature. There are several ways of organising the position of each component, but a general rule is to put the lower temperature exchanger in front of higher temperature one (in the direction of the airflow). This way, the air is progressively heated up and it can still cool down the radiator placed behind.

As there are more and more heat exchangers in front of the vehicle, the heat rate transferred to the air increases as well (compared to the standard case). For the same surface area and ambient air temperature, the airflow needs then to be faster in order to cool down efficiently the different circuits, which in turn calls for an improvement in the control over the fan.

Up until recently, each actuator regulating the temperature of the coolant was controlled mechanically : involving a thermostat in conjunction with an engine-driven fan and pump.

However, these types of control have several drawbacks: they are not highly accurate nor controllable, and driven independently from each other. Moreover, they are designed on the worst case scenario (low vehicle speed, high heat input from the engine and high ambient temperature), happening extremely rarely in real condition. Ideally, a smaller amount of coolant would be sufficient in the radiator if the water flow was adapted. As this is not the case, all the surplus of coolant propelled by the pump goes into the bypass, and it wastes energy.

Additionally, the fan control is also dependant of the engine speed and is often driven too fast, which increases the fuel consumption as well in the end.

This method of control results in frequent overcooling or overheating of the engine, as well as high component temperature fluctuations and thermal stresses, decreasing therefore the lifespan of the components.

All of these drawbacks have been highlighted in several studies. They show a potential reduction in fuel consumption if all of the actuators (bypass valve, pump and fan) were controlled with an electrical servomotor. It would divert less power from the engine, only powering an alternator, used for other auxiliaries as well, and just feeding the optimal amount of energy to the actuators.

A consequence of the electrification of the actuators is that their control signal are not mechanical anymore (wax expansion related), and the thermal circuit needs several sensors to know the coolant temperature at the relevant locations. These sensors sends an electric signal, proportionate to the measured physical variable, to the Engine Control Unit (ECU) of the vehicle which will then process and control the actuators according to a predefined methodology.

However, a major drawback of this electrification of the actuators can be envisaged : if a failure in the electric system appears, the thermal management becomes inoperative and the engine can be completely destroyed due to high overheating if it continues to run. A failsafe system is thus necessary. It is noteworthy that most of the recent vehicles won't work anymore in case of an electricity failure, and the problem is then inconsequential.

1.2 Literature survey

This section is an overview of several studies that have explored different control method of thermal management in vehicles. From these, several conclusions have been drawn. In the end, this work helped to determine the most important parameters to take into account to design a demonstrator, as well as the most promising method(s).

A lot of researches have been done since the emergence of vehicles and, consequently, the database of articles about this topic is huge. To keep this study in appropriate proportions, I based my review only on the most recent articles, with similar level of technology and with an electric control of the actuators.

Each article answers to several questions :

- For what application? Whether the cooling method is applied to an internal combustion engine (ICE), an electric motor (EM) or an hybrid electric vehicle (HEV).
- What is the objective fixed for the thermal management? Maintenance of a constant temperature or minimization of the energy consumption?.
- How were the physical equations put together, what is the model?
- Which are the controlled actuators to reach the objective.
- What are the control laws and control strategies used.
- How the model has been verified in reality to validate the results.
- What are the results of the control method put in place in the study.

An answer to these questions for each article is put in Appendix A. The survey is mainly focused on the internal combustion engine thermal management control (ICE TM), but some articles have been read about some electric motor (EM), battery or hybrid vehicle thermal management systems (VTMS) as they are similar to the ICE TM. It also allows to look at the systems next to the coolant circuit and to take some information about the other systems as well.

The following development broaches the common points and the general conclusions that can be learned.

1.2.1 Model

The reduced order multi-nodal lumped parameter model is the most successful one in vehicle thermal management.

This mathematical model simplifies a spatially distributed system into an elementary one, under certain assumptions, where each component is a discrete entity with their own global characteristics, approximating this way the physical behaviour of the whole cooling system.

It is really effective for the representation of a circuit where a signal (in this case, the coolant flow rate and temperature) propagates, going from one component to the other, which influences the signal in the same time.

Compared to the 3D computational fluid dynamics (CFD), it doesn't allow detailed analysis in each point of the system, but this 1D representation is a low consumer in terms of computational power.

As expected, the articles focus on the main components mentioned in the section 1.1.1, namely : a heat source, a bypass valve, a radiator and a pump.

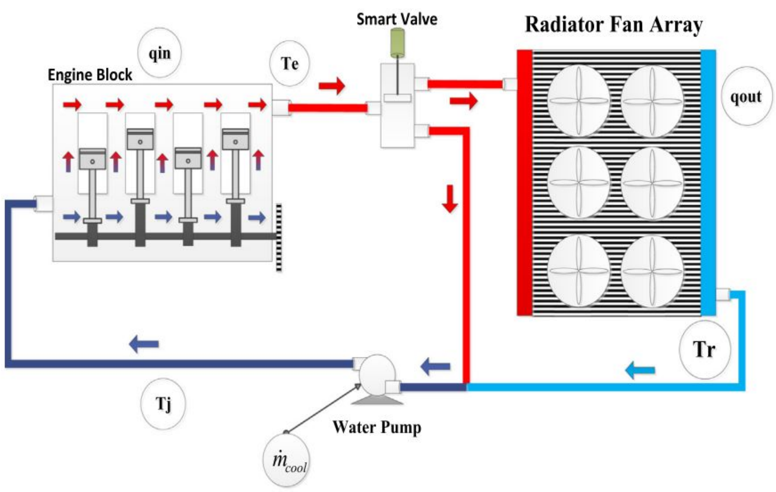

Figure 1.9 – Simplified automotive thermal system [10]

Here are the governing equations of the system pictured on Figure 1.9, representing the main dynamics of the process :

$$C_e\dot{T}_e = -Cp_{cool}\dot{m}_{cool}(T_e - T_j) + \dot{Q}_{in}$$
$$C_r\dot{T}_r = Cp_{cool}H\dot{m}_{cool}(T_e - T_r) - \dot{Q}_{out}$$
$$T_j = (1 - H)T_e + HT_r$$

Where

— $T_j(t)$, $T_e(t)$ and $T_r(t)$ are the coolant temperature at the engine inlet, engine outlet and radiator outlet.
— C_e, C_r, and Cp_{cool} are the specific heat of the engine, radiator and coolant (at constant pressure)
— $\dot{m}_{cool}(t)$ is the coolant mass flow rate, proportional to the pump speed.
— $H(t) \in [0\% \ ; \ 100\%]$ is the opening of the valve. At $H = 0\%$, the valve is fully closed and the coolant goes directly towards the pump inlet. When $H = 100\%$, the valve is fully open and the coolant is directed into the radiator.
— $\dot{Q}_{in}(t)$ represents the engine heat flux due to the combustion process, function of the crankshaft speed and torque of the engine.
— $\dot{Q}_{out}(t) = f(\omega_{fan}, T_{amb}, v_{ram})$ is the heat rejected from the radiator to the ambient air. Its full expression is a complex relation between the contribution of the fan effect and the ram air disturbance (vehicle speed, wind blow), and including the ambient air temperature, the characteristics of the radiator and those of the fan. Interested reader is referred to [11] for more details. A simpler expression, taking into account those uncertainties, can be written as :

$$\dot{Q}_{out} = \dot{Q}_0 + \varepsilon Cp_a\dot{m}_{air,fan}(T_e - T_a)$$

$\dot{Q}_0(t)$ is the radiator heat loss due to the ram air disturbance, $\varepsilon(t)$ is the heat exchanger efficiency, Cp_a is the air specific heat, $\dot{m}_{air,fan}(t)$ is air flow rate given by the fan contribution and T_a is the ambient air temperature (supposed spatially uniform).

An important hypothesis on this model is that the heat loss from the external surface of the components to the ambiance is not considered. This means that all the components are fully thermally isolated and the heat loss only occurs through convective heat transfer in the radiator. To keep the model in its limit, it is also assumed that $\dot{Q}_{in}$ and $\dot{Q}_{out}$ are positive, and T_e is hotter than T_r and T_a.

Sometimes, other extra components are also added to the model. This can be a transmission cooler or an oil cooler, in separated or integrated circuit to the coolant system. There exist then some interactions between the additional fluid and the coolant temperature.

The previous described model is a system of simple differential equations that can be solved quite easily, to determine the general behaviour of the circuit. However a whole vehicle thermal system is very complex : it includes a lot of other components interacting between each other and the governing physical equations are much more complicated, *e.g.* the heat transfer is most of the time a proportion of conduction, convection and radiation. To take into account those complex interactions, some authors use a software (*e.g.* GT-SUITE) where the components are more completely defined, their association is more adaptable, and the model of the engine can be more precise.

Just for information, Figure 1.10 illustrates the integration of a large range of components and its complexity, in an example of a whole thermal systems on a HEV powertrain.

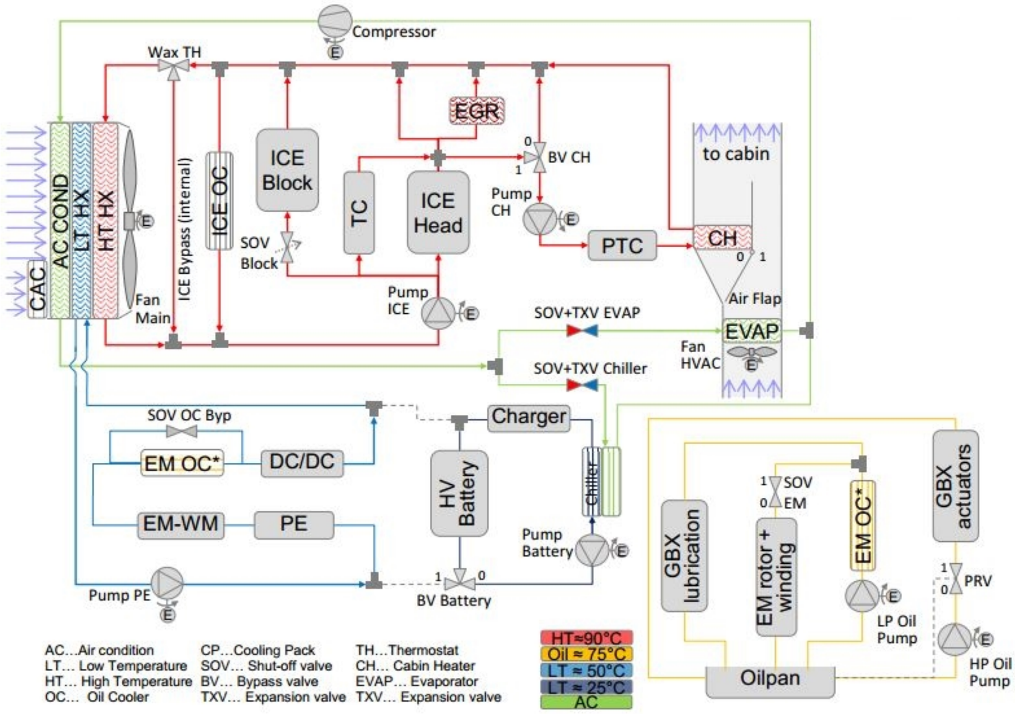

Figure 1.10 – Representation of thermal systems on the powertrain of a hybrid vehicle [12]

1.2.2 Control

What differs the most in each study is the way of regulating the thermal system of engines. It can vary in objective, actuators used and strategy of control.

As mentioned before, there exists only a small range of temperature where the conditions of the combustion process are optimal : The oil is not too viscous nor too inefficient in the lubrication of the moving parts, and the metal is not too hot to overheat nor too cold which increases fuel consumption and emissions. This condition of optimal combustion process has driven for a long time the objective of constant coolant temperature at the engine outlet.

However, the most recent studies show that it is still possible to decrease the fuel consumption by decreasing the energy consumption of the actuators, while maintaining the optimal conditions inside the engine. This is the main reason driving to the electrification of the actuators, which tend to become more flexible in their use, and allowing therefore a more complex control strategy.

Each study has its own way of regulation and differs in the combination of the actuators : sometimes, only the bypass opening varies, sometimes it is a conjunction of control over the pump and the fan speed, and sometimes an other combination can be taken. The non regulated actuator(s) are fixed at 100% (opening or speed).

The simpler method of control is the ON/OFF strategy, also called **bang-bang** control. This method consists in two discrete states of the bypass valve, the fan and/or the pump to keep the coolant temperature in a defined range (Figure 1.11).

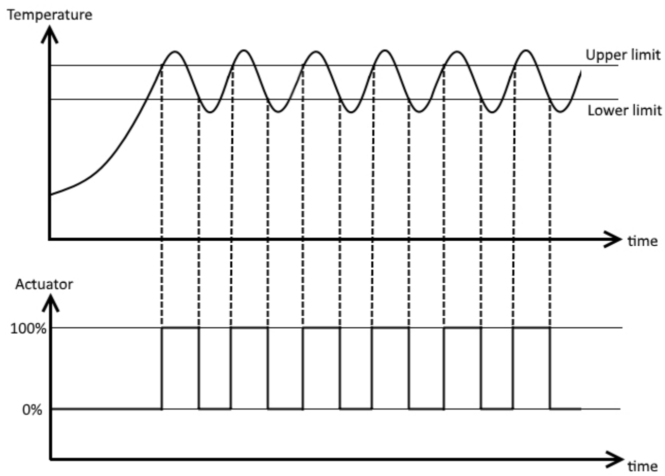

Figure 1.11 – Bang bang control [*Author's illustration*]

If the temperature is below the lower temperature limit, the bypass valve directs the fluid to the engine inlet (bypass position), the pump and the fan are turned off (or driven at a minimal partial load). Then, as the engine brings some heat to the coolant, the temperature of the fluid increases because it is not correctly cooled down in the radiator. If the temperature exceeds a predefined stage, the bypass fully opens to the radiator, the fan/pump are driven at maximal speed. The controlled variable decreases until it reaches the lower limit, where the cycle begins again. This is an hysteresis.

As the system has thermal inertia, a certain time is needed before the temperature returns in the interval between lower and upper limit and will always exceed those values.

The limits can also coincide. That way, the coolant temperature oscillates around a mean value called the set point.

The use of only one actuator may not be enough to always keep the temperature within the predefined interval. In the opposite, running/opening fully the three actuator at the same time would lead to very high and fast fluctuations. Therefore, each actuator can have its own set point value / hysteresis with different temperature thresholds. That way, once an actuator is not able to change the coolant temperature anymore, a second actuator takes over.

Another approach, with less temperature fluctuations, is the **PID** (proportional integral derivative) control. This technique uses an equation that tries to minimize the error $e(t)$ of a state variable (in our case, the temperature) over time, between a desired value and the measured one. The mean of action is the output $u(t)$ of the equation, which gives the value of the control variable that will change adequately the state of the system (*e.g.*the position of the valve or the pump/fan speed). The equation is a combination/addition of different terms, each one modifying in its own way the general behaviour of the temperature response in function of the error measured :

$$u(t) = K_p e(t) + K_i \int_0^t e(\tau)d\tau + K_d \frac{de(t)}{dt}$$

K_p, K_i and K_d are respectively the proportionate, integral and derivative coefficients. These parameters need to be tuned to give a specific and optimal response of the temperature.

The success of this method is based on the fact that there is no need of knowing the process to correctly tune the parameters. Even if several methods exist to help to determine the optimal coefficients, it is often time-consuming and requires some experience and trial-and-errors from the designer of the control. Short transient and high stability are the two most important objective of the response, but sometimes, the optimization of one is opposite to the second and a compromise is needed. The results of PID control can be compared in terms of good temperature tracking and fast disturbance rejection.

This approach is more adapted to the management of only one actuated variable (*e.g.*the fan speed). A combination of several ones is likely to create disturbances between each other and have opposite effect, leading to an instability.

A third method is the **Lyapunov-based backstepping nonlinear control**. It is similar to PID control by the fact that it tracks the setpoint by minimizing an error function between desired and measured state variables (temperature). The innovation of the control comes from the analysis of the main equations governing the model, developed in section 1.2.1, to actuate accurately the control variable(s). It also takes into account some (bounded) uncertainties of the system and ensures the stability of the control.

N.B. : A control based on the governing equations of the system, creating a model of the process, is called a model-based control. These are very efficient due to the fact that it is highly adaptable and customized to the situation and it can predict the main evolution of the state variables, through the equation derivatives for example.

Another control strategy is called **dynamic programming**. This is a type of off-line control which tries to reach the global optimal solution by minimizing a cost function, over a full cycle, under certain constraints. The external conditions are known in advance and the solution is found numerically.

This is opposite to the on-line control, where the external conditions are known in real time. Actual vehicle thermal management is obviously done with on-line control as it is impossible to determine in advance the operating conditions at any moment, on the overall route of the vehicle (such as the thermal load of the engine, the ram air speed through the radiator, etc).

Moreover, on-line optimization is capable of running with a quite low computation power, and be done in real time, while the global optimization takes much more time to find the solution.

A last and promising control strategy is called **model predictive control**. This can be viewed as a mix between on-line model-based control, and off-line control.

The control methodology uses a model of the process to predict the future evolution of the system, according to the present state of the plant. From that information, it will predict an optimal control of the actuators at each time step to minimise a cost function over a finite time horizon.

After one time step, only the according control is applied and a solution to the optimisation problem over a new receding time horizon is computed once again (with the new state).

This method also allows to take into account the (past) disturbances with a feedback and to react accordingly, while meeting the imposed constraints and staying inside the fixed boundaries.

Each study is different and these are the most reviewed topic. There exists other exotic ways of control explored but this paper has not for objective to describe each of them.

Few works use the three actuators at the same time, as it is complicated to develop an optimal control strategy taking a lot of parameters together.

However, such a combination is still described in the recent works [13] (p.19-20 of the slides), [14] (p.8) and [15] (p.11). In the three articles, the authors drive the bypass valve during the warm-up time and the compensation of disturbances is done through model-based control of the fan and the pump speed only, when the engine has reached the desired temperature.

1.2.3 Validation and results

The validation of the study is often done on a small test rig, a small scale thermal management circuit, with lower power input from the heater, and lower temperature than on a real engine. Indeed, the only results needed are a comparison between several control strategies, and how good is the temperature tracking, and this can be done on a small test rig. On these test benches, the heat source can be an electric heater or a heat exchanger crossed by hot water.

Other validation processes use numerical simulations. This is usually done with specified software where the model is more completely defined. This way, the test is easier and faster done and requires less resources, but it is also less representative of the real process, and some simplifications are made, as it is impossible to model all the disturbances.

When the objective of the study is based on the desired temperature tracking, the input of the experiment is mostly a variable temperature signal, a variable heat load from the engine or sometimes a variable ram air speed. The evaluation is then done on their response behaviour to the variation of their input through time.

Alternatively, for a fuel economy objective, the studies are based on a full drive cycle. The results are then evaluated based on the comparison of energy consumption (or the fuel consumption) between several control strategies (detailed in the section 1.2.2).

The results depends obviously a lot on the actuators used, the control strategy or the researched objective. However, the tendency shows that an advanced control can effectively reduce the energy consumption of the auxiliaries and, therefore, the final fuel consumption of the vehicle.

Chapter 2

Demonstrator concept

The objective of this thesis is to deliver a thermal management control demonstrator that will be able to perform different control strategies, to determine their applicability, their performance and which one consumes the least energy. It will also be used for sales and marketing purposes : customer presentations and exhibitions.

In the previous chapter, the basic principles of vehicle thermal management were approached and a review of several articles have been realized. In those articles, different set-ups, objectives, models and methods of control were presented. It allows to understand globally how a vehicle thermal system works, to determine the relevant components and to derive a generic architecture of thermal management controller from these observations.

To implement diverse control methods, the demonstrator necessitates to be flexible and have diversified features. The presentation purpose imposes also that it has to be easily transportable, and should fit in a suitcase.

A particular set-up in the literature survey was found interesting. In several papers [15], [16], [17], Harald Aschemann, Robert Prabel, Saif Siddique Butt, and more occasionally Christian Groß, Dominik Schindele and Robert Grimmecke, members of the Chair of Mechatronics, University of Rostock, Germany, studied several control methods. They tested these methods on a prototypic test-rig, featuring a variable pump, a heating system, a bypass valve and a radiator equipped with a fan, shown on Figure 2.1.

Since the basic idea of the demonstrator is the same as this test rig, only a few adaptations and components were added :

— A secondary radiator : after the main heater (engine), in series, to simulate a cabin heater core. This radiator needs also a fan to extract the heat from the coolant. If no cabin heating is required, the fan is stopped.

— A secondary heat source : placed in parallel of the main heat source + cabin heater branch, to assumes the role of an oil cooler, giving its heat to the coolant. If the oil cooler is not operated, a shut-off valve (SOV) prevent the flow inside this branch.

— An air heater : located in front of the main radiator, to behave as the additional radiators in front of the vehicle.

— An additional fan : in front of the main radiator and the air heater, creates an airflow similar to the ram air disturbance.

All these adaptations can be seen as a disturbance source to the original design.

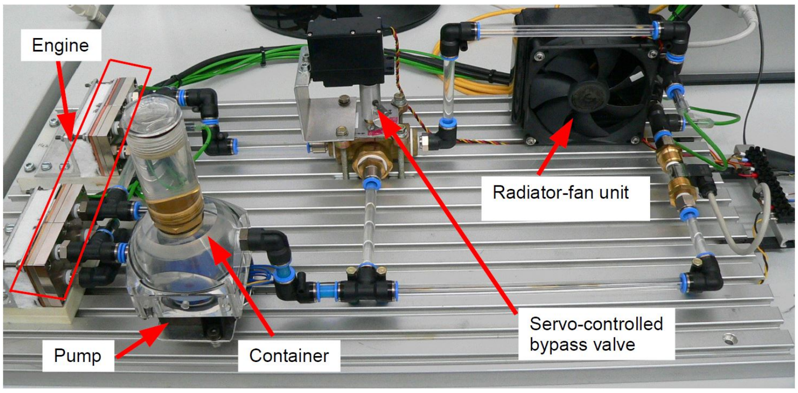

Figure 2.1 – Prototypic test-rig of an engine cooling system at the Chair of Mechatronics of the University of Rostock [17]

The final draft with all the hardware components is presented on Figure 2.2. On this drawing, the locations of the temperature sensors needed for an optimal control are also displayed.

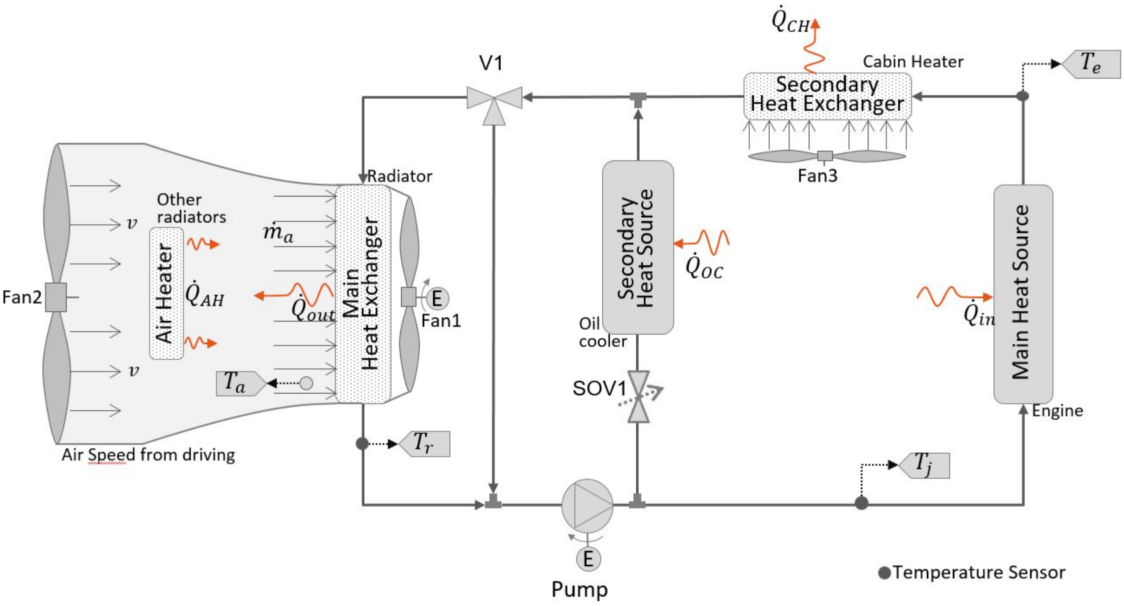

Figure 2.2 – Hardware plant draft [*Author's illustration*]

This way, the demonstrator is very flexible : it has the basic features (heat source, pump, bypass, and radiator), and it has also other specific features, which allows it to simulate different configurations.

It is also possible to imagine that the whole demonstrator is used for an entirely different circuit such as the low temperature circuit in an hybrid vehicle. The main heater would be the electric motor, and the secondary one would simulate the battery cooling. This is a pure question of interpretation. However, as the initial and main goal of the demonstrator focuses on the high temperature coolant circuit, this idea is not developed further.

2.1 HiL simulation

The development method is based on the Hardware-in-the-Loop (HiL) simulation. This technique puts two ways of development of a control system in parallel. On one hand, a control system is used to operate a physical machine (called the plant) connected through actuators and sensors. On the other hand, the same control is applied to a numerical model reproducing the physical processes (called the HiL simulator). A key feature of the model is its high fidelity to the real world process.

Building a model helps firstly in the decision of the right components : Its specifications (given in a datasheet) can be implemented in the model to show that the overall performance of the demonstrator makes some sense.

Testing the model allows then to investigate the control system more easily, more quickly and with less financial means. It shows the feasibility of the control strategy and an error in the control algorithm is also less problematic and more rapidly detected.

The HiL simulation for the demonstrator is explained through the Figure 2.3.

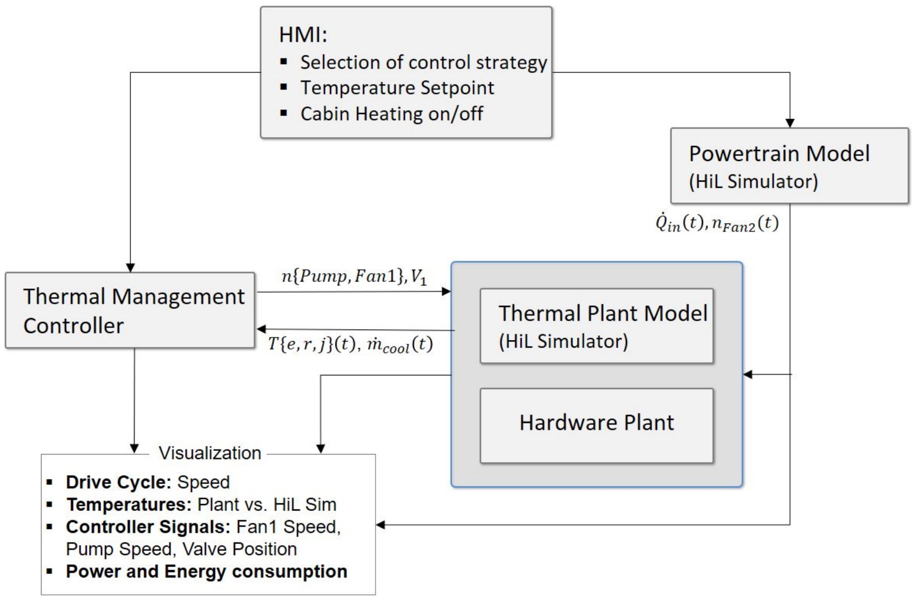

Figure 2.3 – Overview of the demonstrator HiL simulation [*Author's illustration*]

The *Human-Machine-Interface HMI* translates the human choices into inputs for the demonstrator. Those inputs consist in the selection of a predefined thermal management control strategy and it also allows to choose if the cabin heating is needed or if the oil cooler is activated.

The *powertrain model* generates the vehicle speed $v(t)$ (associated to the fan speed n_{Fan2}) and the heat input signals $\dot{Q}_{in}$. Those can be related to a certain drive cycle associated to a specific vehicle and engine.

The *Hardware plant* is the demonstrator, with the heat source, actuators, heat exchangers, sensors, etc. The *thermal plant model* emulates the demonstrator dynamics.

The *Thermal Management Controller TMC* receives the (feedback) signal from the sensors (the temperatures $T_{e,r,j}$, optionally the flow rate $\dot{m}_{cool}$), given whether by the hardware plant, whether by the simulation of it and determines then the according state of the actuators (pump and fan speed n + valve position V_1) based on the control strategy.

Finally, a *visualization interface* serves to show the behaviour of the demonstrator, and to see how the output of the controller are linked to the input. It is also used to compare the results of the thermal plant model to the hardware plant, and tune some parameters if necessary.

2.2 General assembly & characteristics

The test rig at the Chair of Mechatronics is composed of several computer water cooling components. Those will also be used for the demonstrator build-up.

Nowadays, waste heat generation is the limiting factor to develop more powerful computers, using a faster processor, graphic card or integrated circuits. With a few adaptations, it is possible to get around this issue,by cooling down a heat sink, glued to these components, with a water flow. This allows then to take the full potential of processors, graphic cards and others and run them at higher speed and voltage (this is called overclocking) for intensive tasks (*e.g.* video editing and gaming).

Besides the heat sink(s), a general set-up of computer cooling includes a radiator, a pump, fan(s) and tubes in between, that are similar to the engine cooling system, at smaller scale, exactly what is needed for the demonstrator.

An advantage of using computer water cooling components is also this ensures a fast and reliable delivery as there exists a multitude of online retailers (such as *amazon.com, aquatuning.de, mylemon.at, ...*), and the components are low-priced (compared to the automotive industry). Their performances are also well documented all over the internet.

One of the main characteristics of these components is that they usually don't allow water temperature higher than $60°C$. This temperature will thus be the upper working limit for the demonstrator.

The fluid used as coolant will be simple water : that allows to meet the transportability requirement as water is cheap and easily accessible, and the circuit can be flushed out when the demonstrator needs to be moved. No antifreezing additive is needed as the demonstrator won't be used in freezing environment. Likewise, as just said in the previous paragraph, the temperature won't exceed $60°C$, so there is no need to worry about evaporation. Finally, the whole device is not supposed to be continuously filled when unemployed for long periods to avoid algae formation. If so, it is then preferable to add a few drops of an antibacterial and antifungal biocide.

2.2.1 Pump & reservoir

The pump serves to push the coolant through the whole circuit and overcome the pressure drop along the tubes and components. The pump speed control is also possible with supply voltage variation or PWM signal.

It is usually a centrifugal pump (Figure 2.4)and its general characteristic curve (represented on Figure 2.5) is typically expressed in term of the total dynamic head (pressure) H over the flow rate Q. The system loss curve is the ascending one which means that the pressure drop will rise when the flow rate increases.

The pump has a mainly decreasing characteristic curve and the equilibrium point is the intersection P between both trajectories, determining the flow rate and the overall pressure drop in the whole system. If the pump speed is raised, the pump characteristic is displaced upwards and the new equilibrium point P' shows increased flow rate and pressure drop in the circuit. This is the opposite if the pump speed decreases.

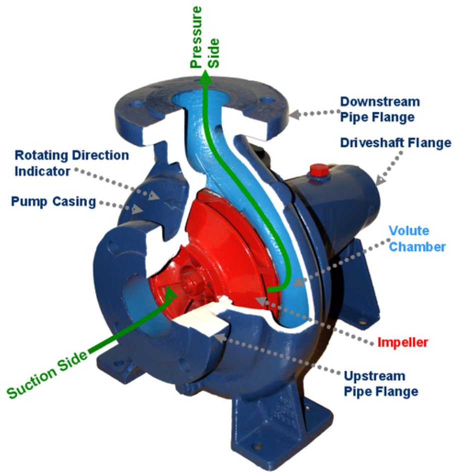

Figure 2.4 – Generic centrifugal pump [18]

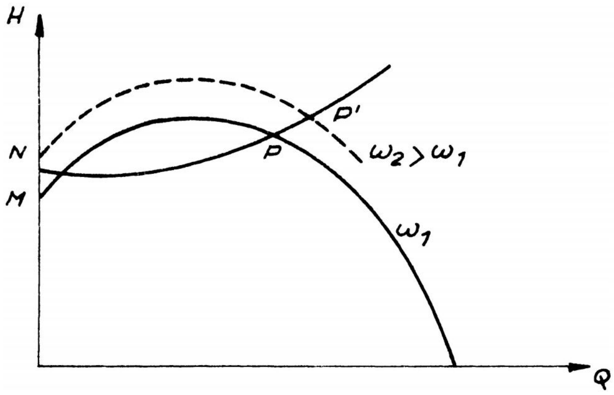

Figure 2.5 – Typical characteristic curve of a hydraulic pump [19]

It is possible to place two identical pumps, either in parallel or in series. The Figure 2.6 shows the corresponding modification of the characteristic curve : The dynamic head pressure is doubled in the series case and there is a two times bigger flow rate in the system for a same head pressure. However, for the same circuit, it is observable the flow rate will be higher with a placement in series.

The reservoir is usually placed on top of the pump and is just used to fill the circuit with water, to allow a small thermal expansion of the fluid, and to collect the residual air bubbles when the system starts running.

2.2.2 Radiator & fans

The radiator and fans are components that have to be looked together. Typical computer cooling radiators are crossflow heat exchangers, with 2 passes for the water : this means that the inlet and outlet are placed on the same side of the radiator. Usually they can support between one and four fans in a row, depending on the heat load of the cooling loop. A higher heat load to dissipate by the radiator, requires a higher surface area (*ceteris paribus*). The fans have a standard size of 120mm or 140mm in diameter, which implies that the radiator has then its highness around the same value and its length is a multiple of it. An example is shown on Figure 2.7.

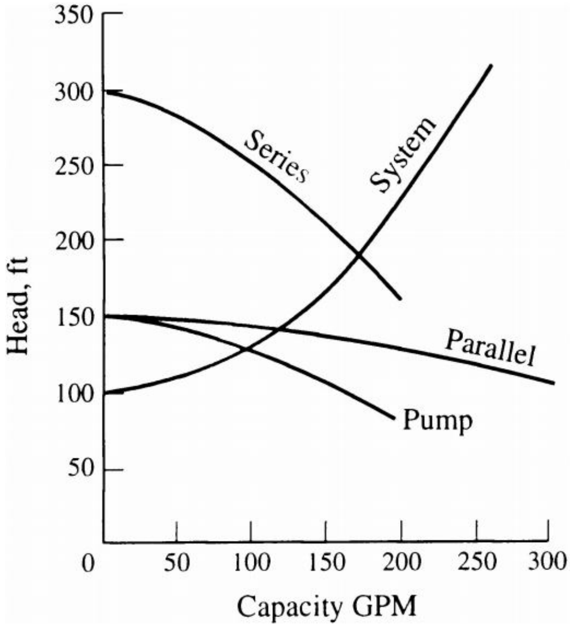

Figure 2.6 – Comparison of hydraulic pumps placed in parallel and in series [19]

If the fans turn more quickly, more heat can be dissipated. The difference of heat dissipation for different size of radiator is represented on Figure 2.8. RS120, RS240 and RS360 are radiators from the same series of the same manufacturer, with the same specifications, except for their length and the number of fans they can accept. They have one, two and three 120mm diameter fans respectively. The water flow rate is fixed to 1,5 Gallon Per Minute (GPM) which is equivalent to 5,678 Liters Per Minute (LPM), a typical flow rate inside the circuit. The ordinate axe is the watts dissipated for a 10°C temperature difference between the ambient air and the water outlet. It is compared in function of the airflow rate on the abscissa, expressed by the fan speed in Revolutions Per Minute (RPM), easier to determine in a test experiment than the air mass flow rate or the air speed through the radiator.

Another characteristics of the PC water cooling radiators is their possibility to accept a fan that pushes the air in entrance and another fan, on the other side of the radiator, that sucks/pulls the air through the radiator. This technique is called *Push-Pull*, in opposition to *Push* or *Pull only*. A comparison of temperature difference between the air and the water flow is put on Figure 2.9. It is also possible to place shrouds between the fan and the radiator to make uniform the airflow, and avoid therefore the zone just next to the electric motor of the fan where turbulence is created.

Placing shrouds and fans on both sides of the radiator increases the efficiency of the heat dissipation and a lower temperature difference is thus observed. However, Figure 2.9 shows that placing two fans on both sides of a radiator (for the same front surface) doesn't double the heat transfer : Indeed, the fan characteristic curve is similar to the pump one (explained in section 2.2.1). Two fans in series increase the total flow rate going through the radiator, but the air pressure drop inside the heat exchanger is also augmented so that the air mass flow is not doubled. Moreover, the heat dissipation efficiency of the radiator isn't either linear with the air flow.

As a fan in a normal engine is positioned to pull the air, so will the actuated fans

Figure 2.7 – Different radiator sizes (manufacturer : Swiftech)

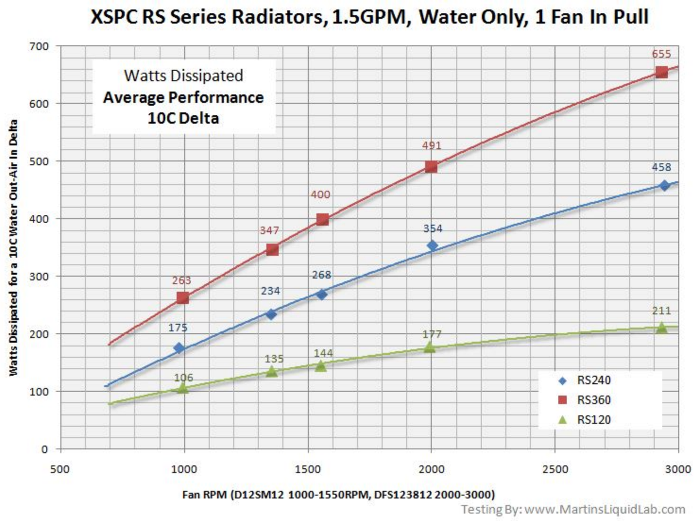

Figure 2.8 – Cooling performance in function of different radiator sizes (manufacturer : XSPC)

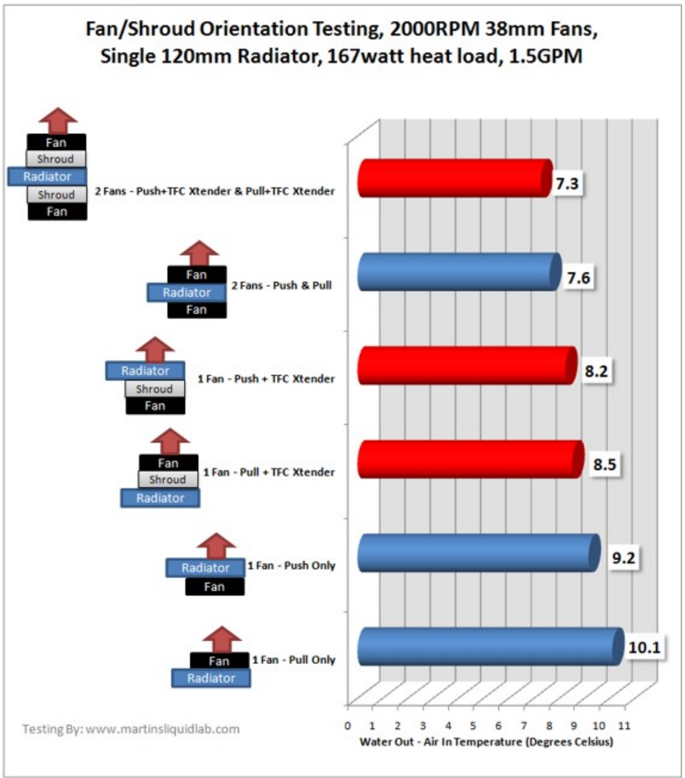

Figure 2.9 – Comparison of different fan dispositions

for the demonstrator (also labelled as main fans). Nonetheless, the fans used to simulate the air speed (sometimes denoted as front fans) will be placed on the other side of the radiator such that it will look like a push-pull disposition. No shroud has been used in the demonstrator.

The other characteristics to be attentive to are the depth of the radiator, which varies usually between 30 and 80 mm, and the number of Fins Per Inch (FPI), typically situated in the range 10-30. A higher value of those specifications improve the heat transfer from the water to the air flow, but increases also the air pressure drop, requiring more powerful (meaning higher static pressure) and faster fans to be really effective.

2.2.3 Water heater

To heat the cooling water with a controllable heat input, with a component reduced in size, and an easily accessible supply source, the choice of an electric heater is the most obvious.

The solution chosen for the main water heater is an assembly of a cold plate with a silicone heater :

A cold plate is made of a copper or stainless steel tube embedded to a thick aluminium plate, as represented on Figure 2.10. The water flow through the tube, which is bended several times at 180°, making 1, 2, 3, 4,... passes over the metal plate.

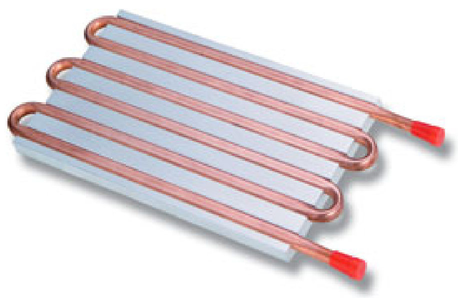

Figure 2.10 – General design of a cold plate [20]

The performances of the cold plates are defined by their pressure drop and their thermal resistance curves. The thermal resistance shows the temperature difference between the metal plate surface and the flow, under a given thermal load. The unit is $°C/W$, which means that for $250W$ transferred to the plate for example, the temperature difference will be 3,75$°C$ at 1,5GPM (0,015$°C/W$)

The higher the number of passes, the lower the temperature difference between the water at the cold plate outlet and the metal, but the higher the drop pressure. Choosing the right cold plate is thus a compromise between those characteristics.

The silicone heater, with an example on Figure 2.11, is a heating foil with a resistance wire embedded between two silicone sheets. The heat is produced by the heat dissipation due to the Joule effect ($P = RI^2$). The foil can be self-adhesive or vulcanized on the metal, which enable a better contact between both materials, so that a better heat transfer. The silicone heater can heat up until 240$°C$ and has a maximum heat output of $3W/cm^2$ if vulcanized. The supply voltage of this device is very flexible and can vary from $12V$ to $400V$, AC or DC.

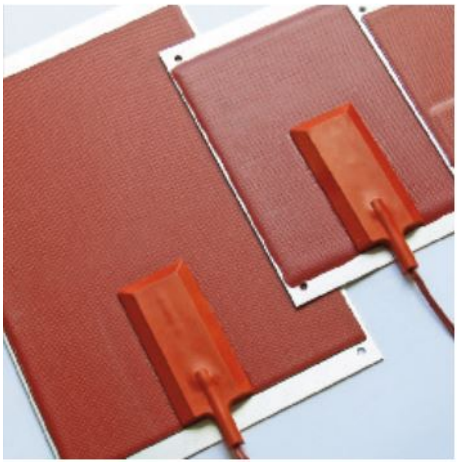

Figure 2.11 – Different sizes of silicone heaters on metal plates [21]

2.2.4 Bypass valve

The bypass valve is a three way valve actuated by a servomotor. Our application requires that the command of the valve defines the percentage of opening, with a quick variation from fully closed to fully open, and has an accurate and fast control. This is not a standard water cooling component.

In a vehicle, the consumption of the servomotor is usually neglected due to its low value, compared to the power required by the pump and the fan.

2.2.5 Tubes & fittings

In water cooling components, the water flows through soft or hard tubes. The soft tube are flexible and made out of rubber, silicone, PVC or other compounds. It can be transparent, colored or opaque. The other option is hard rigid tubing. The common materials are acrylic (plexiglass) or PETG, which can be bended relatively easily with an adapted heat source : their glass transition temperature is situated around $80 - 100°C$. As the demonstrator has an exhibition purpose, it was preferred to use rigid tubes to offer clean, well organized and aesthetically pleasing look.

The tubes are defined by their inner and outer diameter (respectively abbreviated ID and OD), usually expressed in inches, sometimes in millimetres. For hard tubes, the combination is either 3/8" x 1/2" (10 x 13 mm) or 1/2" x 15/8" (12 x 16 mm). To minimize the pressure drop inside the tubes, the flow speed has to be low, which happens when the front section area is bigger (at same mass flow rate). Therefore, the bigger inner diameter (1/2" / 12mm) is chosen for the demonstrator.

To attach together the tubes and the components, fittings are needed. Those have a standard thread size of G1/4 (also named BSPP1/4) in water cooling. This defines every parameters of male and female threads for a perfect match.

There exist also T/Y/X-fittings to divide the flow and put temperature sensors in the system and some adapters to adapt the different thread sizes.

2.2.6 Overall system

After a thorough research of components, to match each one of them together, with their own characteristics (power, pressure drop), it has been decided to use a $500W$ electric main heater, with a 3 x $120mm$ radiator, with fans going up to $3000RPM$. The control will be designed so that the coolant temperature won't exceed $58°C$ to let a safety margin with the maximum temperature of the components ($60°C$).

The radiator simulating the heater core, placed after the heating unit, will only be a one-fan radiator, because it is only used as a disturbance and not as the main heat sink. It only needs to extract a small amount of heat from the system (proportionally).

An air heater, with a nominal heat power of $200W$, will also be used to simulate the other heat exchangers in front of the main radiator. In the case of a combustion engine, it is mainly the air conditioning system, and the charge air cooler in a smaller measure. For an hybrid vehicle, the low temperature radiator for the electric components is also present.

A flow meter has also been added after the pump to know the flow rate at any moment and use it in the controller. Temperature sensors are also obviously needed at the relevant locations (see Figure 2.2).

Due to lack of time during the internship, it has been decided to leave out the implementation of the secondary heater, originally in the test rig, and focus on the main components. Nonetheless, its place has been taken into account, the model can simulate it, and it could easily be installed in a future work / update.

A particular attention was paid to use compatible materials in aqueous solution to avoid galvanic corrosion. This takes place when two metals of different nature (different electronegativity) are in contact in an electrical conductive environment, called electrolyte (like mineralised water). Most of the components are made of brass for their wetted parts, except for the flow meter, made of stainless steel 316L, which couldn't be avoided. In this last case, some attention should be paid over time to the fittings (in brass) touching the flow meter, but the corrosion should be limited.

The particular components and the global model are detailed in the next chapter.

Chapter 3

Thermal plant

In this chapter, the chosen components used for the demonstrator and the overall model, represented on Figure 3.1, are detailed.

The Simulink program has been used for the model. It is included in the MATLAB environment.

The modelling is done through the use of elemental blocks which corresponds to mathematical or logical relations, predefined signals, or other signal processes. It is also possible to use libraries with their own blocks to emulate a certain comportment.

For this work, the *Thermo-Hydraulic Library* (short version : TheLib), developed by Armin Traußnig working in the company AVL, is used. It features every common element of a vehicle thermal management system (complex thermal and fluid networks) to assess its behaviour.

Deeper description will be given throughout this chapter.

In this case, the model is a closed loop where the state of the fluid balances the mass and energy inputs and outputs at any moment.

The global solution to the underlying continuity and energy conservation equations is computed by the *Flow Solver* block of TheLib. It is an iterative solver that is based on the Global Gradient Method (not detailed in this paper), resolved numerically for a fixed discrete time step of 0,1s.

Between each component (characterized by fluid inlet i and outlet o ports), the standard buses convey the mass flow rate $\dot{m}$, the pressure drop Δp and the temperature T signals. In closed loop, the components need nodes between them for a right computation of the solution.

The different information displayed in the *PostProc* subsystem are the temperatures, pressure drops and flow rates calculated in each node by the *Flow Solver* block, and it also gives the number of iterations, the global head error and the error to the continuity equation for each sample time. Those numbers are to be the closest possible to 0. The simulation crashes if they exceed a predefined level.

TheLib can model fluid networks with oil, coolant, air or water. For the demonstrator, the last option is chosen. It is important to note that the properties used are valid for a range of fluid temperatures between -35 and 120°C. If this range is not respected, the simulation crashes.

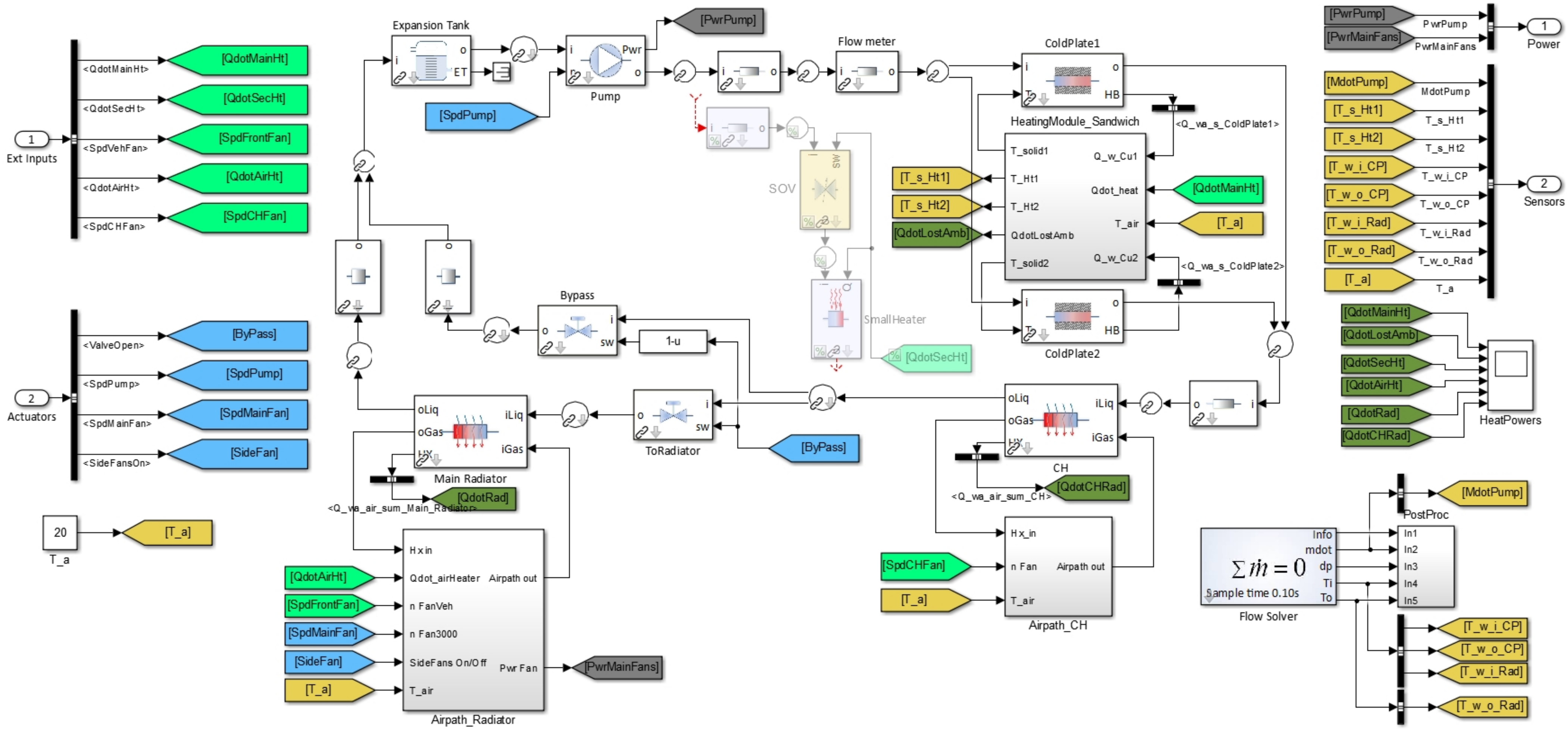

Figure 3.1 – Simulink model of the Thermal Plant Simulator : Water circuit subsystem [*Author's illustration*]

The thermal plant circuit model has in and out signals, conveyed to and from the appropriate element port via the coloured *Goto* and *From* blocks.

The incoming signals are divided in two categories :

1. The 'Ext. Inputs' are associated to the chosen human inputs. It includes :
   — the heating power input of the main heater $QdotMainHt$;
   — the speed of the fans simulating the vehicle speed $SpdVehFan$;
   — the heating power of the secondary heat source (the oil cooler) $QdotSecHt$;
   — the heat input given by the air heater $QdotAirHt$;
   — the speed of the cabin heater fan $SpdChFan$.
   $SpdChFan$ is more dependant of the user request, while the first four inputs are ideally to be related to the driving cycle, even if it could be adapted to some user entry if needed.
2. The 'Actuators' are managed automatically by the thermal management controller (placed outside of this model and described later in the section 4.3) in function of the cooling strategy and the sensors signals. There are :
   — the percentage of valve opening $ValveOpen$;
   — the pump speed $SpdPump$;
   — the actuated fan speed $SpdMainFan$.
   An option has been added to let the possibility for the controller to drive only the middle actuated fan of the main radiator, while both fans on the side could be turned off, to lower the cooling power.
   When the variable $SideFansOn = 1$, all three actuated fans rotate at the same speed. Otherwise, $SideFansOn = 0$ and only the middle fan rotates.
   The control strategy is explained in more details in the next chapter.

The outgoing signals are also divided in two categories :

1. The 'Sensors' are the signals of temperature on significant points of the network and of the mass flow through the heater. The thermal management controller uses these informations to change the state of the actuators according to the control strategy.
   — $MdotPump$ is the mass flow rate ;
   — T_s_Ht1 and T_s_Ht2 the temperatures of the silicone heater ;
   — $T\_w\_i\_CP$ / $T\_w\_o\_CP$, are respectively the fluid temperature at the heating unit inlet / outlet ;
   — $T\_w\_i\_Rad$ / $T\_w\_o\_Rad$ are the fluid temperature at the radiator inlet / outlet ;
   — T_a is the ambient air temperature and is fixed at $20°C$ in the model.
2. The 'Power' output records the power used by the pump and the actuated fans.

About the signal units, :
— the speed is in RPM ;
— the heat power in W ;
— the mass flow in kg/s ;
— the pressure drop in Pa ;
— the temperature in $°C$.

The heat transfer powers can also be displayed on a monitor device.

This rest of chapter is organised with the description of each specific component followed by its detailed model in Simulink.

Each block of the library is defined with specific parameters to generate the same behaviour than the real component. Over a first phase, the parameters entered in the model are found on the internet or fitted to emulate the same performances if they are not directly available. These parameters can later be updated to reproduce the exact behaviour of the component, after their reception and some tests made, to confirm the alleged performances found.

3.1 Heating unit

The main heating element of the demonstrator is an assembly of an aluminium plate in sandwich between two cold plates **Lytron CP10G14**, separated by the silicone heaters from the **HORN** company, as represented on Figure 3.2 with the dimensions of the different basic elements. The parts are pressed and fixed together with screws, within the square hole areas made to avoid that the screws pierce the fragile silicone heaters. The aluminium plate in the middle is added to give extra thermal inertia to the heating unit. This way, the heat power variations to the coolant are tempered, and if the heat input stops, the overall metal temperature will decrease slowly. The heater behaviour is therefore more similar to a real engine block.

The cold plates are placed in parallel in the fluid network to limit the pressure drop across the heating unit.

The global heating power of the module has been fixed at $500W$, which means that each silicone heater has a nominal power of $250W$.

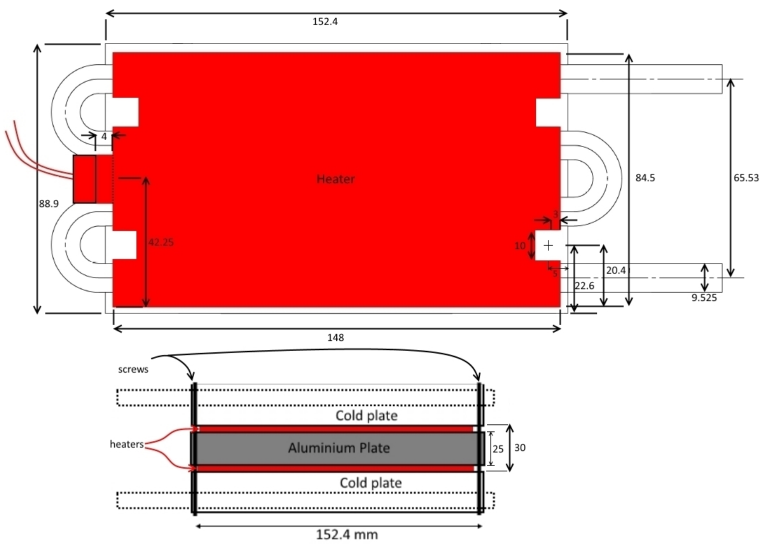

Figure 3.2 – Schematic of the heater module (measures in mm) [*Author's illustration*]

Each cold plate has 4 passes of a 9,5mm diameter copper tube and their dimensions are 152,4 x 88,9 x 12,7 mm (6" x 3,5" x 0,5").

Their performance charts are given on Figures 3.3 and 3.4, for the CP10 - 6" - 4pass. ($1GPM = 3,785LPM = 0,0631kg/s$)

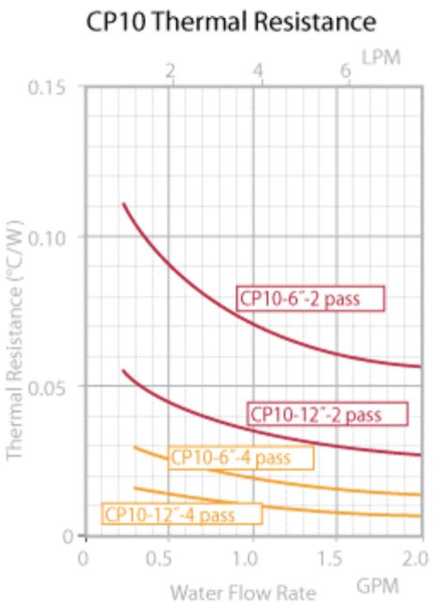

Figure 3.3 – Thermal resistance of the CP10 cold plate series (case : 6" - 4 pass) [20]

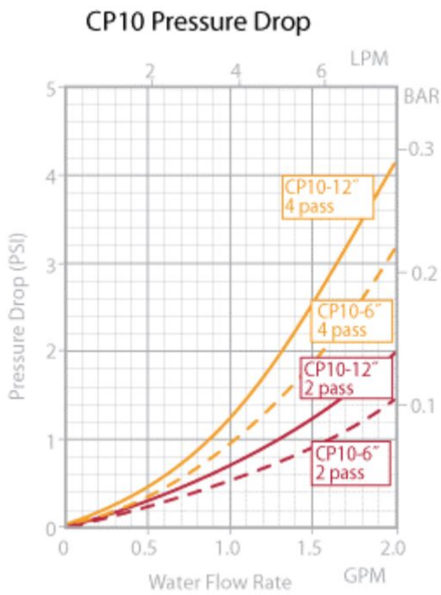

Figure 3.4 – Pressure drop of the CP10 cold plate series (case : 6" - 4 pass) [20]

Each silicone heater of $250W$ are pressed between a cold plate and the aluminium plate.

They are designed such that the electrical connector, thicker than the rest of the element, is placed out of the heating surface. Their supply voltage is $230V$ AC.

As their surface power density is quite high ($\frac{250}{14{,}8*8{,}45} = 2W/cm^2$), it is essential to ensure a perfect contact between both elements, to guarantee an efficient heat transfer to the metal so that no overheating appear, which could destroy the heating device otherwise. So, the heaters have been ordered with an integrated temperature sensor (T_s_Ht1 and T_s_Ht2 signals), with a main purpose of monitoring, and to check that it doesn't exceed $240°C$.

Model

The heating unit specific model is shown on Figure 3.5. The complex heat transfer between both plates is modelled in the subsystem, detailed on Figure 3.6.

Both cold plates blocks are a *Heat Bridge* block from TheLib, which calculates the convective heat transfer between a solid and a fluid flowing through the component. More than the standard input and output ports concerning the fluid ($\dot{m}$, Δp and T), this block requires the temperature of the solid Ts in input and outputs (through HB port) the heat flowing from the solid to the fluid $Q\_wa\_s\_ColdPlate$ and other useful specific factors, such as the heat transfer coefficient h, the Nusselt number Nu, the Reynolds number Re, and the thermal resistance R_{th}.

The parameters inside the *Heat Bridge* are divided in three categories : 'General' (concerning dimensions, fluid and initial temperature), 'Flow' (concerning the pressure drop) and 'Heat transfer'.

The pressure drop is here defined by a second order polynomial (fitted from the datasheet information) and the heat transfer is defined via the use of the Gnielinski correlation ($Nu = f(Re, Pr)$, with the Prandtl number Pr).

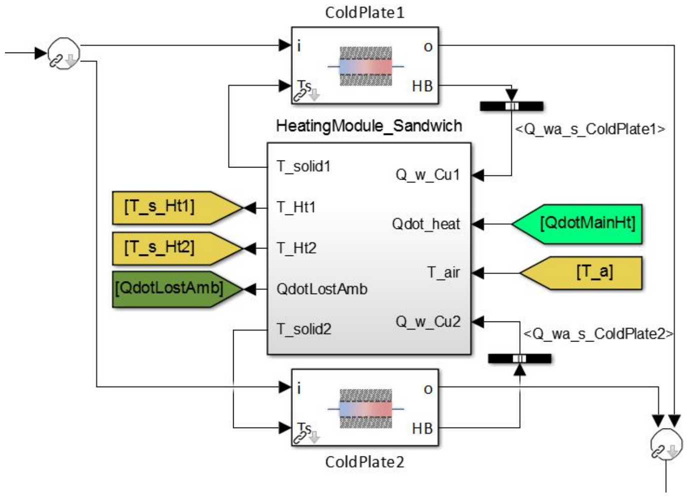

Figure 3.5 – Model of the cold plate circuit + thermal subsystem [*Author's illustration*]

The information of the heat power $Q\_wa\_s\_Coldplate$ from the fluid to the solid is taken to feed (through the port Q_w_Cu) the thermal subsystem HeatingModule_Sandwich linking both plates (Figure 3.6).

The inputs of the subsystem are the ambient air temperature T_a and the heat powers from the water Q_w_Cu and from the electrical input $Qdot\_heat$. Its results give the metal and silicone heater temperatures (respectively T_solid and T_Ht).

The subsystem simulates mainly the conduction (with the *Conduction* blocks) between the different element of the heating unit : cold plates ($Coldplate1$ and $Coldplate2$), silicone heaters ($Foil1$ and $Foil2$), and the Aluminium plate (AP).

The *Lumped Mass* block from TheLib works as heat storage, with the sum of incoming and outgoing heat flows in input and the temperature of the element (determined by its specific heat and mass) in output.

For this subsystem, the *Lumped Mass* are used for the heating foils, but are also employed in the cold plate and Aluminium plate subsystems :

As T_solid is the temperature of the Copper of the cold plate in contact with the water flow, a little more elaborate model Coldplate has been produced to simulate the inner heat transfer between the face exposed to the silicone heater, the copper in contact with the water flow and the natural convection to the ambiance. The model is shown on Figure 3.7.

A *Lumped Mass* acts as the copper tube. It exchanges heat with the water flow (input of the subsystem), a part goes to an intermediary lumped mass that acts as a heat storage, and the last part goes directly through convective transfer to the ambiance because a fraction of the copper tube is in contact with the air. The intermediary thermal mass looses a fraction of its energy to the ambiance, and the rest of the balance has a thermal connection through conduction with a thin layer of aluminium (1,5mm thick) in direct contact with the heater

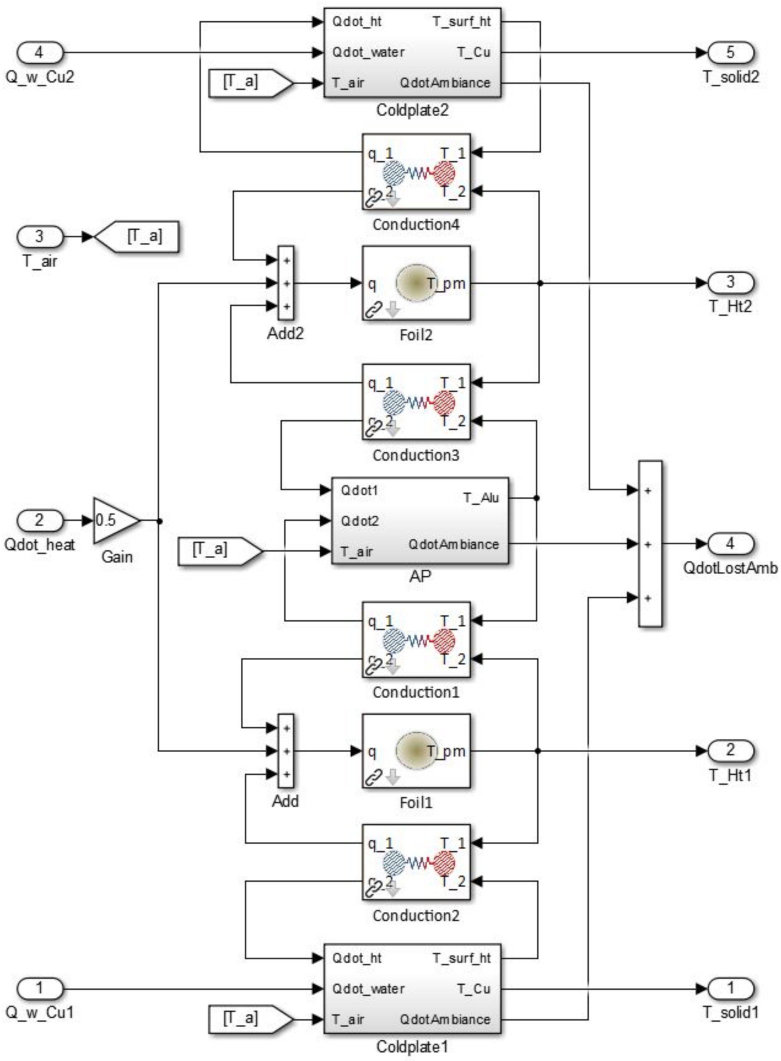

Figure 3.6 – Thermal subsystem of the heating unit : HeatingModule_Sandwich [*Author's illustration*]

The model Coldplate has then been tested to compare its thermal resistance to the performance provided by the manufacturer of the cold plate. Its comparison is shown on Figure 3.8, with the blue line. The model underestimates a little the real thermal resistance, except for low flow rates, where it overestimates and diverges a little more from the given performance. However, the overall error stays acceptable.

The same idea as the cold plate subsystem applies for the Aluminium plate, on Figure 3.9. The storage lumped mass is thus surrounded by heat exchanging surface :

- two thin metal layers are in direct contact with the silicone the heaters. This is simulated by two small lumped masses.
- the storage mass interacts also with the ambiance, proportionally to the rest of the plate external surface.

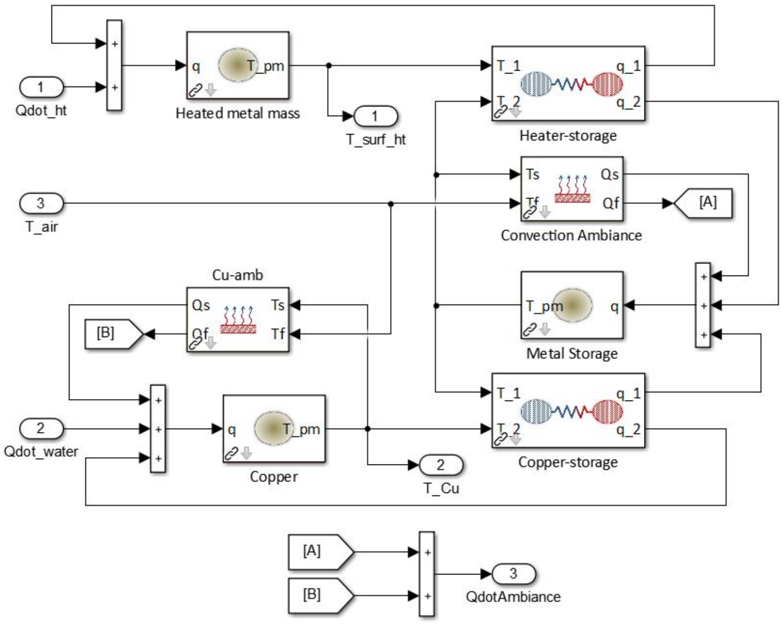

Figure 3.7 – Coldplate heat transfer model : Coldplate [*Author's illustration*]

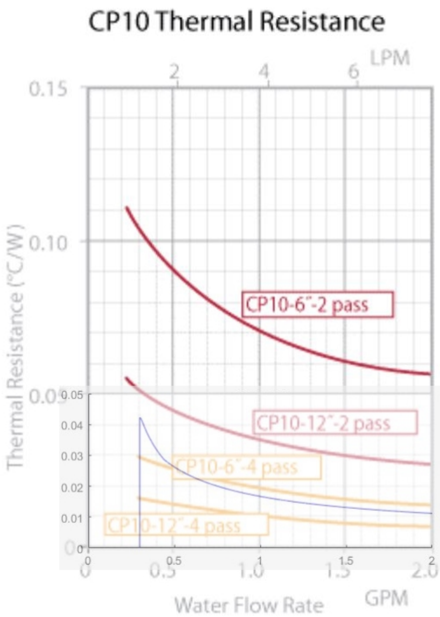

Figure 3.8 – Validation of the cold plate model [*Author's illustration* + [20]]

3.2 Cabin heater unit

The secondary heat exchanger is placed after the heating unit.

It is a **Phobya G-changer 140**, a 140mm-fan, 60mm thick and 12FPI radiator. Its characteristic curves are given on Figure 3.10 and 3.11 (the black line is not relevant). This radiator was especially chosen for its low pressure drop. A particular specification is to have two G1/4 at each inlet and outlet port, that allows to have several tubes or sensors

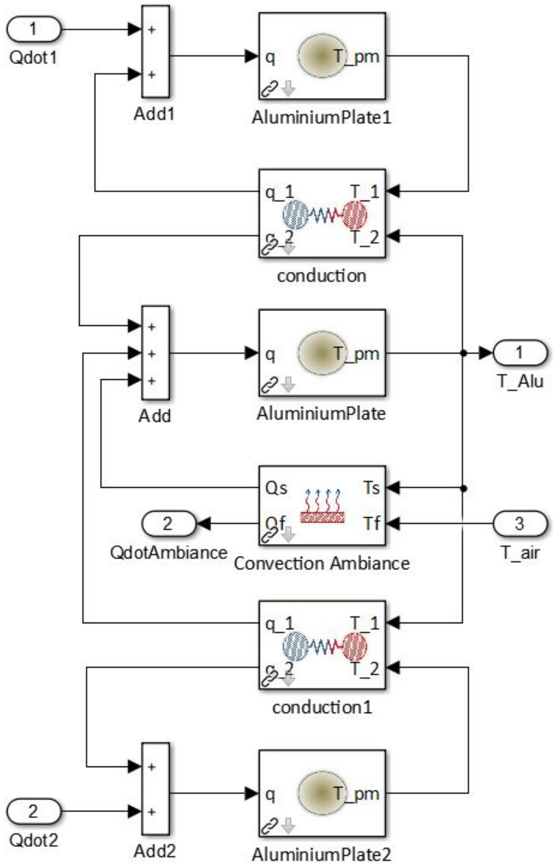

Figure 3.9 – Aluminium plate heat transfer model : AP [*Author's illustration*]

connected to the same node.

The fan, a **Noctua NF-A14 industrialPPC-2000 PWM**, has a thickness of $25mm$ (standard size in water cooling fans) a rotational speed range between $500RPM$ and $2000RPM$, which corresponds to a maximum air flow of $182{,}5m^3/h$ and with a maximum static pressure of $4{,}18mmH_2O$.

Model

The model of the cabin heater unit is represented on Figure 3.12. It uses the *Fin Tube Heat Exchanger* block from TheLib and an other subsystem Airpath_CH to determine the air flow rate, expanded on Figure 3.13.

As no information was found on the internet about the fan characteristic curve, the data was scaled down from a standard vehicle fan curve (used by my company supervisor Armin Traußnig), based on the nominal power and static pressure of the computer cooling fan.

In the Airpath_CH subsystem, there is a *Fan* block from TheLib which calculates a pressure increase/drop polynomial $dp(m)$, a pressure increase/drop dp and the power consumed Pwr for a given mass flow mfl, air temperature $Tair$ and rotational speed n.

The balance between the pressure increase polynomial from the fan and the pressure drop polynomial from the radiator (modelled by the *Fin Tube Heat Exchanger* block) are

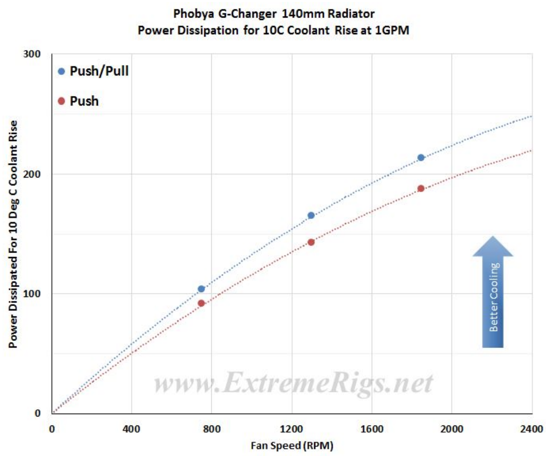

Figure 3.10 – Heat dissipation characteristic of the secondary radiator

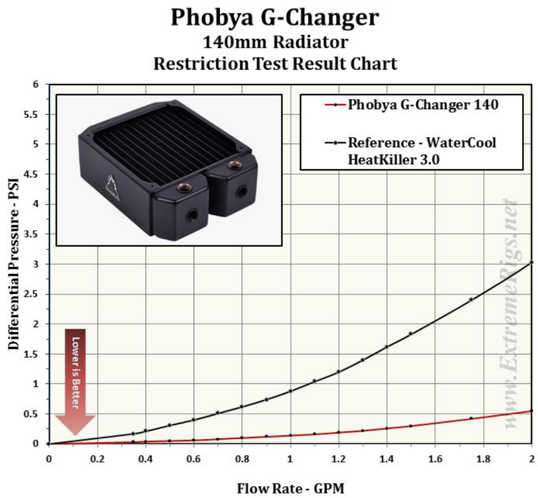

Figure 3.11 – Pressure drop characteristic of the secondary radiator

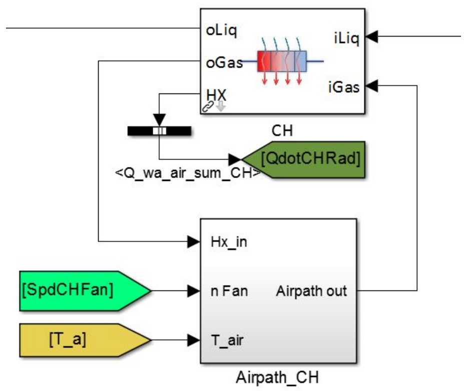

Figure 3.12 – Model of the secondary radiator + air path subsystem [*Author's illustration*]

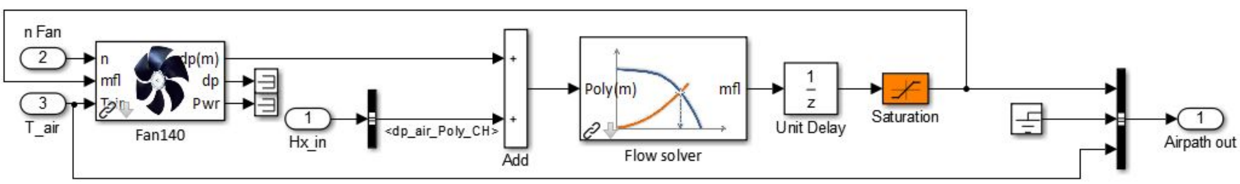

Figure 3.13 – Air path subsystem model : Airpath_CH [*Author's illustration*]

then solved together via the *Flow solver* block to obtain the resulting air mass flow going through the radiator.

The *Unit delay* block, which delays the response from one time step, serves for the feedback to mfl. As for the *Saturation* block, it is used to ensure the existence and the stability of the solution for very low flow rates, very close to $0 kg/s$.

The *Fin Tube Heat Exchanger* block, *CH* on Figure 3.12, replicates the behaviour of a louvered fin heat exchanger (Figure 3.14), with heat transfer correlations developed by Chang and Wang [22] on the air side and Gnielinsky correlation on the water side. Its inputs and outputs are the characteristics of the incoming and outgoing water and air flows. Additionally, the heat transfer coefficients, temperatures, heat flows of both mediums and for the individual heat exchanger cells are given as output.

However, computer radiators have triangular fins (Figure 3.15) and the underlying equations of the model are not applicable. Some parameters of the louvered fin heat exchanger (fin efficiency, louver angle, louver pitch, and wetted perimeter, some shown on Figure 3.16) have been fitted to the performance measured to adopt a similar heat response (Figure 3.17).

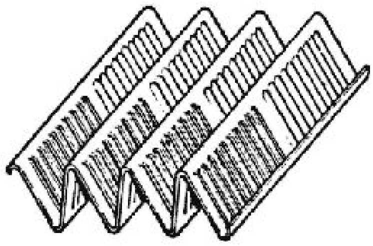

Figure 3.14 – Louvered fins [23]

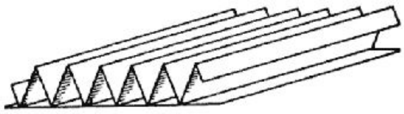

Figure 3.15 – Triangular fins [23]

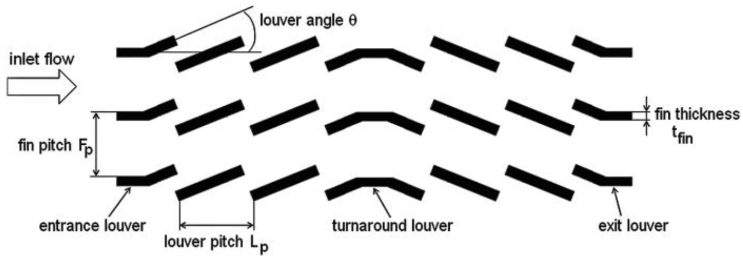

Figure 3.16 – Louvered fin heat exchanger parameters [24]

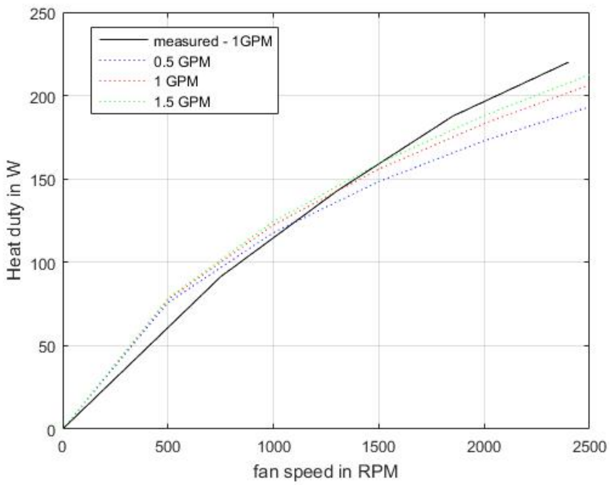

Figure 3.17 – Validation of the secondary radiator model [*Author's illustration*]

The black continuous 'measured' line shows the alleged performance for a $1GPM$ flow rate ($= 3{,}785LPM$ or $0{,}06309kg/s$). The dotted lines brings to light the characteristic curve for the same water flow rate in the model as well as its evolution for an increasing water flow rate.

A script was written to automatically tune the parameters, to fit perfectly the known curve ('measured' line), but no solution was found, so the best compromise has been searched manually. Compared to the real curve, the heat dissipated by the radiator in the model will be higher for low fan speeds (and thus low air flow) and will be underestimated for high fan speeds.

The heat dissipation of a radiator is not very sensitive to the water flow rate variation.

3.3 Bypass valve

The bypass valve **VDE/ML S O C 24V PASSO-PASSO** shown on figure 3.18, is controlled by a stepper motor (explain in the next chapter). Its pressure drop characteristic appears on Figure 3.19. The path A leads to the bypass branch and the path B to the radiator.

Figure 3.18 – Bypass valve [25]

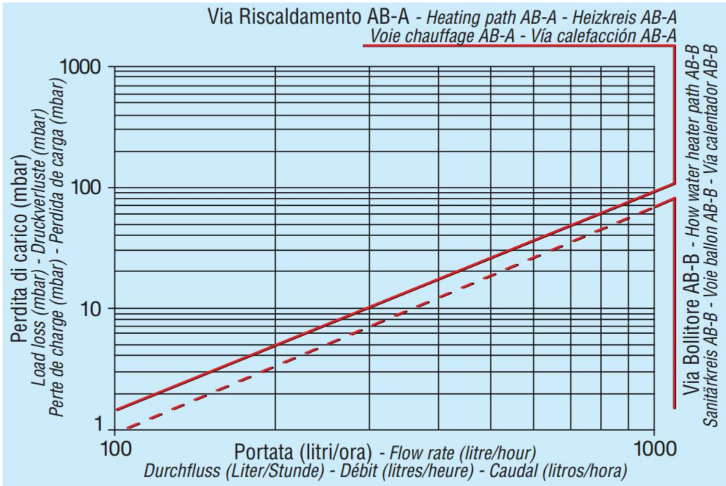

Figure 3.19 – Bypass valve performance [25]

Model

The model of the valve is visible on Figure 3.20. It is a combination of two *Map Valve* blocks from TheLib.

The *Map Valve* is fully open (lowest flow resistance) if the control port $sw = 1$ and fully closed (highest flow resistance) if $sw = 0$. In the interval [0;1], the valve resistance is given by the Zeta curve (defined as a parameter). If one valve opens, the other one closes.

The pressure drop in one branch is linked to the Zeta coefficient by the formula :

$$\Delta p = \zeta \frac{\rho V^2}{2}$$

As this valve was already used and characterized by my company supervisor, he furnished the Zeta curve used in the model, on Figure 3.21.

3.4 Main radiator unit

The main radiator, a **Hardware Labs Black Ice SR2 360 MultiPort**, is a 3 x $120mm$-fan ($60mm$ thick and $9FPI$) version, with the heat transfer and pressure drop

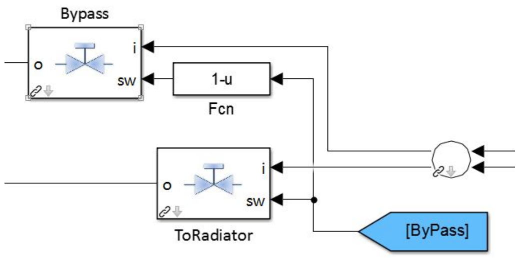

Figure 3.20 – Valve model [*Author's illustration*]

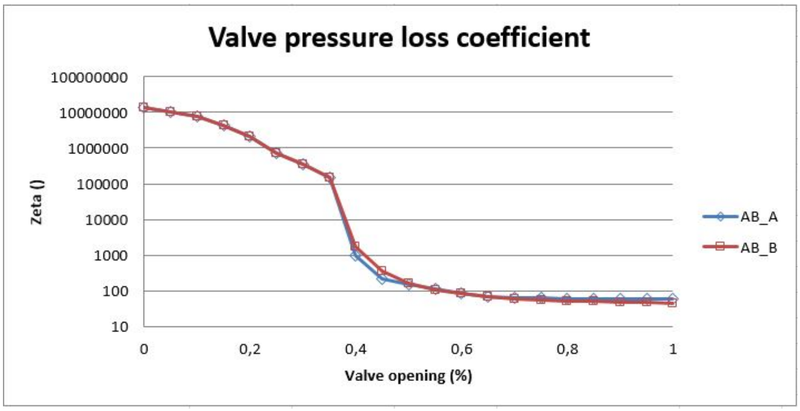

Figure 3.21 – Valve Zeta coefficient [*Courtesy of Armin Traußnig*]

characteristics on Figure 3.22 and 3.23 respectively. It has also several ports at the inlet and outlet for tubes and sensors.

Figure 3.22 – Heat dissipation characteristic of the main radiator

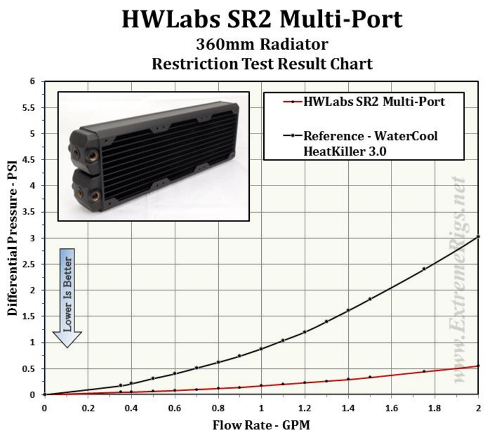

Figure 3.23 – Pressure drop characteristic of the main radiator

The three actuated (main) fans **Noctua NF-F12 industrialPPC-3000 PWM** have a large rotational speed range between $750RPM$ and $3000RPM$, with a maximum air flow of $186{,}7m^3/h$ and a maximum static pressure of $7{,}63mmH_2O$. Like on a real vehicle, they are placed to pull the air through the radiator, behind it (from the airflow direction viewpoint).

A high maximum fan speed increases also the low limit fan speed. As the fans simulating the vehicle speed (sometimes called in this paper : vehicle fans or front fans) have only a disturbance purpose and that it would be better to be able to create low vehicle speed, the choice went to the **Noctua NF-F12 industrialPPC-2000 PWM**, with a minimal rotational speed of $450RPM$ (other specifications include a maximum speed = $2000RPM$, a maximum air flow = $121{,}8m^3/h$ and a maximum static pressure = $3{,}94mmH_2O$). Those three fans are placed in front of the radiator.

Finally, the electric air heater, the **Stego HV 031**, Figure 3.24, is placed between the middle front fan and the radiator. The version used can be powered by up to $200W$, connected on the power grid ($230V$ AC). It should not be powered without any airflow through the radiator.

Figure 3.24 – Air heater **Stego HV 031** [26]

Model

The model, visible on Figure 3.25, is an evolved version of the cabin heater unit model : The air heater and the front fans have been added. The option of driving only the middle fan is also possible. As the purpose of the demonstrator is to decrease the overall energy consumption of the actuators, the instant power of the actuated fans can be monitored via the output $PwrFan$ of the air path subsystem Airpath_Radiator, detailed on Figure 3.26. The input signals are coloured in green and the outputs in red.

Inside Airpath_Radiator, three subdivisions have been made, corresponding each time to the solution of the air mass flow through one front fan (*Fan2000* block), the related part of the radiator and one actuated fan (*Fan3000* block). The submodel is on the Figure 3.27).

The Airpath_MiddleFan subsystem has additionally a *Flow Resistance* block for the pressure drop caused by the air heater placed in the way (Figure 3.28).

The pressure drop polynomials of the fans are added because they are placed in series with the radiator. In this model, the difference between a fan pushing or pulling the air has been neglected.

Coming back to Figure 3.26, the powers from the fans and the air mass flows from the subdivisions Airpath_SideFan(1+2) and Airpath_MiddleFan are added to give their global value.

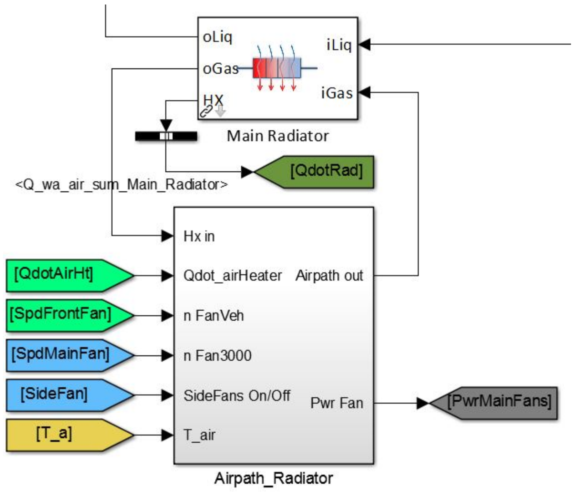

Figure 3.25 – Main radiator model [*Author's illustration*]

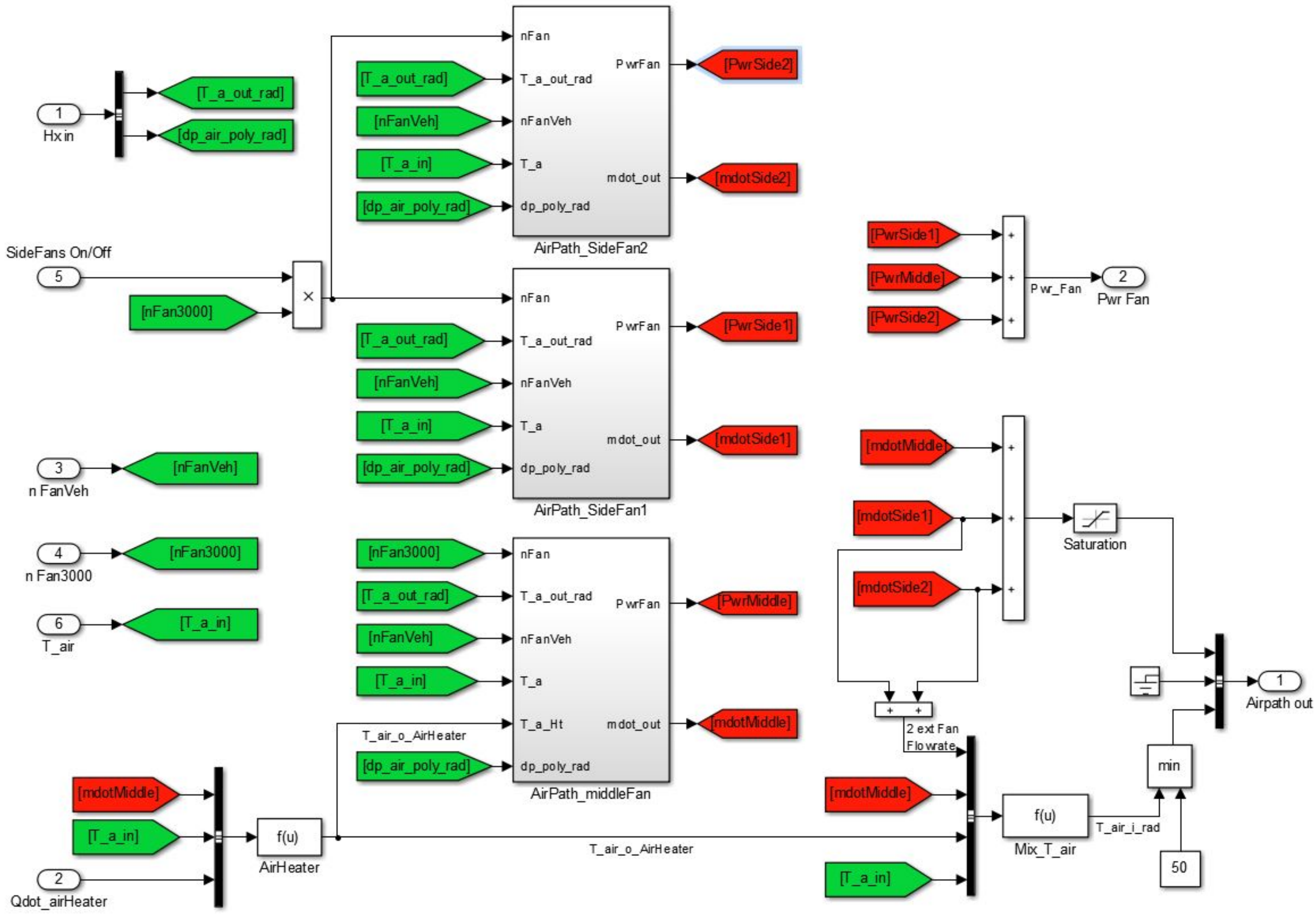

Figure 3.26 – Main radiator air path model : Airpath_Radiator [*Author's illustration*]

The temperature of the air flow *Airpath out* entering the radiator is a weighting of the ambient air temperature T_a_in and the air temperature after the air heater $T\_air\_o\_AirHeater$,

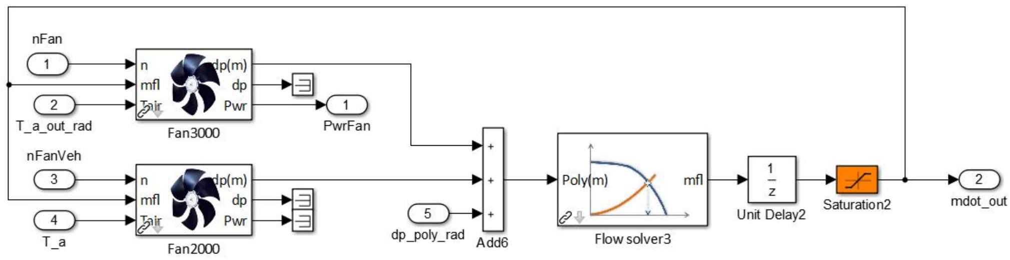

Figure 3.27 – Model of the air path on the side of the main radiator : Airpath_SideFan [*Author's illustration*]

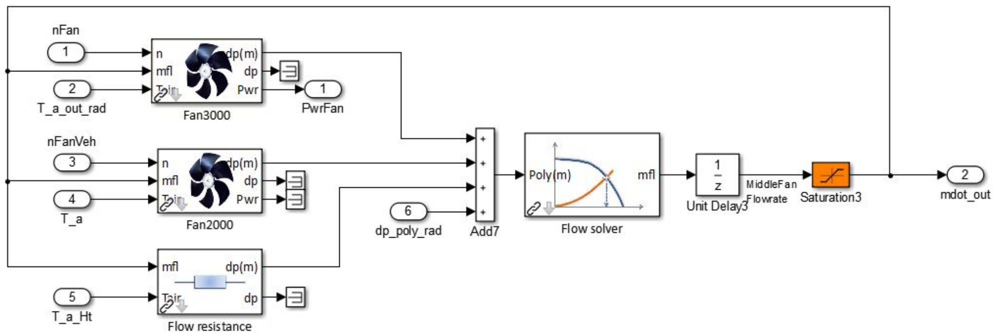

Figure 3.28 – Model of the air path in the middle of the main radiator : Airpath_MiddleFan [*Author's illustration*]

according to the air flow through each fan :

$$T_{air,o,AirHeater} = T_{air,in} + \frac{\dot{Q}_{AirHt}}{\dot{m}_{air,MiddleFan} * Cp_{air}}$$

$$T_{air,i,rad} = \frac{(\dot{m}_{air,SideFan1} + \dot{m}_{air,SideFan2}) * T_{air,in} + \dot{m}_{air,MiddleFan} * T_{air,o,AirHeater}}{\dot{m}_{air,SideFan1} + \dot{m}_{air,MiddleFan} + \dot{m}_{air,SideFan2}}$$

$(Cp_{air} = 1005J/kg.K)$

The upper limit of 50°C has been implemented for the stability of the model with very low air flow.

Finally, the validation of the airpath model with the fitted parameters for the *Fin Tube Heat Exchanger* block is visible on Figure 3.29.

3.5 Pump unit

The pump unit comprises the pump **Swiftech MCP35X** and its adapted reservoir, the **Swiftech MCP35X Reservoir**. The assembly is visible on Figure 3.30. The pump can rotates from 1300 to 4500RPM. Its curve, at various speeds, is represented on Figure 3.31

Model

The data from the pump has been fitted with a polynomial, which has then been introduced in the *Pump* and *Expansion Tank* blocks from TheLib (Figure 3.32), along with

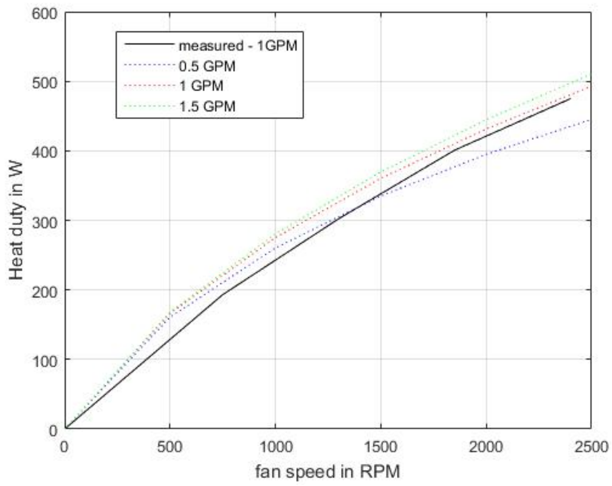

Figure 3.29 – Validation of the main radiator model [*Author's illustration*]

Figure 3.30 – Pump + reservoir assembly [27]

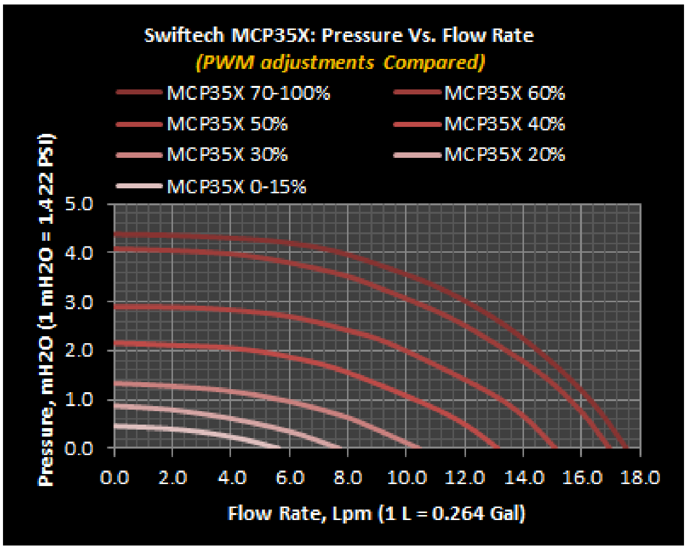

Figure 3.31 – Pump curve [27]

the dimensions of the reservoir and the pump impeller diameter.

The *Expansion Tank* block is just used for inertia in the system, but has not any other particular function. It can give the pressure, the air volume and the liquid volume inside it.

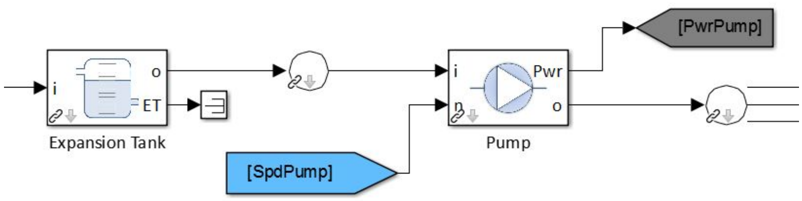

Figure 3.32 – Pump model [*Author's illustration*]

For the validation of the parameters, the Figure 3.33 shows the pump curve of the model at $4500RPM$

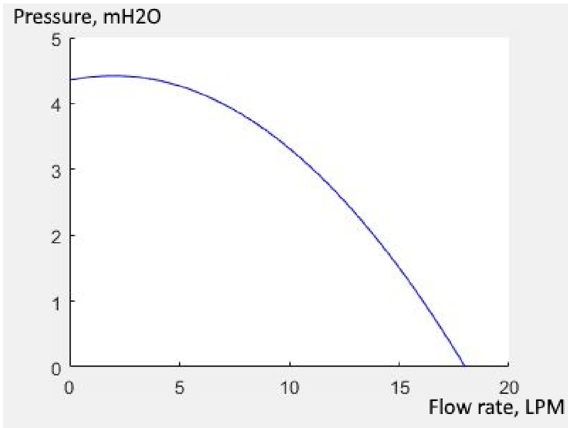

Figure 3.33 – Pump model curve at $4500RPM$ [*Author's illustration*]

3.6 Tubing

The tubes are transparent, in acrylic.

They appear in the model as *Flow resistance* blocks, which only impose a pressure drop to the flow. In this model, they are placed to only simulate the longest tubes of the hardware plant, the smallest ones are neglected. Their parameters are approximated in function of the bends and the length of the tubes, but it should be updated after some calibration tests, to fit the flow measured on the real device.

The flow meter is simulated the same way in the model. It is placed in the main heater branch to know the flow rate inside the device and to relate it to a control signal.

3.7 Secondary heater

The secondary heater hasn't been used on the real hardware. However, a *Heated Pipe* block from TheLib has been implemented at its expected place to be able to simulate it if it is one day inserted in the demonstrator (see Figure 3.34).

A shut-off valve (SOV Valve) is also necessary to cut the flow if the heater is not used. It is either open (if $sw >= 1$) or closed ($sw < 1$). A very high back pressure has been parametrized when it is closed to avoid an influence on the whole network.

The main difference of the *Heated Pipe* with the *Heat Bridge* is that the heat power input is directly transferred to the flow, without other heat transfer correlations.

Another component to add if a secondary heater is connected is an adjustable pressure drop component (*Flow resistance* block in the model) to avoid that a high flow rate goes into this branch. This could happen as the main heater branch, in parallel with the heater,

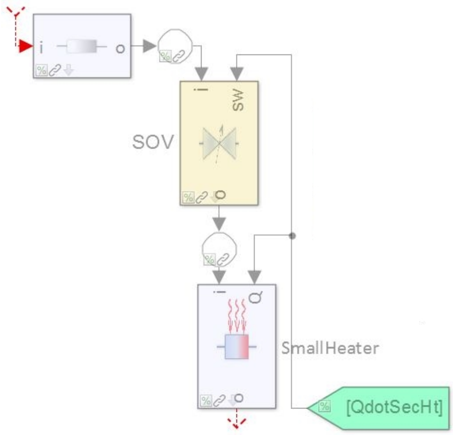

Figure 3.34 – Secondary heater model [*Author's illustration*]

has potentially a higher pressure drop characteristic than the secondary heater. A good behaviour would be a lower flow rate in the oil cooler branch than in the cold plate one.

3.8 Flow meter

The **ifm Efector SM6004**, visible on Figure 3.35, is a flow meter with a range between 0,1 to 25 LPM, with a response time inferior to 0,15s. It is also able to measure the temperature between -20 and 80°C, but with a response time of 20s. It is therefore not used for the actuation.

Figure 3.35 – Flow meter [28]

It can also display the measurements and be adjusted on a small screen.

Its pressure drop characteristic is shown on Figure 3.36.

It is placed downstream of the pump, and in order to obtain the most correct measurement, the flow meter needs have enough space before and after any disturbance source (like a bend or a component of the demonstrator).

3.9 Hardware plant

Some ordered components had not arrived when the internship finished : the bypass valve, the air heater, and the silicone heaters. The Figure 3.37 is a picture made at that time which shows the assembly of available components.

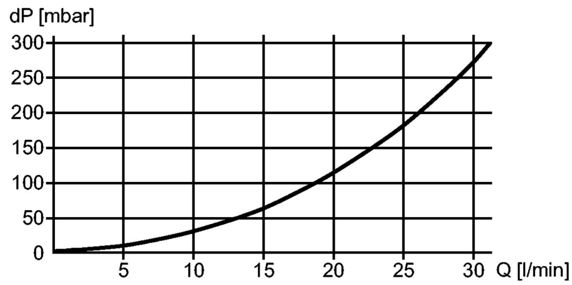

Figure 3.36 – Pressure drop characteristic of the flow meter [28]

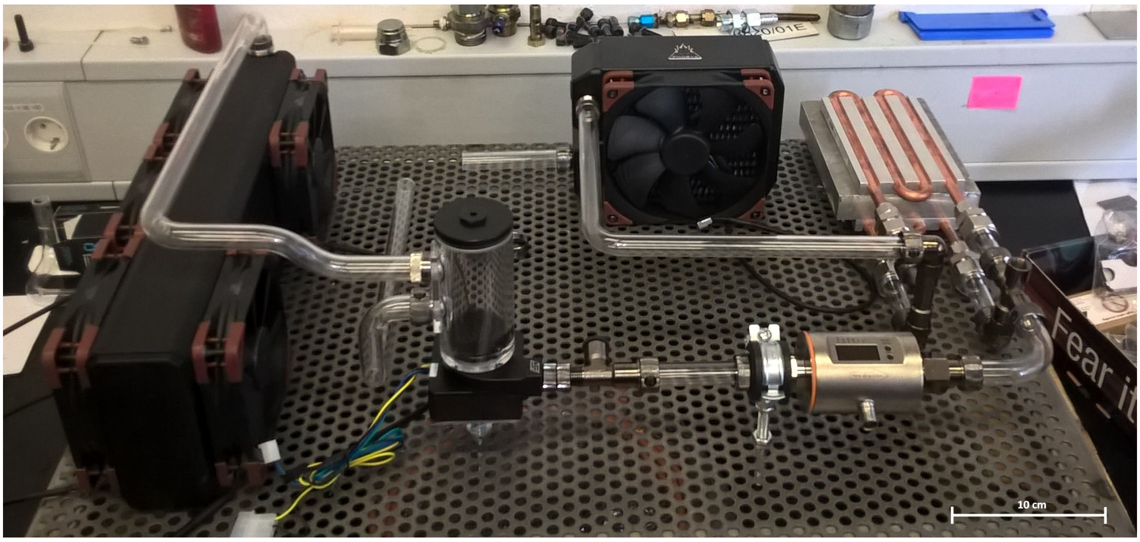

Figure 3.37 – Thermal management demonstrator [*Author's illustration*]

The support frame is a thin pierced Aluminium plate with 70 x 50cm dimensions, surrounded by 3 x 3cm frame, also in Aluminium.

The air is blown from the inner side to the outer side of the plate. The actuated fans are therefore on the left side of the radiator on the picture. The reason is a lesser effect of the convective heat transfer (not modelled in the simulation) between the airflow and the elements.

(The middle front fan is not assembled on the radiator, as the air heater, coming in between was not available.)

Finally, even if some components are missing, the overall performance can still be assessed for the demonstrator with the model. After having specified each of the elements, it shows that the point of equilibrium for a maximum pump speed (4500RPM), with the radiator branch open, is for a 32.830Pa pressure drop (=3,35mH_2O) and a flow rate of 0,163kg/s (9,78LPM - 2,58GPM). The temperature difference will be near of 10°C for a maximum heat input, with intermediate fan and pump speeds and no other input.

Chapter 4

Signals & control

This chapter describes all about the signals that drives the hardware and model plant. It explains the inputs, the basic control strategy put in place and develops also the electrical signals.

At the end of this chapter, the hardware plant becomes functional and autonomous.

The overview of the whole simulator is presented on Figure 4.1.

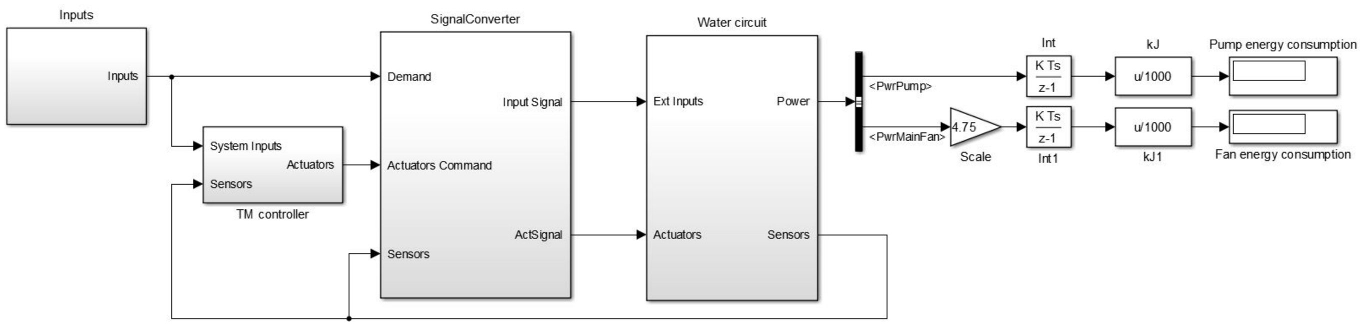

Figure 4.1 – Overall model of the Hil Simulator [*Author's illustration*]

The Water circuit subsystem has just been described in the chapter 3 about the Thermal plant.

The Inputs subsystem covers the external inputs and conditions desired to test the control strategy (non actuated signals).

Along with the '*Sensors*' signal from the plant, these '*Inputs*' are sent to the TM controller subsystem. The control strategy is defined at this place and it will determine, according to the inputs, the value of the signals for each actuators, to regulate the demonstrator.

The Signal converter subsystem converts then the signals from the inputs and the actuators to the signals readable by the simulator and the hardware plant. These ones depend on the characteristics of the specific components.

Finally, each power calculated in Water circuit is integrated over time to get the energy consumption, and the J unit are then transformed into kJ. In this way, the energy consumption over the full cycle can be monitored and compared between several control strategies.

The electric power absorbed by the fan has been scaled up to be more representative of real vehicles. In a standard car, the pump nominal power equals to $200W$ and the fan nominal power reaches $500W$ (approximately). For this demonstrator, this is respectively $18W$ and $3{*}3,16 = 9,48W$. To keep the same proportion, the power of the fan is multiplied by

$$\frac{500}{200} = \frac{x * 9,48}{18} \Rightarrow x = \frac{18 * 500}{9,48 * 200} = 4,7468 \approx 4,75$$

To pass from the model to the real hardware plant, the Inputs TM controller, and Signal converter are kept to drive the demonstrator, and the Water circuit model is switched with the hardware device. More information is given in the following section 4.5.

4.1 Hardware signals

The electrical components need to be driven with specific signals to be controlled adequately. For this purpose, the Arduino board is the most adapted microcontroller. For the demonstrator, a Arduino MEGA 2560, represented on Figure 4.2, has been used. This microcontroller platform will take the role of the "brain" of the demonstrator, as it can't give more than $20mA$ for a $5V$ pin, but can generate complex electrical signals. What is called the "muscles" is simply the supply voltage that powers the assembly (delivered through a converter for example). A great advantage of this particular device is the vast documentation available over the internet, on various control topics and projects. Moreover, *Shields* are little add-ons that can enhance the board in numerous ways (bringing WiFi communications for example).

Figure 4.2 – Arduino MEGA 2560 [29]

The rest of this section talks about the electrical signals needed to drive the electrical elements of the demonstrator. The commands are initially sent from the MEGA 2560, but can be filtered and adapted through passive or active components before arriving to destination.

4.1.1 Power supply

The electrical components need first a supply voltage.

The power for the heaters, will be provided from the power grid.

The pump, the fans and the microcontroller, are supplied by an external $12V$ voltage. Those $12V$ are generated by a **DIN rail power supply**, visible on Figure 4.3. These are converters, transforming the $230V$ AC input into $12V$ DC output, with a maximum of 4,5A ($54W$). It as an built-in fuse in case of short circuit to protect the components downstream.

The maximum supply power is well above the total power of the low voltage components (which sums up at $35W$ for the $12V$ elements and $14W$ for the $24V$ elements).

Figure 4.3 – DIN rail power supply used for the demonstrator [30]

The stepper motor for the bypass valve and the flow meter need a $24V$ DC supply. 2 DIN rail power supplies of $12V$ are put in series to reach this voltage.

4.1.2 Pump and fans

Most fans and pumps used in computers (water cooled or not), have a supply voltage of 12V DC (direct current). Two possible ways of controlling their speed exist :

— **Voltage control** : the actuators have a connector of 3 pins : one pin is linked to the ground, one to supply voltage and one is allocated for the tachometer. This tachometer sends a square signal of 5V with a frequency equals to twice the frequency of the fan. This signal is thus a sensor for the fan speed.
The fan (or the pump) is defined by its nominal speed N_n at its nominal supply voltage $V_n = 12V$. If the supply voltage V progressively decreases, the rotating speed does the same. In this way, a characteristic curve can be drawn. To each voltage corresponds a rotating speed (Figure 4.5). When the supply voltage becomes too low (around $5V$ for example), the fan goes abruptly from a threshold minimum speed to zero. Starting from 0V and 0RPM, the speed stays at 0 if the voltage increases up to the threshold voltage, and then the fan starts suddenly at minimum speed. This behaviour is represented on Figure 4.4

— **PWM Control** : An extra pin is added on top of the three other ones. This pin receives a Pulse Width Modulation (PWM) signal, governing the fan rotational speed, while the supply voltage pin is maintained at 12 V. The PWM signal is rapidly switched on (*e.g.* to 5V) and off (0V) to create a square wave. It can be modulated by changing the duty-cycle : the proportion of time the signal spends

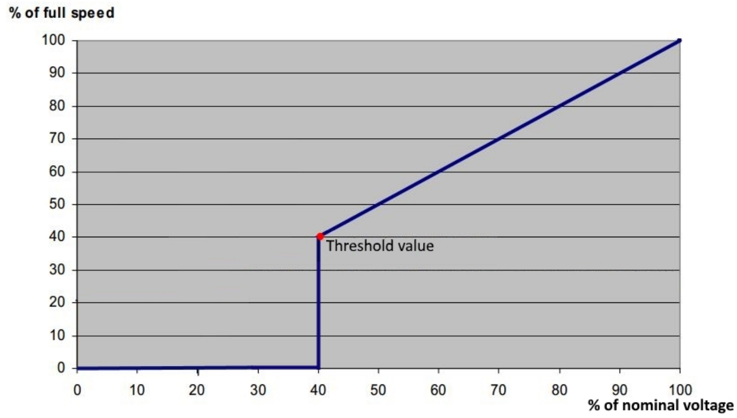

Figure 4.4 – Example of a fan PWM relation with voltage control [*Author's illustration*]

on. It is illustrated on Figure 4.5. The higher the duty-cycle, the higher the mean value of the signal voltage and the faster the fan rotation. For computer fans, the frequency of the PWM cycle is fixed on 25 kHz, with an acceptable range between 21 and 28 kHz.

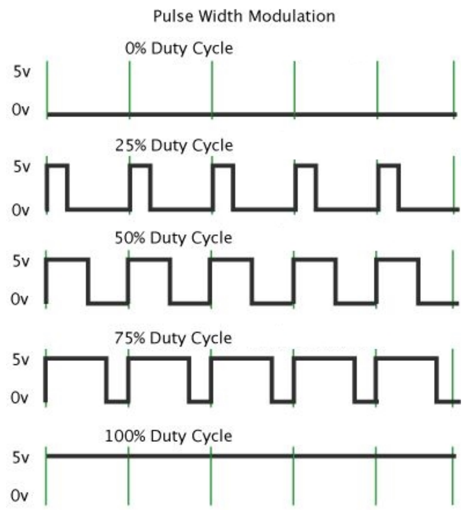

Figure 4.5 – Different PWM duty-cycles [29]

The relation between duty-cycle and percentage of nominal speed is similar to the characteristic curve of the fan voltage control. The minimum speed and duty-cycle has however to be lower than 30% of the nominal value, imposed by the processor manufacturer. Below this minimal value, most of the fans will have a constant minimal speed (even with a 0% duty-cycle), as shown in Figure 4.6.

The PWM signal from the Arduino is linked to the ground via a $10kOhm$ pull-down resistor, as represented on Figure 4.7. This allows to maintain the PWM voltage to its desired value (5 or $0V$). Otherwise, any disturbance can affect the wire and the logic level is therefore undetermined.

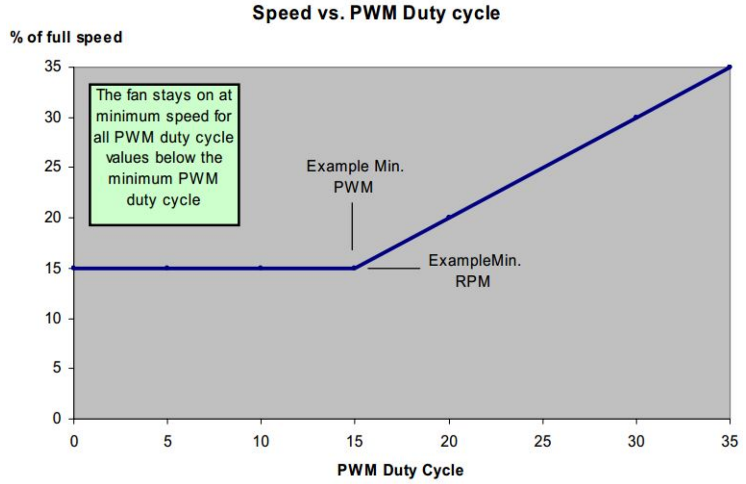

Figure 4.6 – Minimal PWM duty-cycle behaviour for most of the computer fans [31]

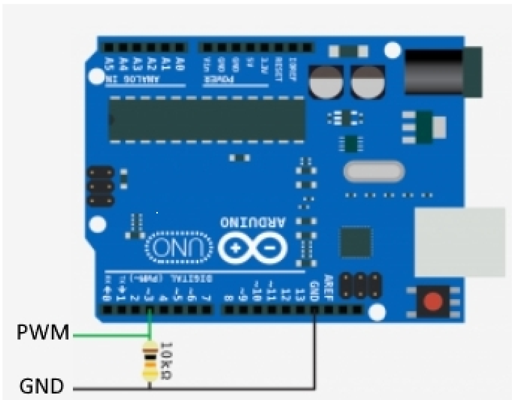

Figure 4.7 – Arduino circuit for PWM control [32]

Note : The picture of the similar Arduino UNO is a representation, but this is well the MEGA 2560 that is employed in the final system.

The fans and pump of the demonstrator are all driven by the PWM signal of $5V$. As those elements have a non zero rotational speed for a 0% duty cycle (refering to Figure 4.6), they also need the adding of a MOSFET between the controller (MEGA 2560) and their supply voltage to switch it off if the command imposes it. The configuration is shown on Figure 4.8. The N-Channel MOSFET used in the actual device is the **FQP30N06**, with the same function.

The binary signal ON (1 / $5V$) or OFF (0 / $0V$) is sent in this example from the pin 3 of the Arduino board. The resistor is also a pull down resistor.

The diode in parallel of the motor is used to protect the Arduino and the MOSFET from peak reverse voltage, happening when the motor is switched off. This voltage, up to several hundred volts, could destroy those elements. The diode allows that voltage burst to flow back to the coil.

When the signal from the pin (*e.g.* 3), connected to gate G, is ON, then the MOSFET allows0 the current to flow between drain D and the source S. If the voltage of G is $0V$, then the current is stopped and the device doesn't work.

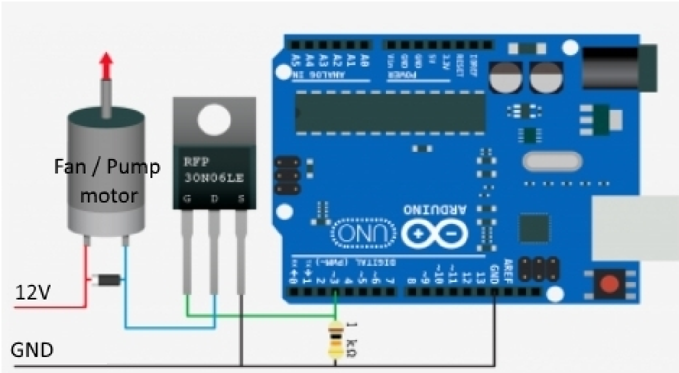

Figure 4.8 – MOSFET circuit for On/Off control [32]

A mean of measuring the electrical consumption of these actuators should be integrated in future works. A temporary solution is a light bulb in series with the power supply. It gives a qualitative measurement and would be sufficient to achieve the exhibition purpose. Including a shunt resistor in series to measure the (small) voltage drop and link it to the power consumption of the main device is the best solution.

4.1.3 Stepper motor

The bypass valve is controlled by powering a bipolar stepper motor of $24V$.

A stepper motor is a DC motor that moves in discrete steps increments. The rotation, one step at a time, is produced by energizing multiple coils (regrouped in different phases) with the proper sequence of input pulses. The steps allow a precise positioning, while the speed of the motor is controlled by the frequency of the input pulses.

Bipolar motors refer to the winding disposition. Those coils are always energized, once positively, once negatively, in opposite to the unipolar windings which alternate between a winding supply voltage switched on and off.

The sequence to drive the stepper motor of the bypass valve is represented on Figure 4.9.

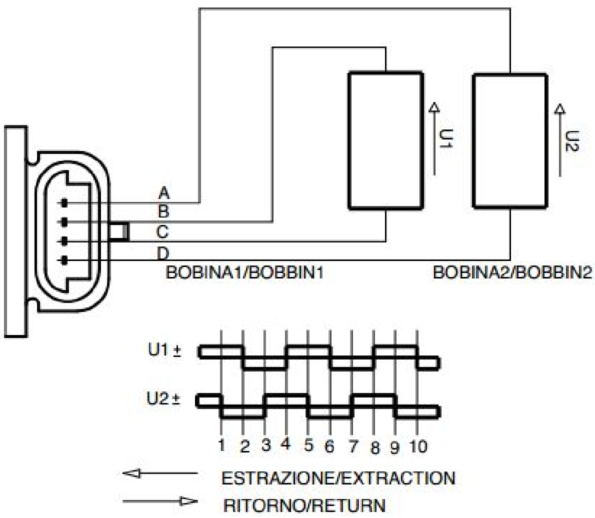

Figure 4.9 – Pulse sequence of the valve bipolar stepper motor [33]

The shield **VMA03** from Velleman (Figure 4.10) can be added on top of the Arduino board to create this pulse sequence, with an external supply voltage of $24V$ DC, and controlled via the 4 selected pins of the microcontroller board. An illustration is given on Figure 4.11.

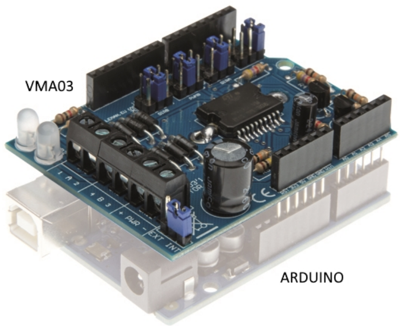

Figure 4.10 – VMA03 shield on top of a Arduino UNO [34]

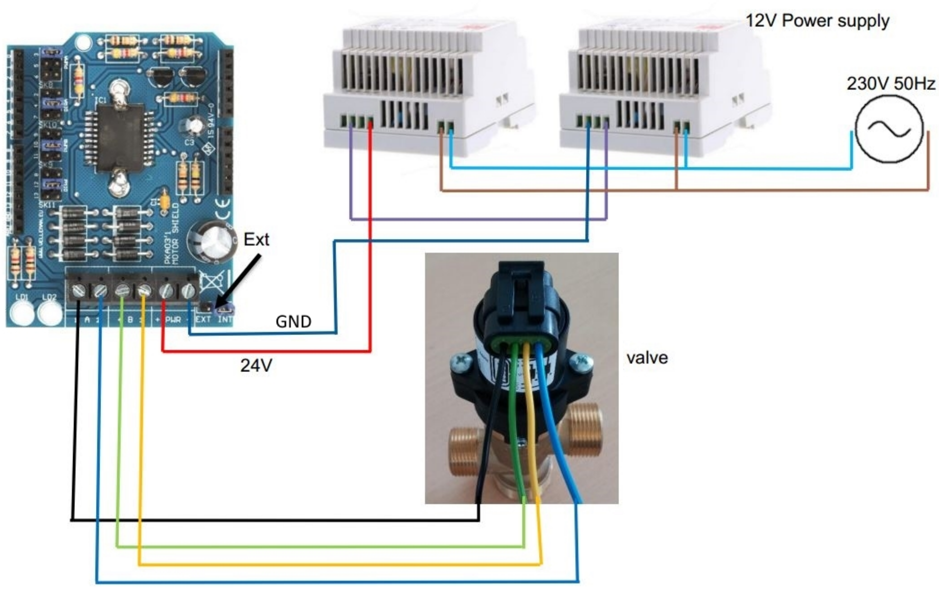

Figure 4.11 – Diagram to power the VMA03 shield and the bypass valve [*Courtesy of Dominik Gößler*]

4.1.4 Triacs

The silicone heaters dissipate heat based on the Joule effect, and can't modify their power by themselves, as it depends on the built-in resistor. To vary this heat input in the system, a Triac is inserted between the heating device and its supply voltage.

The principle is to switch rapidly the incoming $230V$ AC to lower the RMS (root mean square) voltage felt by the heater. The RMS voltage is the DC voltage that would be necessary to apply to the heater to produce the same power (as the heater is only a resistive load). It is similar to a mean value, like the PWM control, but with the difficulty of the AC current.

The phase control used here is described via the Figure 4.12. It receives the $230V$ AC from the power grid and switch it off when the $0V$ is crossed. After a specific delay (t_1), it is switched on again by an adapted signal from the controller. This way of functioning decreases the RMS voltage, which depends on the time delay t_1.

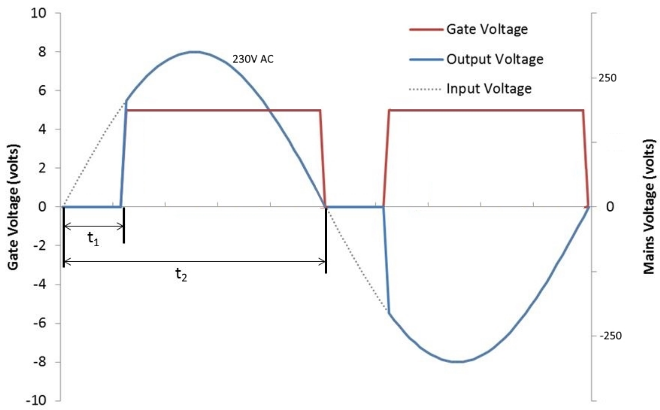

Figure 4.12 – Triac input/output signals [29]

The Triac is switched via an optocoupler, allowing a galvanic insulation between both circuits, to keep away the elevated voltage away from the low voltage of the Arduino. It is enabled when there is a high logic level on the control pin, and disabled when there is a low logic level on the pin.

Therefore, a zero cross detector is needed. As its name indicates, it detects when the AC voltage crosses $0V$. Then, it sends a short signal to the Arduino, that resets the time delay t_1 and wait the proper moment before triggering the Triac.

About the specific hardware, the **Triac Nanoshield** and the **Zero Cross Nanoshield** from Circuitar Eletrônicos are used. Figure 4.13 is an illustration of their electrical connexions.

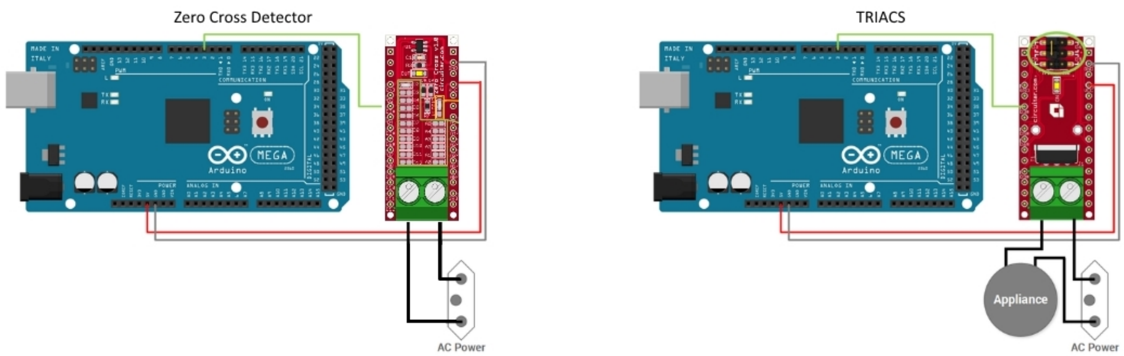

Figure 4.13 – **Zero Cross** and **Triac Nanoshields** [35]

4.1.5 Sensors

The Arduino analogue input is a 10-bit analog to digital converter. This means that the input voltage between 0 and $5V$ will be assigned to a proportional value between 0 and 1023. The resolution is therefore $5/1024 = 0.0049V$.

Flow meter

The flow meter is powered by $24V$ DC and has an analogue current output I between 4 and $20mA$, scalable to the water flow rate range that should be measured. To transform this current into a voltage readable by the Arduino board, a resistor of $R = 217,7\Omega$ is put in parallel of the pin, represented on Figure 4.14.

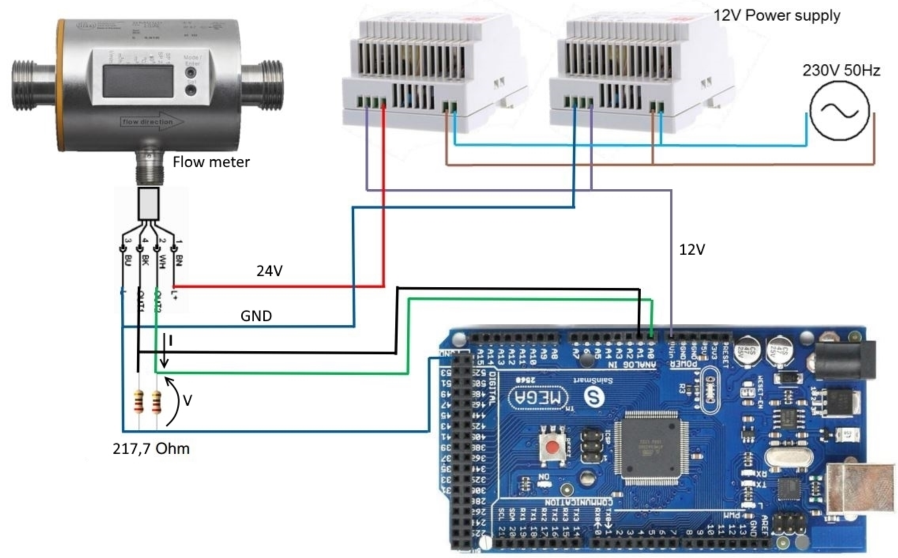

Figure 4.14 – Flow meter connexions [*Courtesy of Dominik Gößler*]

The flow meter is set up for $4mA = 0LPM$ and $20mA = 12LPM$. Indeed, a maximum flow rate of $12LPM$ seems to be an appropriate value due to the test of page 46, which predicted a maximum flow rate of 9,78LPM. A safe margin is applied for some possible variations compared to the model. However, if the maximum flow rate is not as expected, this limit can still be modified.

The voltage V at the extremities of the resistor for a current I from the flow meter will be :

$$V = R * I = 217,7I$$

The Arduino impedance is supposed infinite (this is actually a $100M\Omega$ resistor)

For a $12LPM$ flow, the voltage at the pin will equals $0,02 * 217,7 = 4,354V$, and a $0LPM$ flow will be seen by as $0,004 * 217,7 = 0,8708V$. This gives a resolution of :

$$\frac{12 * 5}{(0,02 - 0.004) * 217,7} * \frac{1}{1024} = \frac{17,2255}{1024} = 0.0168LPM$$

(with $\frac{12}{0.0168} = 712$ steps)

The flow meter can also measure the temperature and sends the information via another wire to the Arduino.

Temperature sensor

The temperature sensors are thermocouples of type J. The thermocouple functions with the voltage production related to the temperature at the junction between two different conductors (made of Iron and Constantan for the type J) : this is the Seebeck effect.

The thermocouples are protected by a metal tube (with high thermal conductivity) to be inserted in a water flow. The sensors have been chosen with a small diameter tube (3,18mm) to have a fast response time to temperature change. It is visible on Figure 4.15. Its has a temperature range between -60°C to 350°C.

The temperature sensors are inserted inside specific threaded fittings to be incorporated into the system (see Figure 4.16).

Figure 4.15 – Thermocouple (type J) [30]

Figure 4.16 – Thermocouple fitting [30]

The sensors are then connected to the analogue temperature transducer **LKM 211** (see Figure 4.17) to convert the specific voltage from the thermocouple into a proportional analogue current output of 4..20mA. Its supply voltage is also 24V DC.

Its connection to the Arduino is similar to the flow meter (without connecting the ground directly), with the diagram visible on Figure 4.18.

Figure 4.17 – Analogue temperature transducer **LKM 211** [30]

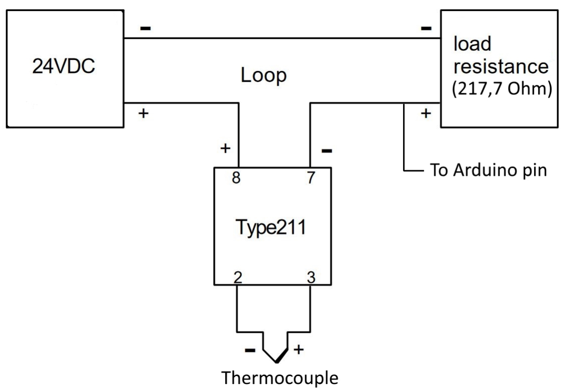

Figure 4.18 – Transducer connexions [36]

4.2 External inputs

The external inputs can either be chosen by the user or, for some of them, generated automatically, *e.g.* the heat input and the front fan speed can respectively assume the role of an engine heat dissipation and the vehicle speed occurring during a driving cycle.

Note : The values and parameters presented in this section are just used as a guide and can be changed later by the user of the demonstrator.

The *QuasiStatic Simulation Toolbox* (QSS TB), developed by the ETH Zürich, is an open source Simulink library used to easily reproduce any driving cycle from Europe, Japan or the USA. This driving cycle is applied on any vehicle and the corresponding engine, predefined by several parameters. The QSS TB blocks used in the model are visible on Figure 4.19.

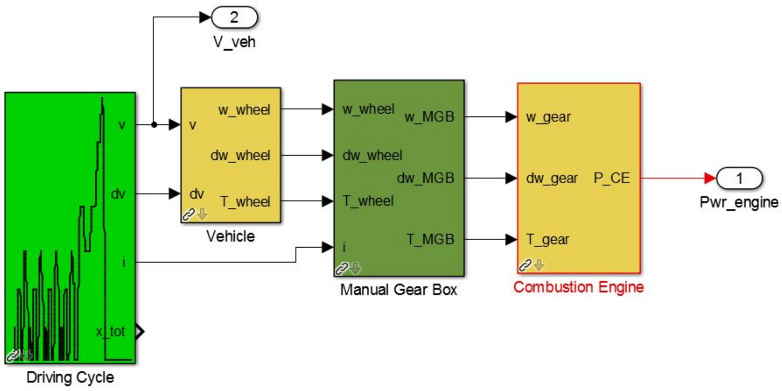

Figure 4.19 – QSS TB blocks, creating the inputs related to a driving cycle : Driving cycle subsystem [*Author's illustration*]

Firstly, a driving cycle is chosen, which determines the speed v of the vehicle, its acceleration dv, the gear number i and the distance travelled x_tot. For the demonstrator, the NEDC (New European Driving Cycle) has been chosen as the reference. The speed of the wheel, its acceleration and the torque is then calculated inside the *Vehicle* block. The parameters of a typical car of $750kg$ are inserted. The *Manual Gear Box* block gives the speed, acceleration and torque of the flywheel, and the *Engine* block transforms those signals into total power delivered by the engine (which could be linked afterwards to the fuel consumption).

The interested reader can refer to "The QSS Toolbox Manual" [37] for more information.

The vehicle speed V_veh and the power output of the engine Pwr_engine are converted (rescaled) to give the adequate input signal for the demonstrator, along with the other external inputs, Figure 4.20.

As Pwr_engine is the engine power, in W, one third is transferred to the coolant (ref. 3). As the maximum power over the cycle is still near $20kW$, the signal value is divided by 40 to get a maximum of $500W$ to the silicone heaters (signal $= QdotMainHt$).

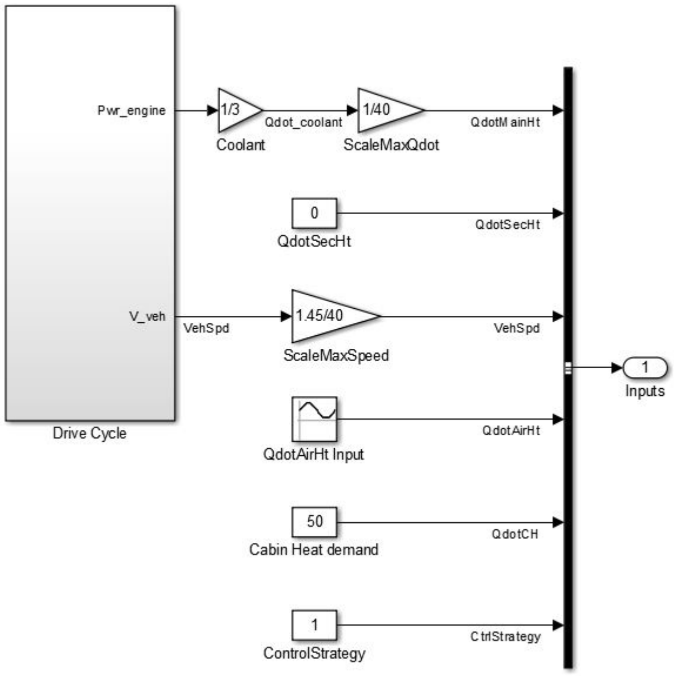

Figure 4.20 – Inputs of the demonstrator : Inputs subsystem [*Author's illustration*]

As the secondary heat source is not installed, its input $QdotSecHt$ is equal to 0.

In a real scenario, the air speed coming from the front of the vehicle (signal $= VehSpd$ for the demonstrator, in m/s) is equal to the speed of the vehicle. Thus, the same reasoning that for the engine power is applied here. The scaling factor is equal the maximum air speed given by the fan (1,45m/s according to [38]) over the maximum vehicle speed (140$km/h \approx$ 40m/s).

In this case, a sinusoidal signal is affected to the power input from the air heater $QdotAirHt$. The maximum power allowed is 200W.
As a reminder, the air heater takes the place of the other radiators, namely the condenser of the air conditioning, the charge air cooler and eventually the low temperature radiator in case of an hybrid electric vehicle.

The heat power demanded from the cabin heater radiator is equal to 50W in this example.

Finally, it is also possible to choose the control strategy (*CtrlStrategy* signal). Each different control strategy is numbered. The adequate number needs to be entered in the small box to switch to this particular control. More information is given in the next section 4.3 about the thermal management controller.

In the future, a possibility is to insert a CAN shield for the Arduino. $QdotMainHt$, $VehSpd$, $QdotAirHt$ and $QdotSecHt$ could then be provided, generated by a small test rig or another simulator and sent through a CAN bus for example. (A CAN bus, for Controller Area Network, is a standard vehicle bus protocol)

Moreover, a small user interface could also be implemented to choose the control strategy, the temperature in the cabin for the heating, and/or the other inputs if not delivered by a CAN bus. Eventually, a smartphone App' (such as Blynk) can be envisaged, with a WiFi shield linked to the MEGA 2560.

This would allow to avoid predefined inputs and more flexibility for the presentation purpose.

4.3 Thermal management controller

This section develops the different thermal management controller signals and control strategies to drive the actuators accordingly. The corresponding Simulink model is represented on Figure 4.21.

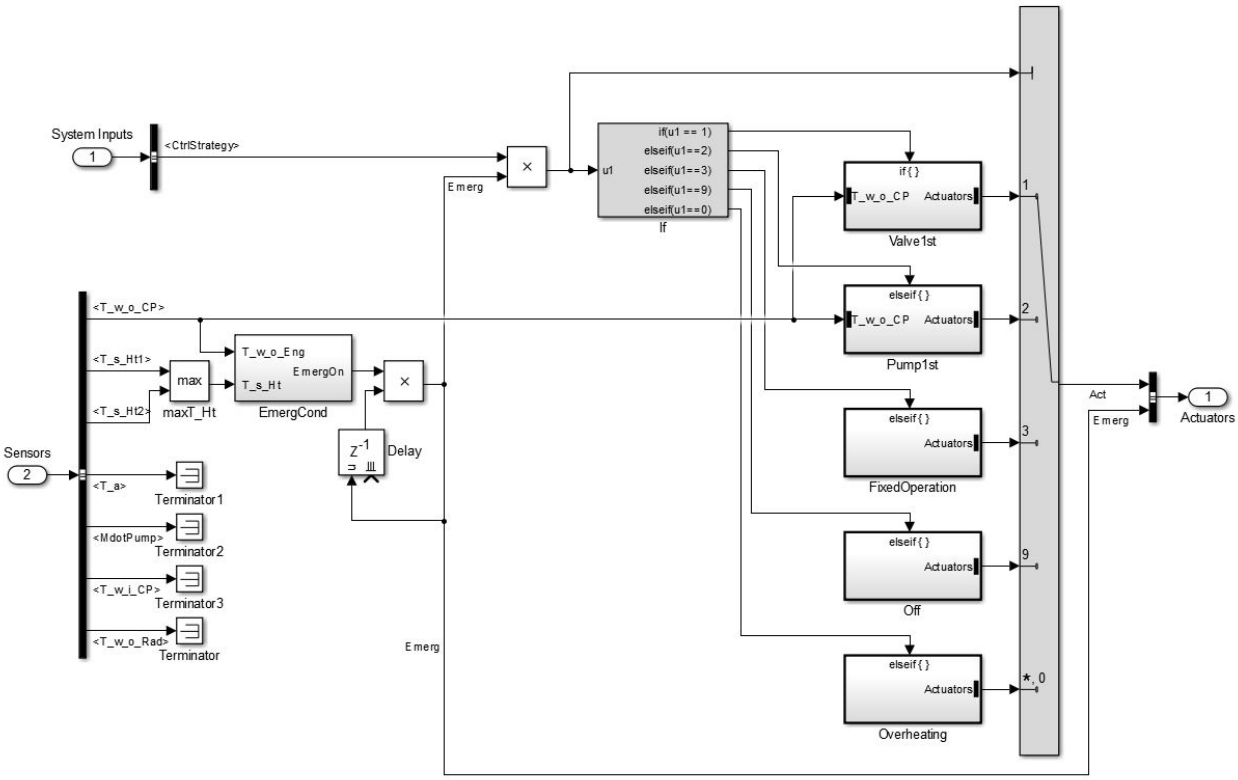

Figure 4.21 – TM Controller subsystem [*Author's illustration*]

The control strategy is chosen in the Inputs. The number given determines which strategy to use, through a selector. They are described in the rest of this section.

The 'Sensors' signal in input of the subsystem is decomposed in each of its variables. Each one (given in the section 3) can be used for a specific control strategy.

In output, the 'Actuators' signal includes :
- the bypass valve opening $ValveOpen$
- the pump PWM duty cycle $PwmPmp$

— the actuated fan PWM duty-cycle $PwmFanRad$
— the signal $SideFansOn$ to switch on or off the actuated fans on the side of the main radiator (mentioned on page 29)
— $Emerg$ is an emergency flag which shut down all the external inputs. This function is detailed in at the end of the current section.

All these signals have a range between 0 and 1 (for 0 and 100%)

Note : In this section, when 'fan speed' is employed, it means the rotational speed of the actuated fans, if not specified otherwise.

The goal of the thesis and the internship were focused on the development of the demonstrator. Therefore, only basic control has been implemented. For now, the water temperature at the main heating unit outlet $T\_w\_o\_CP$ is the single controlled variable for this demonstrator, but new strategies can be developed and coded in Simulink in the future to be tested. For example, several complementary strategies, defining the best set of actuator signals in a given situation, could be put in parallel. Then a selection program would determine which one is the most adapted to the situation. Other non exhaustive possibilities include a model-based control or a model predictive control approach.

4.3.1 Valve1st

The control strategy Valve1 is a mix between linear and On/Off control, depicted in the state of the art. Each actuator is controlled separately, as represented on Figure 4.22.

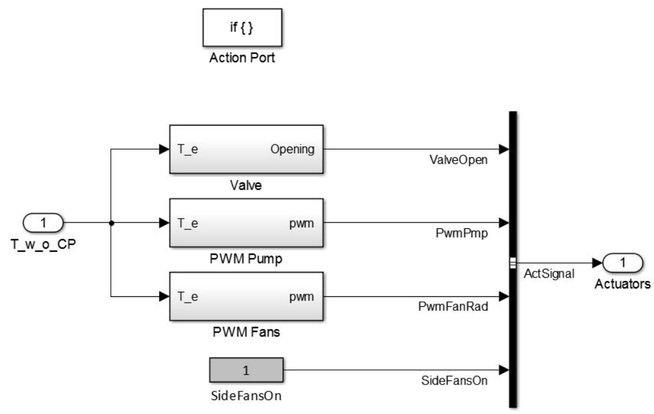

Figure 4.22 – Control strategy subsystem : Valve1st [*Author's illustration*]

The strategy consists in opening the valve linearly between two water temperatures (at the heater outlet) $T\_w\_o\_CP$, with an hysteresis, like on Figure 4.23.

If the temperature increases, the valve is fully closed at $23°C$ and fully open at $25°C$ ($\Delta T_{BP} = 2°C$). A deadband width of $1°C$ is applied, so when the temperature $T\_w\_o\_CP$ decreases, the closing is situated between 24 and $22°C$. If the variation of $T\_w\_o\_CP$ inverts its direction while the valve is not at its boundary, the valve stays at its last position until $T\_w\_o\_CP$ has changed of a value superior or equal to the deadband width $DB_{BP} = 1°C$.

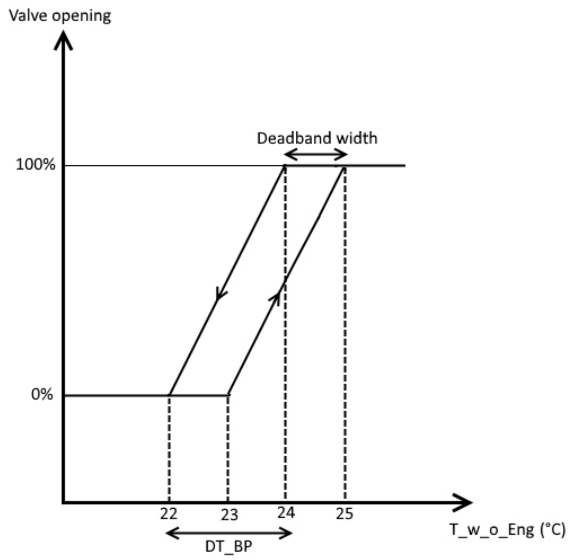

Figure 4.23 – Opening curve of the bypass valve (for Valve1st control) [*Author's illustration*]

The corresponding model is the Figure 4.24. The *Backlash* block allows the deadband behaviour. The falling (-) and rising (+) functions ($FallingFCn$ and $RisingFcn$) are defined with the relation ($T_e = T\_w\_o\_CP$; and in Simulink, u is the standard input vector of a function.) :

$$ValveOpen = \frac{T_e - (22,5 \pm \frac{DB_{BP}}{2})}{\Delta T_{BP}}$$

It is activated with a rising of falling edge of the temperature $T\_w\_o\_CP$ (through the *Backlash*). The delay acts like a memory and give the previous value of opening if the $T\_w\_o\_CP$ (filtered by the *Backlash*) hasn't changed. Finally, the *Saturation* block restricts the valve output between 0 and 1. The test of the control model for a determined sequence of input temperatures in the adequate range is shown on Figure 4.25, to check that the behaviour is as expected.

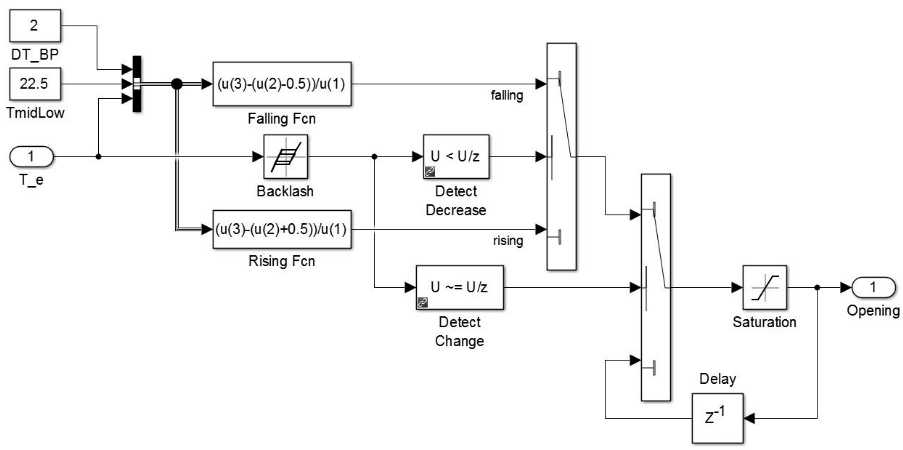

Figure 4.24 – Valve control model (inside Valve1st) [*Author's illustration*]

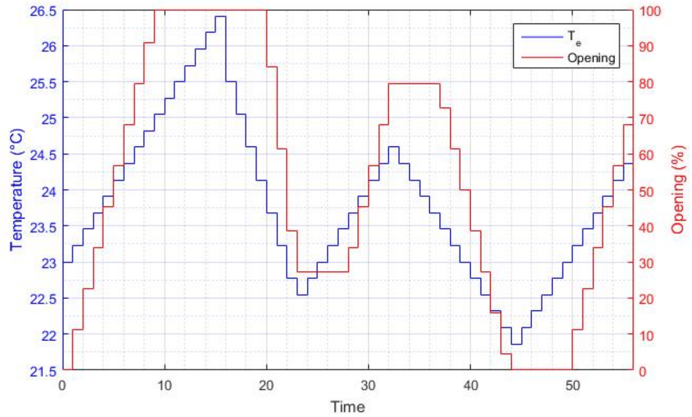

Figure 4.25 – Validation of the Valve control model (inside Valve1st) [*Author's illustration*]

When the valve is fully open and $T\_w\_o\_CP$ is still increasing, the pump starts to turn faster, by stages, and also with an hysteresis. The thresholds are at 27°C and 29°C when $T\_w\_o\_CP$ is going up, and 28°C and 26°C when going down. Around the lower level (26-27°C) the pump speed oscillates between 1300 and 2750RPM (15 and 40% PWM duty cycle). For the upper level (28/29°C), the pump speed goes up to full speed (4500RPM / 100% PWM). This behaviour is represented on Figure 4.26.

The lower limit is set to 1300RPM to ensure that the water is always flowing.

The hysteresis is necessary as changing abruptly the pump speed can decrease $T\_w\_o\_CP$. The controller would then go back suddenly to lower pump speed and the system would oscillates rapidly. An hysteresis of 1°C allows to have a more stable control.

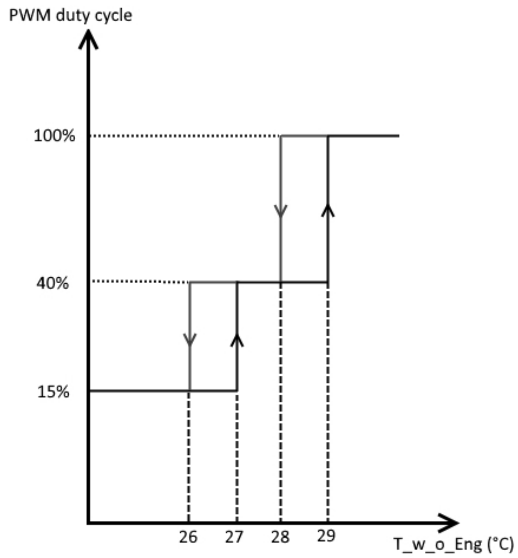

Figure 4.26 – Pump speed stages (for Valve1st control) [*Author's illustration*]

The corresponding model is the Figure 4.27. The *Relay* block *med* (resp. *high*) switches ON if $T\_w\_o\_CP > 27$ (resp. 29) and OFF if $T\_w\_o\_CP < 26$ (resp. 28). The on/off state is not affected by input between the upper and lower limits. The validation of this model is on Figure 4.28.

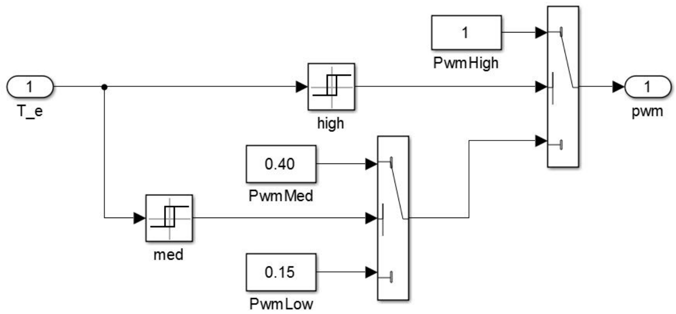

Figure 4.27 – PWM Pump control model (inside Valve1st) [*Author's illustration*]

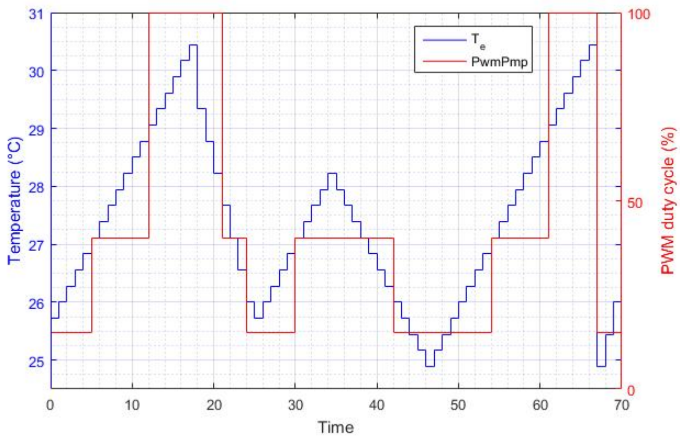

Figure 4.28 – Validation of the PWM Pump control model (inside Valve1st) [*Author's illustration*]

About the fan, it starts at low speed when the valve begins to open (with the same *Relay* block between 22 and $23°C$) to ensure a minimum air flow through the radiator, for an effective heat transfer with the ambiance.

Later, if the temperature is still increasing after the pump is at full speed, the main fans go gradually faster. It has the same base of control that the pump. The distinct stages are visible on Figure 4.29.

And the corresponding model is visible on Figure 4.30, with the control of the right comportment (Figure 4.31). The logic is the same that with the pump control model.

This control strategy has been motivated by the conclusion of [39], and reasserted in [10], that an efficient control to decrease the energy consumption of the actuators is : to adjust in the first place the valve, then to increase the pump speed, and finally to boost the heat rejection with the fan speed.

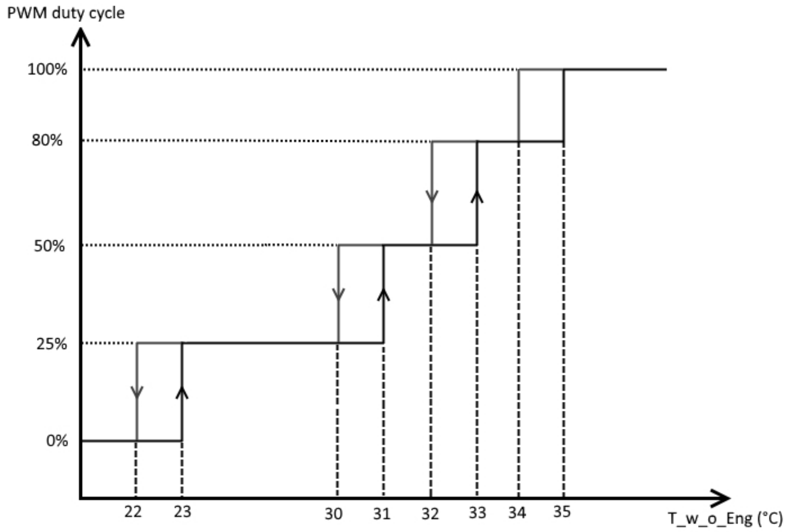

Figure 4.29 – Fan speed stages (for Valve1st control) [*Author's illustration*]

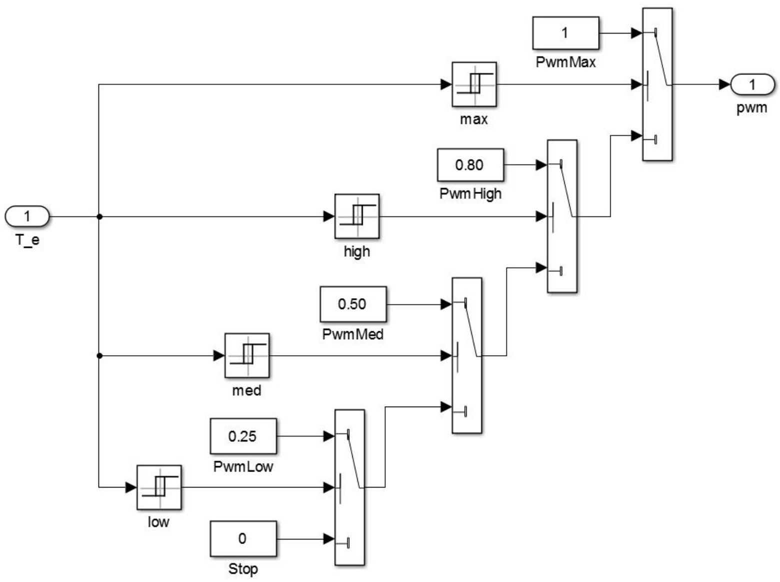

Figure 4.30 – PWM Fans control model (inside Valve1st) [*Author's illustration*]

4.3.2 Pump1st

The second control strategy is based on a standard thermal management control in vehicles, which tries to limit the temperature difference across the engine. To achieve this, this is the pump speed which is increased in the first place, followed by the opening of the valve and lastly the actuation of the fan. So, the valve control and the pump one are inverted compared to the Valve1st strategy (in relation to $T\_w\_o\_CP$).

The parametrized temperature stages are visible on Figure 4.32, 4.33 and 4.34.

Except for the values of the parameters, it is the same model that in the Valve1st subsystem and it is therefore not displayed.

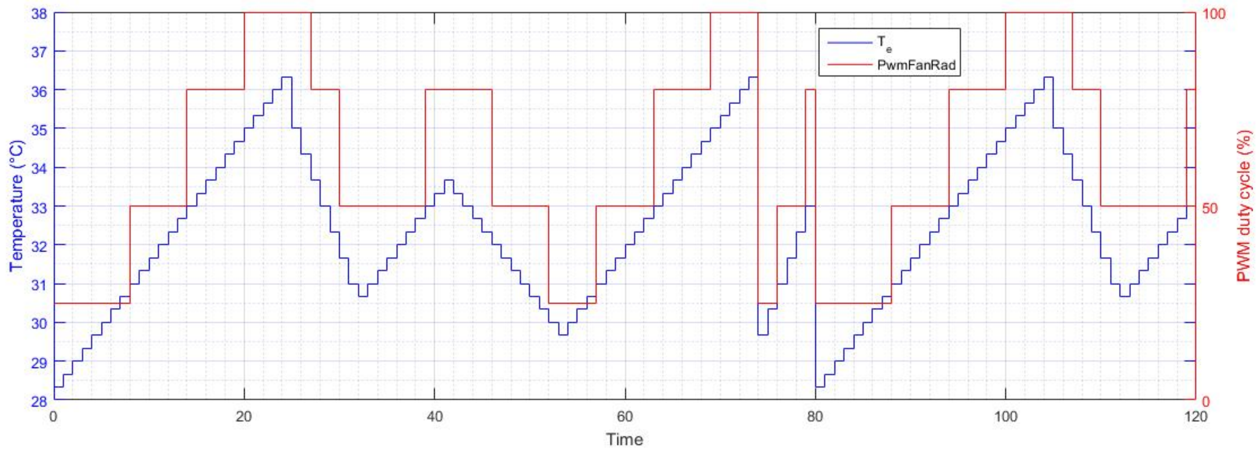

Figure 4.31 – Validation of the PWM Fans control model (inside Valve1st) [*Author's illustration*]

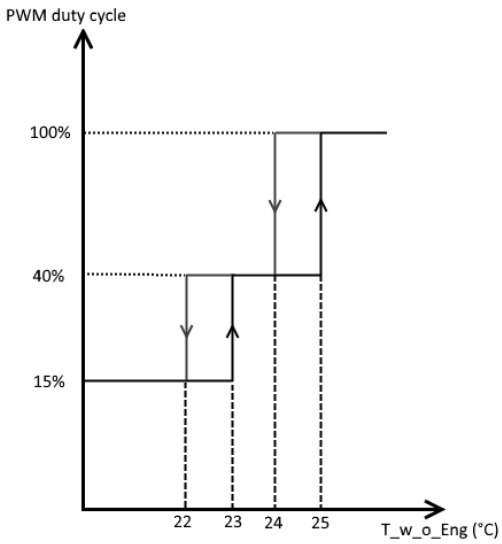

Figure 4.32 – Pump speed stages (for Pump1st control) [*Author's illustration*]

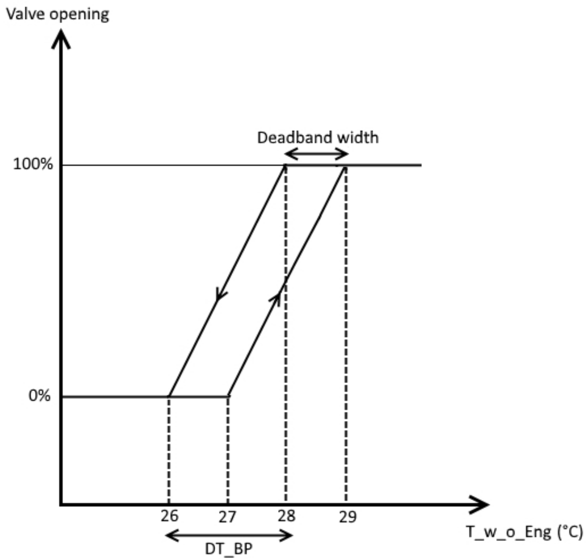

Figure 4.33 – Opening curve of the bypass valve (for Pump1st control) [*Author's illustration*]

A remark can be added for the elevation of the starting of the fan. Indeed, the radiator branch is closed until the valve begins to open, and the condition is not met before $27°C$. If there isn't any flow in the radiator, this is not necessary to turn on the fan, which consumes energy.

4.3.3 FixedOperation

This system is not really a control strategy, but applied to determine easily the equilibrium state of a fixed operating point. Here is an example on Figure 4.35.

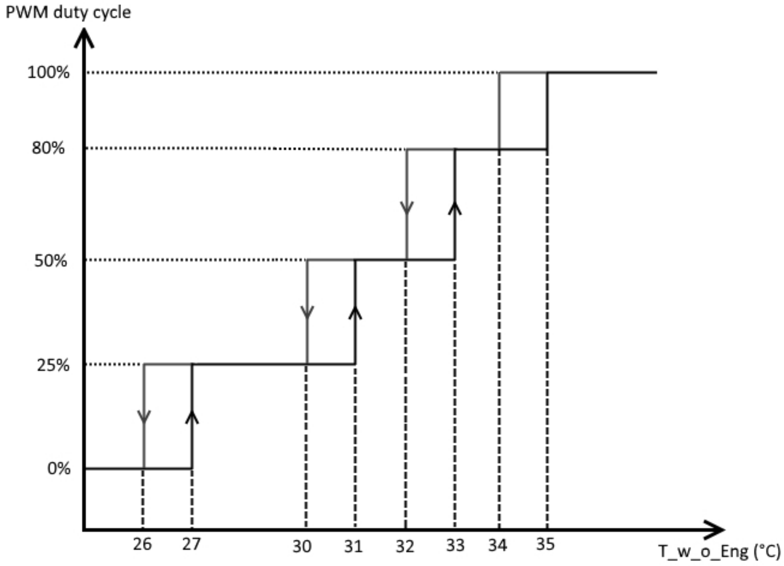

Figure 4.34 – Fan speed stages (for Pump1st control) [*Author's illustration*]

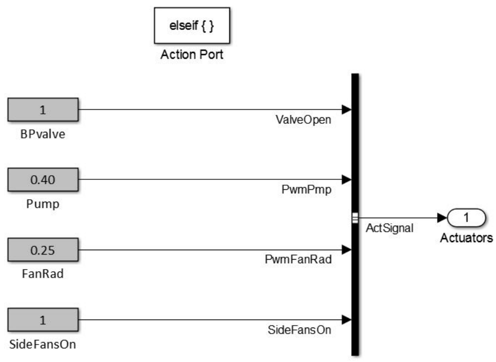

Figure 4.35 – Example of FixedOperation control strategy [*Author's illustration*]

4.3.4 Off

As the previous approach, this one has fixed parameters and shut off every actuator. It is used to keep the demonstrator turned on, but without functioning. To appreciate fully this function, a HMI or a selection program is required, in order to switch easily - manually or automatically - to another strategy,

4.3.5 Overheating

An emergency condition has been implemented in case of overheating : if the water exceeds $58°C$ or if the one of the silicone heater exceeds $130°C$. Its model is on Figure 4.37.

The limit of $58°C$ is fixed based upon the maximum water temperature for the hardware components, with a small margin. Moreover, the model shows that the silicone heater stabilizes around $105°C$ for a cold plate outlet temperature of $T\_w\_o\_CP = 60°C$, with $500W$ heat input and minimum main fan and pump speeds (respectively 235 [1] and

1. This value is lower than the declared minimum rotational speed of the fan. This inconsistency is explained in the next section, with the characteristic curve of the fan

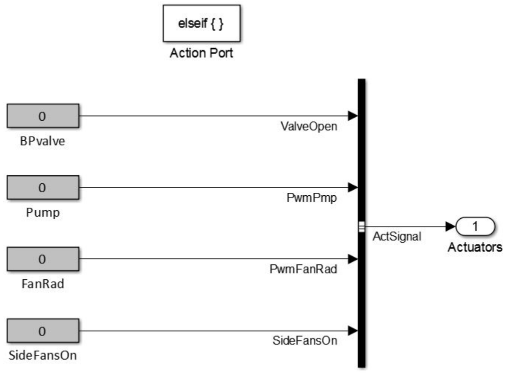

Figure 4.36 – Off control strategy [*Author's illustration*]

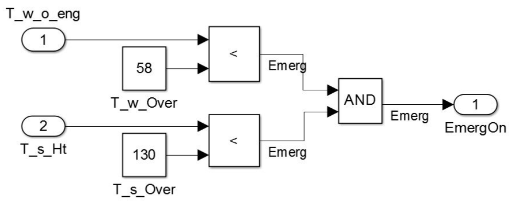

Figure 4.37 – Emergency condition subsystem EmergCond [*Author's illustration*]

$1300RPM$). The results are visible on Figure 4.38. Reaching $T\_s\_Ht = 130°C$ (by taking a safe margin) would mean that there is definitely a problem in the system.

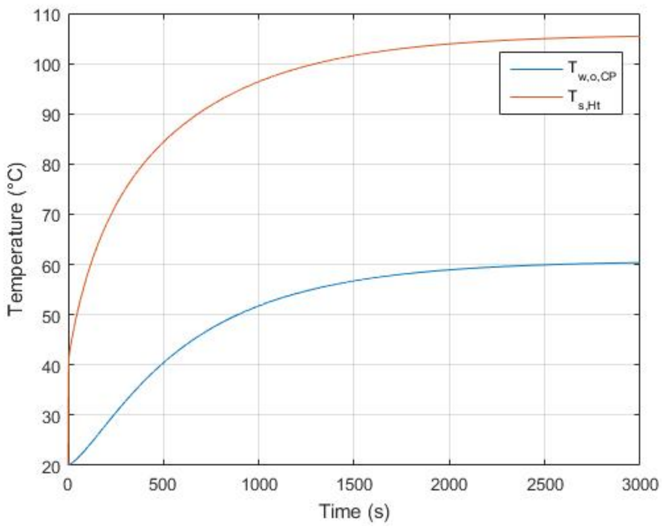

Figure 4.38 – Model stabilized at $60°C$ (with $500W$ heat power input)

Normally, the $Emerg$ signal carries 1. If the emergency condition is met, it passes to $Emerg = 0$ and stays at this level indefinitely. A reset can be applied to the delay if necessary to go back to normal (not implemented).

When the emergency is activated, the control strategy desired is overpassed and becomes 0, for the Overheat control. This is opening fully the radiator branch, and drives the fans and pump at maximum speed, while stopping the heat inputs and other external signals.

4.4 Signal converter

The signals passing from the input and the controller are not directly readable by the model nor the hardware devices. It needs to be filtered through the SignalConverter block, represented on Figure 4.39, relating the signals to the characteristic of the hardware devices.

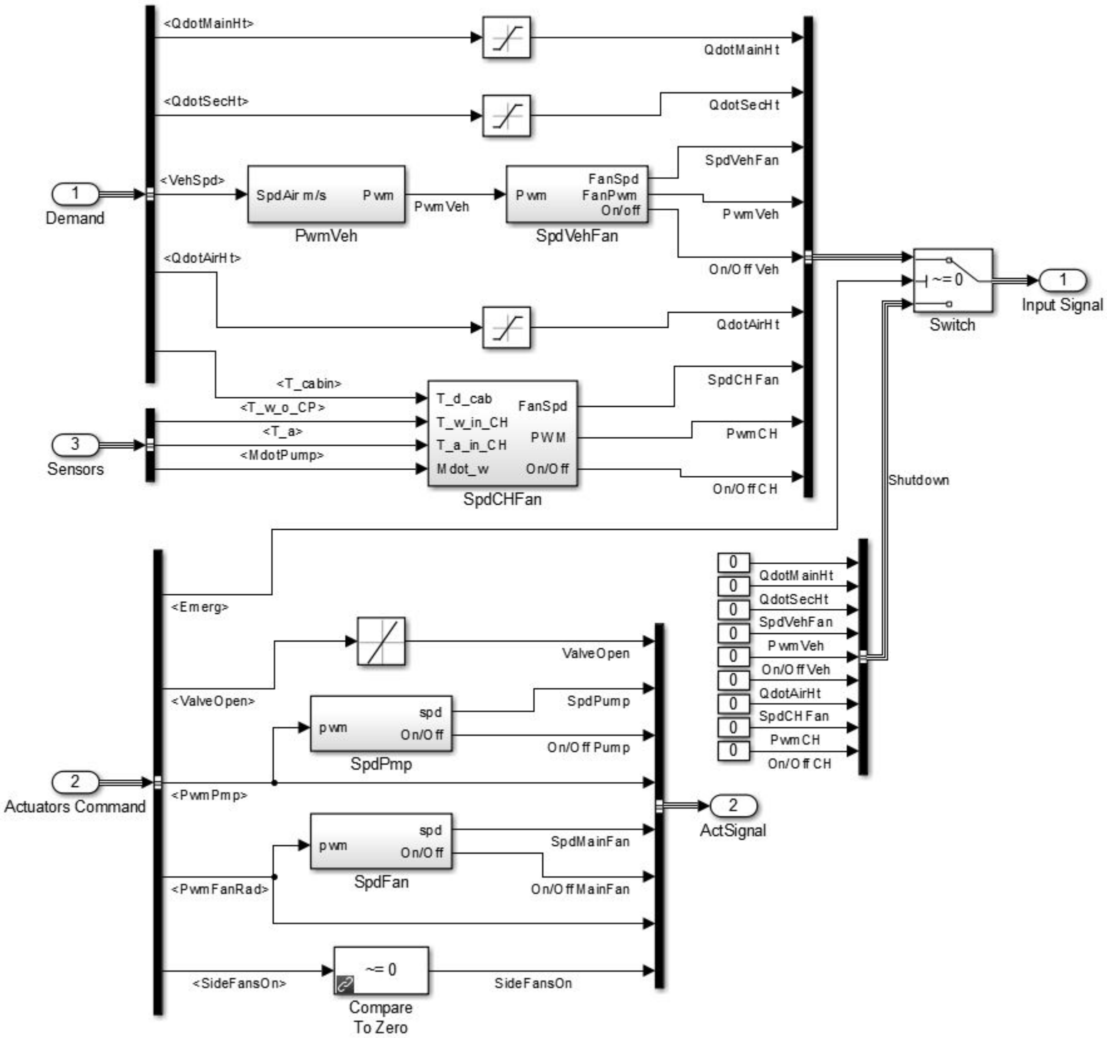

Figure 4.39 – SignalConverter subsystem [*Author's illustration*]

Some signals are simply bounded with a *Saturation* block, like $QdotMainHt$ ([0 500]), ($QdotSecHt$, not currently used, [0 200]) and $QdotAirHt$ ([0 200]).

$ValveOpen$ is restrained in its speed variations, with a *Rate Limiter* block, which translates that the valve can't reach the desired state instantly. According to [25], the full path of the valve can be crossed in 2 seconds with a synchronous motor version. In first approximation, this time is taken for the stepper motor as well. The rate is thus limited to [-0,5 0,5].

$SideFansOn$ is imposed as a boolean variable.

A website [38] reviewed various fans, and the Noctua used in this demonstrator are among them. In these reviews, the author recorded the fan speed and the air speed 6" (15,24cm) away from the radiator, and these results were related to the PWM duty cycle. Those characteristic curves are visible on Figures 4.40, 4.41 and 4.42. ($100FPM = 0{,}5m/s$)

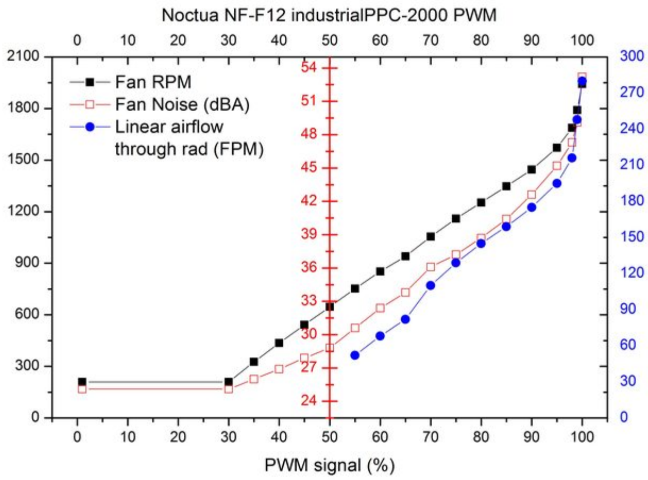

Figure 4.40 – Front fan characteristic curve [38]

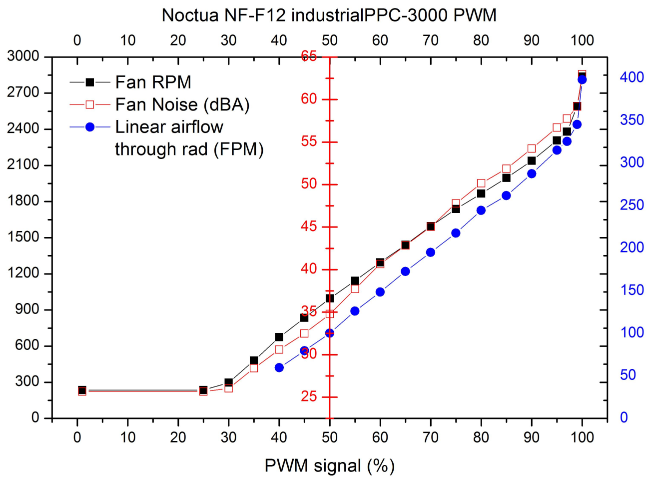

Figure 4.41 – Main fan characteristic curve [38]

Keep in mind that each fan can have a slightly different speed range as it can vary between ±10% and 20% compared to the performance declared by the manufacturer. Those performances should be reasserted once the fans in our possession.

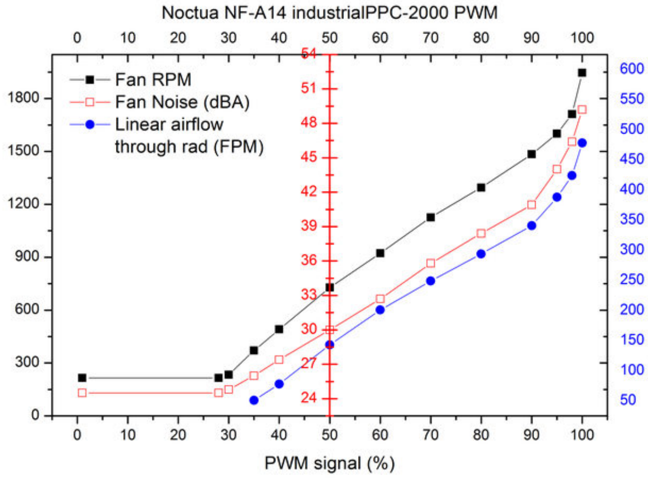

Figure 4.42 – Cabin heater fan characteristic curve [38]

Based on these results, the vehicle speed entered in input $VehSpd$ (in m/s) is firstly translated into a PWM duty cycle and then transformed back into a rotational speed. Both functions are respectively modelled on Figure 4.43 and 4.44.

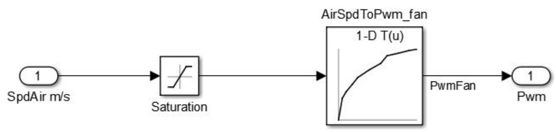

Figure 4.43 – PwmVeh subsystem [*Author's illustration*]

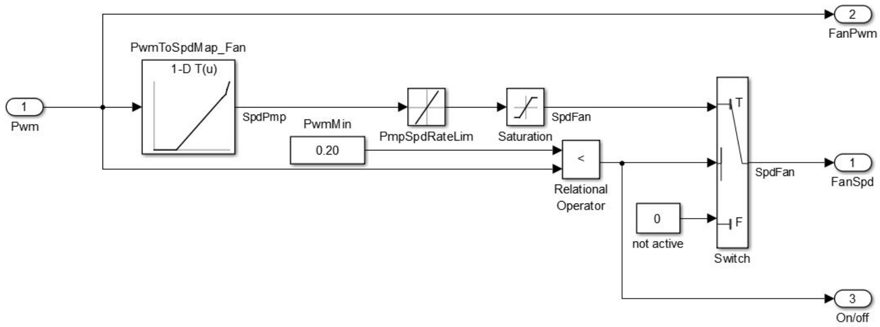

Figure 4.44 – SpdVehFan subsystem [*Author's illustration*]

In the same way, the PWM signals $PwmPmp$ and $PwmFanRad$ of the actuators are transformed into rotational speed with the models on Figures 4.45 and 4.46

3 outputs of PWM driven subsystems are possible : the 'PWM' and 'On/Off' signals are used in the microcontroller, detailed in the next section, where as the 'Spd' signal, which represents the rotational speed of the component goes to the HiL simulator.

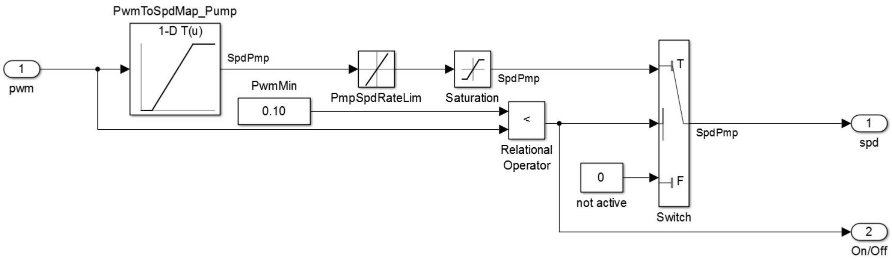

Figure 4.45 – SpdPmp subsystem [*Author's illustration*]

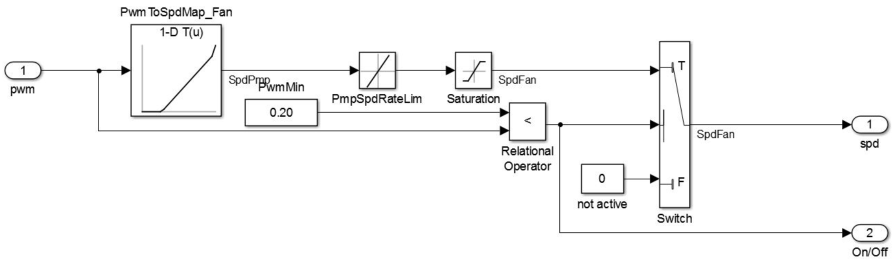

Figure 4.46 – SpdFan subsystem [*Author's illustration*]

The performances (on Figures 4.40, 4.41 and 4.42) have been documented in a *Lookup Table* block : a function defined by determined point. The values in output of these tables are interpolated between two data points. These are the curved charts blocks in the models in Figures 4.43, 4.44, 4.45 and 4.46.

The *Saturation* blocks are related to the maximum values found in the characteristic curves : *e.g.* for the front fan, $VehSpd$ is limited to a maximum of 1,5m/s (300FPM).

The *Rate Limiter* blocks in SpdVehFan and SpdFan are parametrized randomly to [-750 750] RPM/s to avoid an instant speed variation. For the pump, as water has more density than air and thus requires a more important torque from the pump, the variation is limited to [-500 500] RPM/s. This information is mainly used in the main model of the HiL simulator Water circuit.

As the PWM driven actuators doesn't turn off for a 0% PWM duty cycle, a On/Off signal is added, as explained in the section about PWM control, page 51. The lowest admissible PWM duty cycle is fixed at 20% for the fans and 10% for the pump (whose PWM characteristic curve is on Figure 4.47, to relate to the Figure 3.31, page 43).

About the heat demand for the cabin heater radiator, the relation is based on the map of the radiator linking the heat dissipated and the fan speed. As the heat power varies a little compared to the water flow (Figure 3.17, page 37), this variable is neglected for the demand. This could be improved in a future version.

About the *Switch* block, as mentioned previously in section 4.3.5, when $Emerg = 0$, all the input signals are stopped.

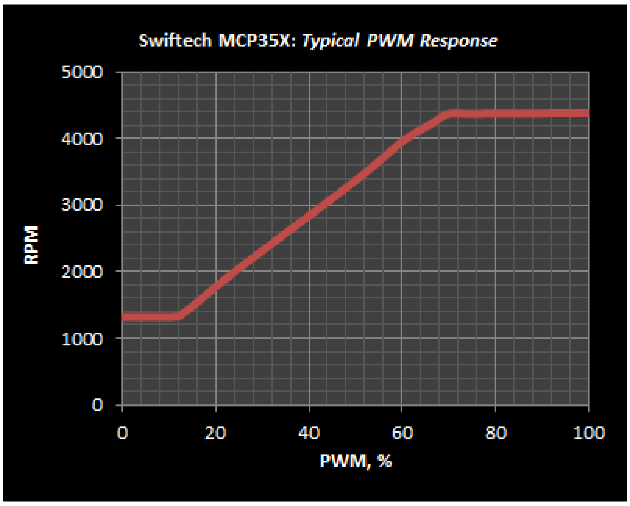

Figure 4.47 – Pump PWM response [27]

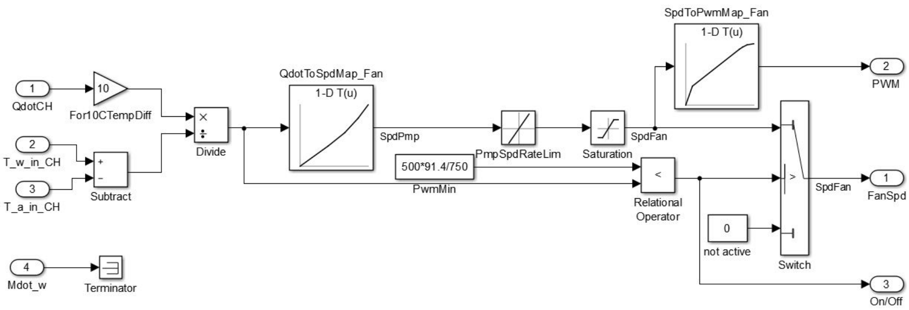

Figure 4.48 – SpdCHFan subsystem [*Author's illustration*]

4.5 Arduino program

The Arduino MEGA 2560 is well suited for this application with its specific features :
- It can receive 16 analogue inputs, *i.e.* the electric signals from the sensors
- It has 54 digital input/output pins (of which 15 can be used as PWM outputs)
- It is powered either by a USB cable either by an external supply between 6 and $20V$
- The main output voltage is 5V, like the PWM sensors of the fans.
- There exist a "Simulink support package for Arduino hardware", created by the MathWorks company, that allows to code this platform with Simulink blocks. Otherwise, it is coded with its own programming language, similar to C. It can either be linked to the computer or to run standalone.
- It supports various shields and has several communication dedicated pins.

This version of the microcontroller was preferred to the Arduino UNO due to its larger number of pins, which would have been too short for this application.

The section details the algorithm developed on Simulink, thanks to the support package, and then downloaded on the board.

The overall algorithm regulating the microcontroller is represented on Figure 4.49. Compared to the HiL Simulator, the Water circuit model has been switched with the ArduinoOutputs, managing the appropriate electrical signals sent to the hardware device. Another Sensors input subsystem appears, which interprets the electrical information coming from the sensors to the Arduino, into the related physical values (T - $°C$ - or $\dot{m}$ - kg/s). All the other subsystems are the same.

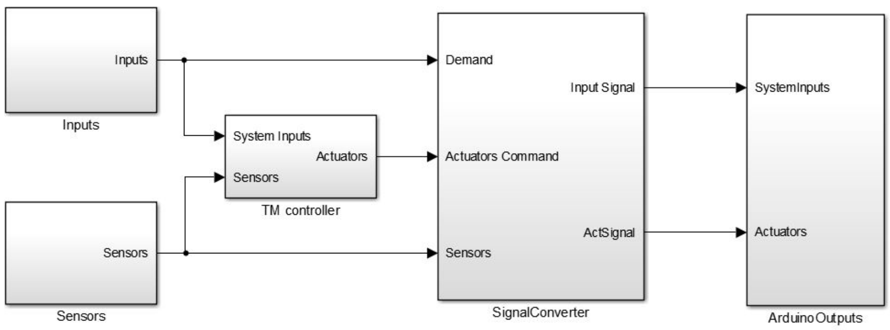

Figure 4.49 – Overall control model of the hardware plant [*Author's illustration*]

4.5.1 Sensors

The Sensors subsystem is expanded on Figure 4.50.

The *Analog Input* blocks are specifically built to assign a value between 0 and 1023 to the signal, proportional to the measurement made between 0 and $5V$. Then, this 10-bit signal is assigned the 'double' type, which is the standard class of signal for Simulink, with the *Convert* block. Finally, the value between 0 and 1023 is scaled to the physical value of the variable, depending on the defined range of the sensor.

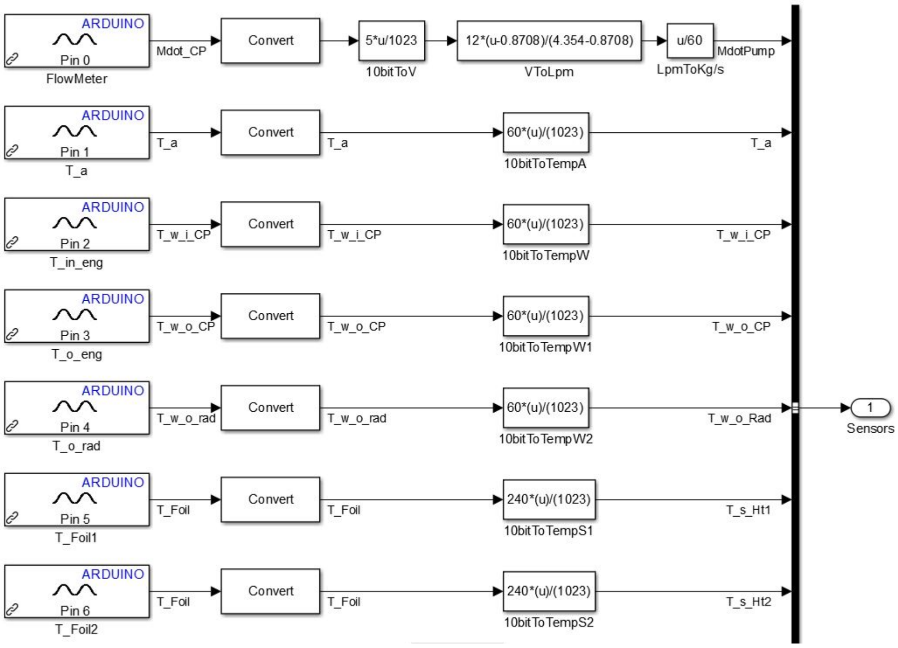

Figure 4.50 – Sensors subsystem [*Author's illustration*]

4.5.2 Outputs

The outputs are modelled in the ArduinoOutputs subsystem, Figure 4.51.

The On/Off signals are just digital output pins with 2 different possible state : High ($5V$) or Low ($0V$)

The others signals are a little more complex and detailed just after.

Heaters and triacs

The air and main heaters are controlled with the **Triac Nanoshields** and their control model is detailed on Figure 4.52 and 4.53.

One digital input pin of the MEGA 2560 detects change of logic level from the **Zero Cross Nanoshield** and this signal serves to reset the time delay before the activation of the Triac.

This delay d is related to the angle α of the sinusoidal voltage at $f = 50Hz$ with the formula:

$$d = \frac{\alpha}{2\pi f} = \frac{\alpha}{100\pi}$$

The output power depends on this firing angle according to the relation (found in [40]) :

$$P_{out} = P_{out,max} * \left(\frac{\alpha - \frac{1}{2} sin(2\alpha)}{\pi} \right)^{\frac{1}{2}}$$

with $P_{out,max} = 500W$ (for the main heater) and $\alpha \in [0\ \pi]$

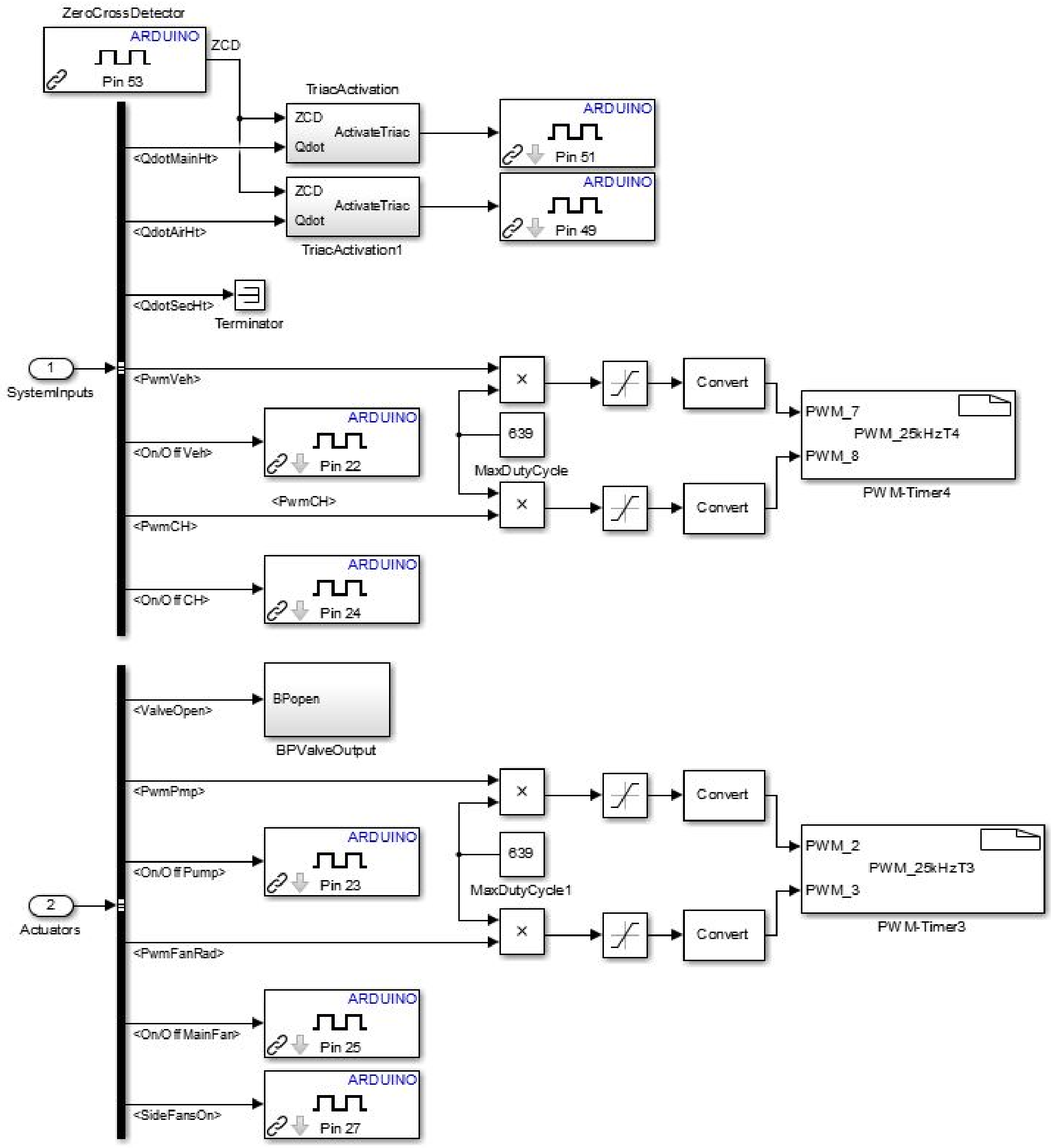

Figure 4.51 – ArduinoOutputs subsystem

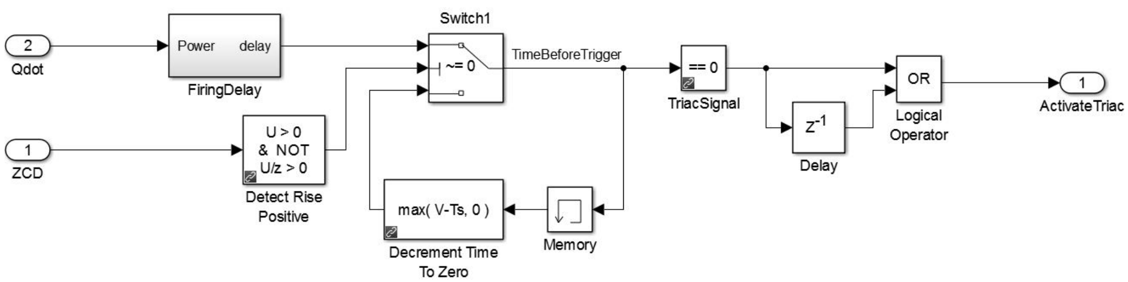

Figure 4.52 – TriacActivation subsystem [*Author's illustration*]

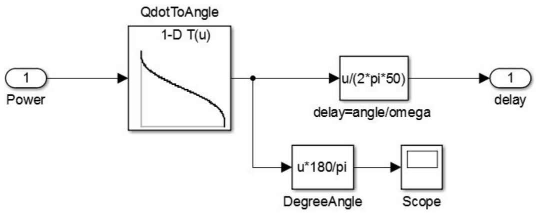

Figure 4.53 – Firingdelay subsystem [*Author's illustration*]

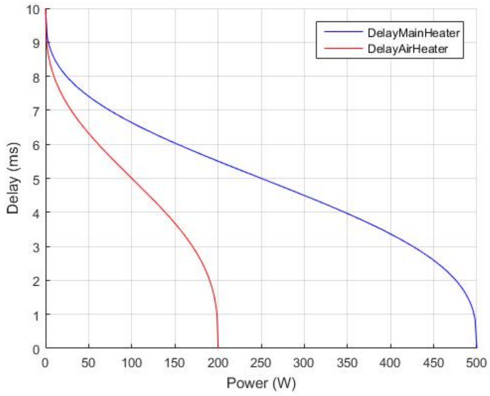

Figure 4.54 – Firing delay according to the power required by the heaters [*Author's illustration*]

To avoid the computation of the solution for each time step, it is recorded for the interval of powers [0 500W] (main heater) and [0 200W] (air heater) in a *Lookup Table*.

The Figures 4.54 shows the graph of the delay to wait before triggering the Triac compared to the power required by the main and the air heater.

The zero cross detector has a high logic level in the period [-0,5 ; 0,5] ms, centered on the AC crossing of $0V$. This causes to decrease the time step Ts to $0,5ms$ to detect it.

The test to validate the good functioning of the TriacActivation is visible on Figure 4.55.

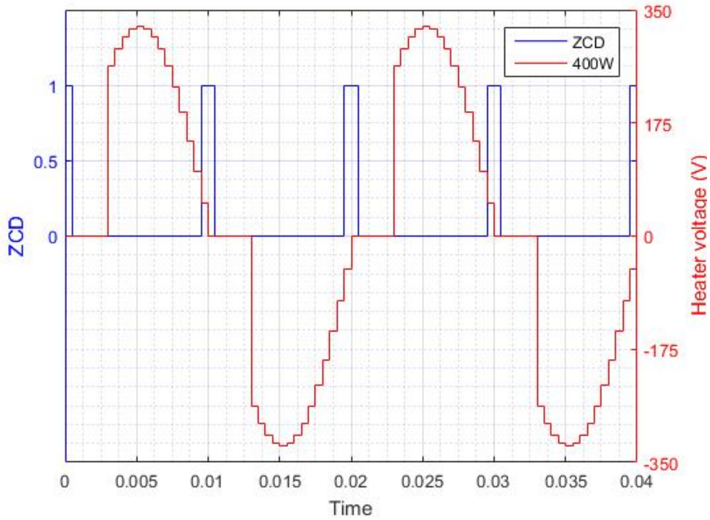

Figure 4.55 – Test of the Triac triggering for $400W$ input to the main heater

Stepper motor control

The stepper motor control signals are managed by the BPValveOutput subsystem, detailed on Figure 4.56.

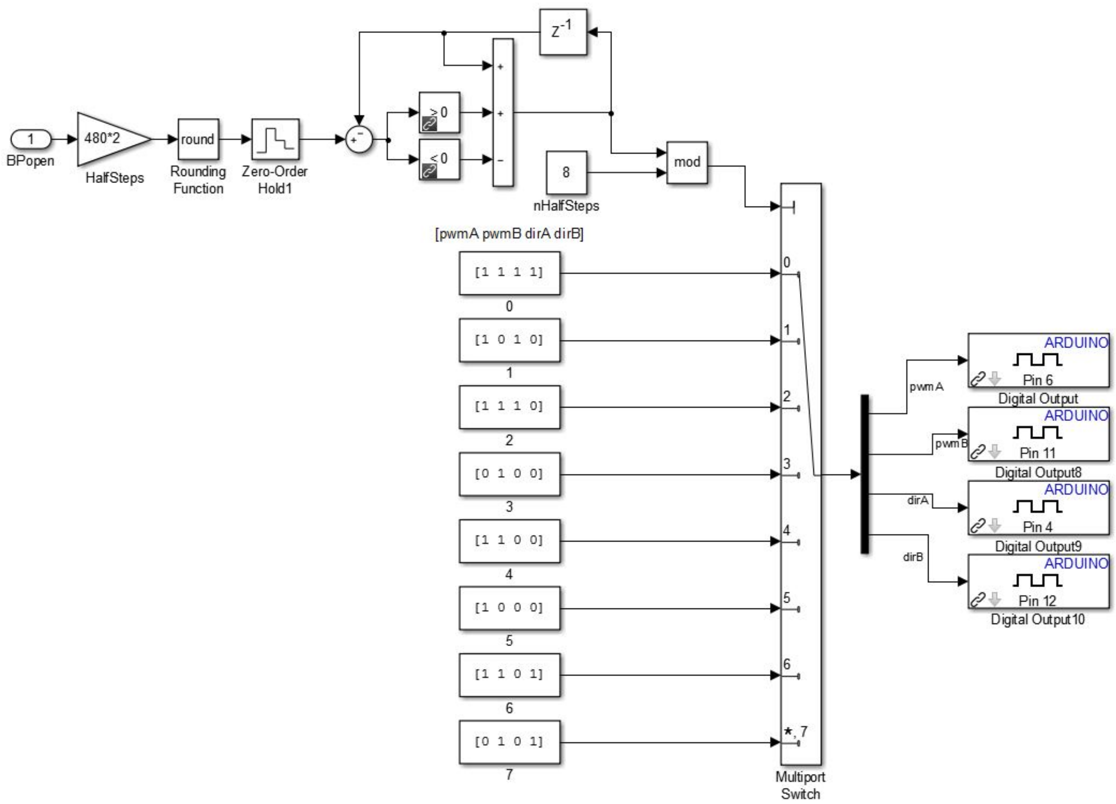

Figure 4.56 – Control model of the stepper motor : BPValveOutput subsystem [*Author's illustration*]

The stepper motor shield **VMA03** has 4 input pins $DIRA$, $PWMA$, $DIRB$, $PWMB$ and is driven, according to [41], with a repeating sequence of 8 half steps in one way (*e.g.* opening the valve) and the inverse sequence in the other way (*e.g.* closing the valve). The algorithm is inspired from the same source.

As for the stepper motor itself, its full path (from fully closed to fully open and vice versa) is made of 480 steps.

A checking of the good functioning of the stepper motor should evidently be in application after the connexions made.

About the algorithm model, it compares the actual position of the valve with the desired one, and run the sequence according to the difference of position. The sample time for the delay fixes the speed of the sequence and thus the speed of the motor. A delay of $0{,}002s$ between each half step is applied to have a full course that lasts $0,002 * 480 * 2 = 1,92s$. The *Zero-Order Hold* block makes compatible the different time steps together.

PWM signals

The *Arduino PWM* block from the support library only generate a fixed $490Hz$ PWM signal, which cannot be read by the fans, working with a $25kHz$ PWM signal. A custom function is therefore needed to generate this signal.

The S-function builder generate a function file that can be read both by Simulink and the Arduino, using the C programming language.

The source code is situated in appendix B.

Chapter 5

Results

Now that the model has been developed in the chapter 3, as for the control method in chapter 4, the results of the whole simulation are approached.

When the internship ended, every pieces had not arrived at the company. Among them, the DIN rail power supplies and the bypass valve were missing for example. Therefore, it was impossible to test the hardware devices and this section focuses on the HiL simulator results.

The comparison is mostly made between the Valve1st and Pump1st, detailed in the section 4.3, page 59.

As the different combinations and the behaviour of the inputs can be infinite, just a few specific example cases have been approached. They have the main objective to give an insight of the functioning of the demonstrator to the reader. These cases will be presented throughout this chapter, with their relative results.

5.1 Full power - 500W

Firstly, it is suited to determine how the demonstrator reacts with a constant full input power of $500W$, and how the disturbances (vehicle speed, air heater, cabin heater) affect it.

Main heating alone - Valve1st

The simulation is done over a period of $900s$, with the Valve1st control strategy and no disturbance. Over a first phase, only the first $300s$ are shown of the evolution of the temperature (Figure 5.1), how the actuators regulate the system (Figure 5.2), how is linked the heat powers (Figure 5.3), and what is the flow rate through the components (Figure 5.4).

At the beginning of the simulation, the temperature $T_{w,o,CP}$, at the cold plate outlet, starts to rise of about $2°C/50s$. $T_{w,i,Rad}$, the temperature at the inlet of the radiator (in the simulation, it is the same than in the bypass valve), and $T_{w,i,CP}$ are delayed compared to $T_{w,o,CP}$, as the water take some time to flow through the components. As the flow through the radiator is blocked, no increase in temperature at the end of the radiator is observed.

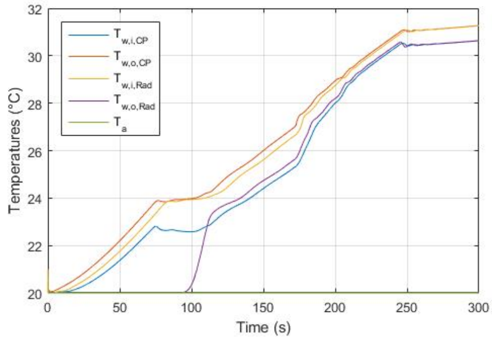

Figure 5.1 – Temperature evolution for a $500W$ heat input, Valve1st control

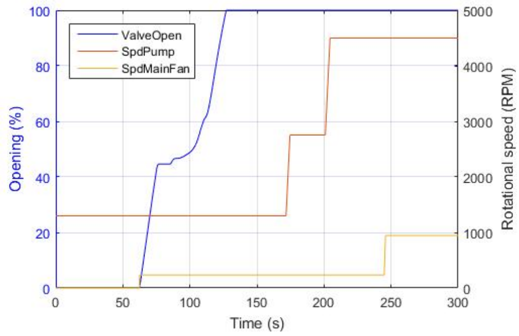

Figure 5.2 – Actuators state for a $500W$ heat input, Valve1st control

[*Author's illustrations*]

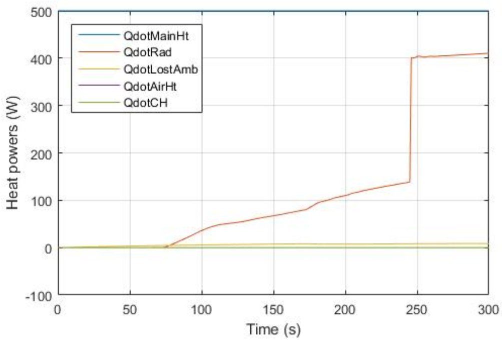

Figure 5.3 – Heat transfer evolution for a $500W$ heat input, Valve1st control

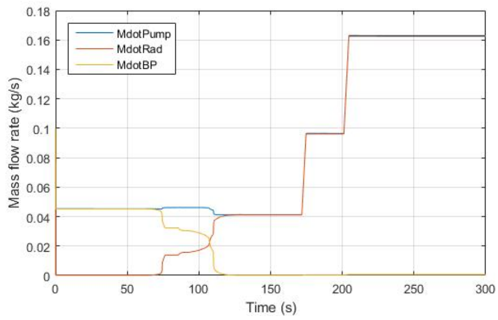

Figure 5.4 – Mass flow rate evolution for a $500W$ heat input, Valve1st control

$T_{w,o,CP}$ reaches $23°C$, around $60s$, the bypass valve starts to open ($ValveOpen$), but the pressure drop inside the branch going to the radiator is still very high and the flow still goes mainly in the bypass branch.

Due to the control strategy, the actuated fans also turns on. That could be improved as there is not any flow inside the radiator.

Around $75s$, the deviation of the flow to the radiator begins to be really effective. The flow entering this component pushes the water. As it is mainly non compressible, the water at the other extremity of this heat exchanger, which is still cold, enters the pump. There is almost a stagnation of the temperature $T_{w,i,CP}$ as this cold water mixes with the flow coming from the bypass. This in turn lead to a stagnation of $T_{w,o,CP}$ (and $T_{w,i,Rad}$). During this time, the valve still opens slowly.

At $100s$, the warm water going into the radiator reaches the end. The rise of $T_{w,o,CP}$ starts again, which opens fully the valve for $T_{w,o,CP} = 25°C$ around $125s$: the flow rate through the pump and through the radiator are equals.

It is worth noting that the total mass flow rate (through the pump) is slightly lower when the water goes through the radiator than when it goes through the bypass due to the higher pressure drop in the former component.

When $T_{w,o,CP} = 27°C$, around 170-175s, the pump speed increases, so does the flow rate, which reduces the temperature difference between $T_{w,i,CP}$ and $T_{w,o,CP}$.

The same thing happens when $T_{w,o,CP}$ reaches $29°C$ (at $200s$) and the pump speed is still increased.

At $245s$, $T_{w,o,CP} = 31°C$ this is the turn of the fan speed to be augmented. This decreases a lot the rising rate of $T_{w,o,CP}$, as the heat power dissipated through the radiator is much higher.

The figures 5.5, 5.6 and 5.7 show the state of the overall simulation. (The detail of the mass flow rates in the system doesn't bring more information and is therefore not displayed.)

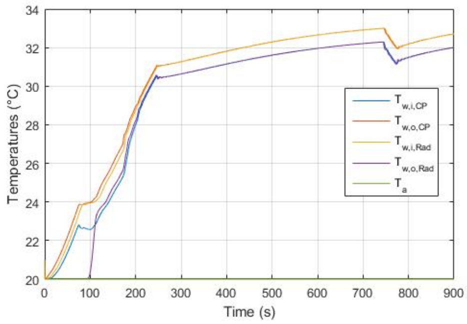

Figure 5.5 – Temperature evolution for a $500W$ input, Valve1st control

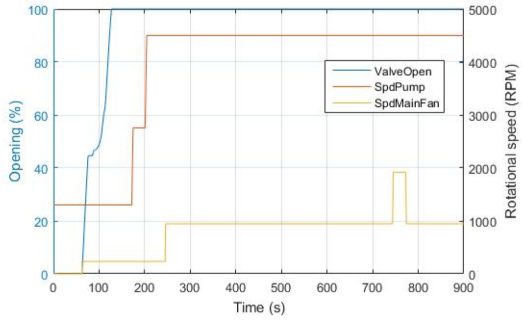

Figure 5.6 – Actuators state for a $500W$ input, Valve1st control

[*Author's illustrations*]

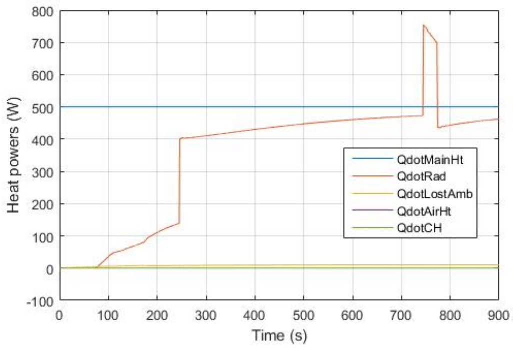

Figure 5.7 – Heat transfer evolution for a $500W$ input, Valve1st control

When $T_{w,o,CP} = 33°C$ (at $750s$), the fan speed is one more time increased. This improves the heat dissipation of the radiator more than the heat input. This makes abruptly decrease $T_{w,o,CP}$, to $32°C$ where the previous fan speed starts again. This way, the temperature will oscillate indefinitely in the hysteresis between the second and the third speed stages of the fan.

It is observable that the heat dissipated through the radiator is mainly dependant of the fan speed and of the temperature difference between $T_{w,i,Rad}$ and T_a. Therefore, the main goal of increasing the pump speed is not for the heat dissipation of the system, but to contribute to lower the temperature difference between the cold plate inlet and outlet.

The heat lost to the ambiance is near $10W$ and the power of the air heater and lost for the cabin heating stays at $0W$, as required.

The total energy consumed by the actuators is 70,42kJ for the pump and 4,969kJ for the fan.

Main heating alone - Pump1st

For the alternative Pump1st control strategy, the simulation over $300s$ is visible on Figures 5.8, 5.9, 5.10 and 5.11.

The behaviour of the system is identical to the Valve1st strategy after this period.

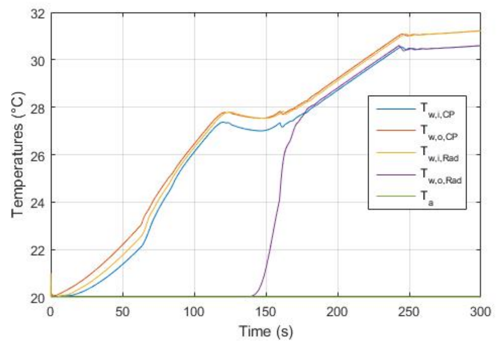

Figure 5.8 – Temperature evolution for a $500W$ heat input, Pump1st control

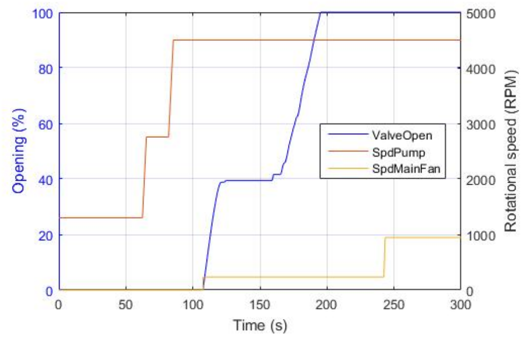

Figure 5.9 – Actuators state for a $500W$ heat input, Pump1st control

[*Author's illustrations*]

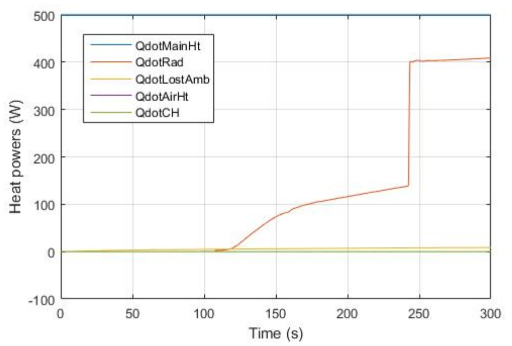

Figure 5.10 – Heat transfer evolution for a $500W$ heat input, Pump1st control

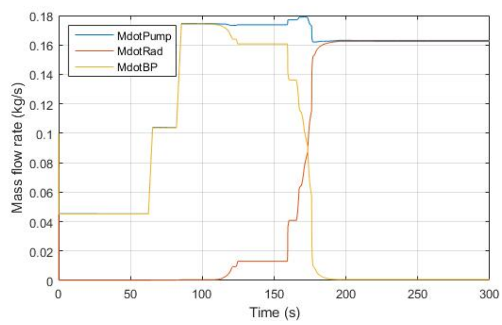

Figure 5.11 – Mass flow rate evolution for a $500W$ heat input, Pump1st control

The evolution is similar, except that the pump speed is increased earlier and the valve opens later. A high flow rate is then distributed between the bypass and the radiator branch. The warm-up of the heating unit is faster over a first phase, when the bypass valve is closed, but the system takes the same time to attain the temperature of the second fan speed stage : the heat dissipated for a longer time in the first case (because the radiator branch is opened earlier) is negligible.

The temperature difference is reduced : when the maximum between $T_{w,i,CP}$ and $T_{w,o,CP}$ reached 1,5°C for Valve1st, and was superior to 1°C between 50s and 200s; the maximum of temperature difference in this strategy is equal to 1°C, with 0,5-0,75°C most of the time.

What changes significantly is the energy consumed by the pump : 81,96kJ over 900s compared to 70,42 for Valve1st. This is due to a longer period running at high speed (around 120s). Due to the observations made just above, the fan consumes more or less the same quantity of energy than before : 4,979kJ.

Ram air disturbance - Valve1st

A maximum air speed of 1,45m/s in input, corresponding to a rotational speed of the front fans of 2000RPM, is then applied to the demonstrator. The results are visible on Figures 5.12, 5.13, 5.14 and 5.15 for a simulation of 900s and the Valve1st control strategy.

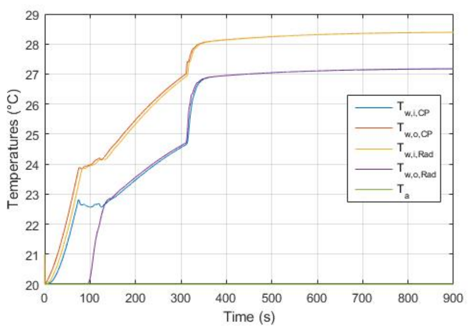

Figure 5.12 – Temperature evolution for a 500W input with ram air disturbance, Valve1st control

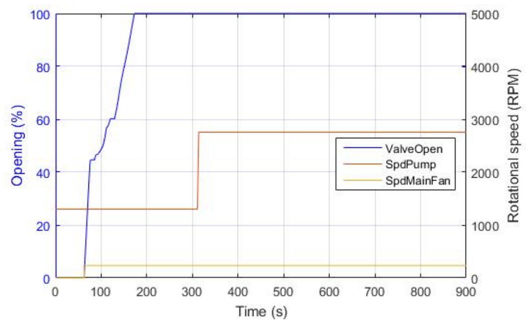

Figure 5.13 – Actuators state for a 500W input with ram air disturbance, Valve1st control

[*Author's illustrations*]

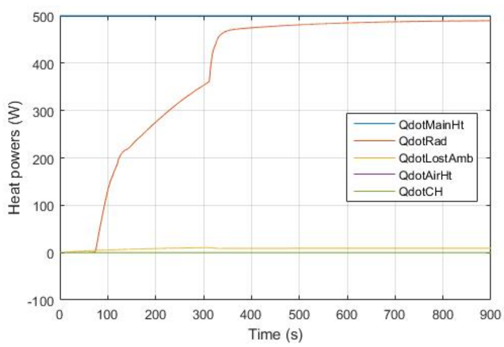

Figure 5.14 – Heat transfer evolution for a 500W input with ram air disturbance, Valve1st control

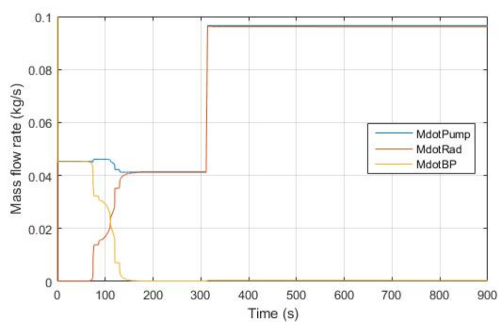

Figure 5.15 – Mass flow rate evolution for a 500W heat input with ram air disturbance, Valve1st control

As the air flow through the radiator is already high, the actuated fans are not necessary to cool down the water. Even with a small water flow, the radiator dissipates a lot of heat and the temperature rises slower than in the previous cases. When the pump speed is increased, this decreases the temperature difference between the silicone heaters and the water flowing through the cold plates. This, combined with a shorter time for the water to travel through the tubes, increases the water temperature much faster, and the associated heat dissipation in the radiator.

Modifying the pump speed and the water flow (with a sufficient air flow through the heat exchanger) can be seen as a fast way to reach the equilibrium state, *i.e.* to reduce the response time of the demonstrator, even if it doesn't change fundamentally the equilibrium point.

Ram air disturbance - Pump1st

The same inputs than the previous case are taken : full power for the main heater, full air speed. The alternative control strategy is used. The results are presented on Figures 5.16, 5.17, 5.18 and 5.19.

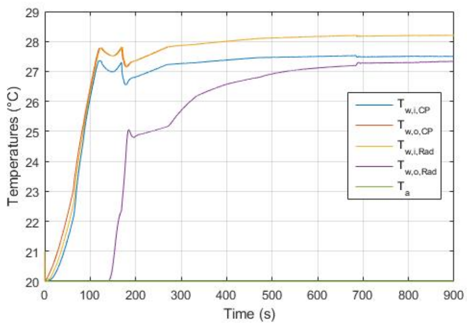

Figure 5.16 – Temperature evolution for a $500W$ input with ram air disturbance, Pump1st control

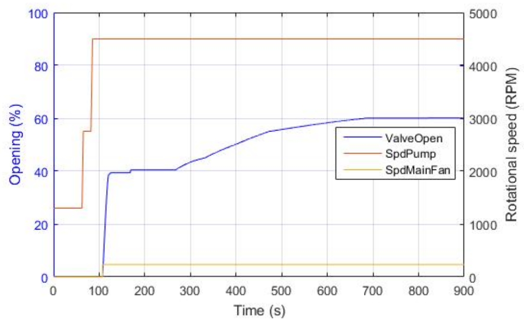

Figure 5.17 – Actuators state for a $500W$ input with ram air disturbance, Pump1st control

[*Author's illustrations*]

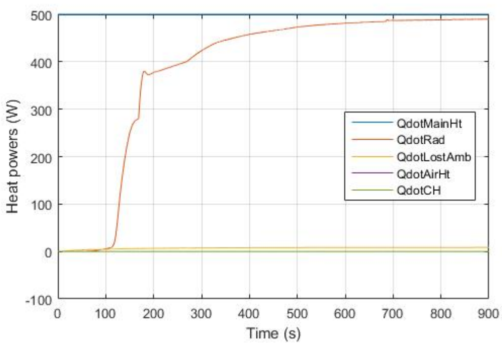

Figure 5.18 – Heat transfer evolution for a $500W$ input with ram air disturbance, Pump1st control

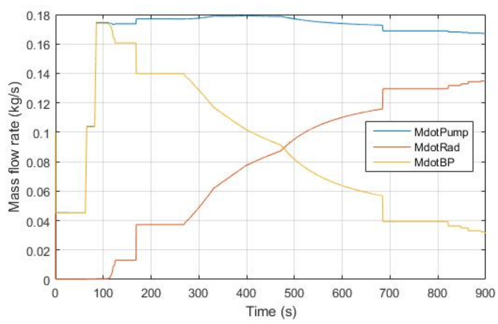

Figure 5.19 – Mass flow rate evolution for a $500W$ heat input with ram air disturbance, Pump1st control

The interesting thing to highlight for this case is that when the system is stationary, the flow is still divided in the bypass and the radiator branches. The part going in the bypass branch is useless to the cooling of the cold plate and increases the pump consumption.

This is a typical problem of the standard control strategy, as explained in the "State of the art" chapter.

Ram air disturbance + Air heater - Valve1st

In this case, the air speed is reduced a little to $1m/s$ and the air heater is put at maximum power input : $200W$. The results are the Figures 5.20, 5.21, 5.22 and 5.23, for the Valve1st strategy.

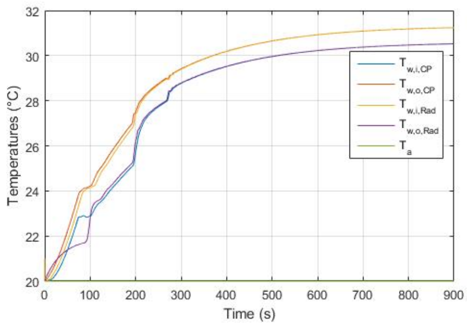

Figure 5.20 – Temperature evolution for a $500W$ input with heated ram air disturbance, Valve1st control

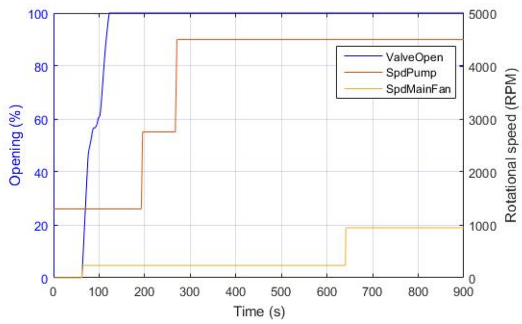

Figure 5.21 – Actuators state for a $500W$ input with heated ram air disturbance, Valve1st control

[*Author's illustrations*]

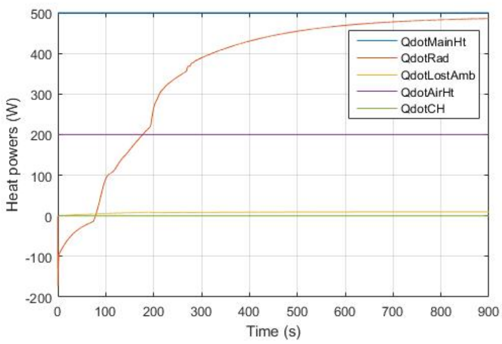

Figure 5.22 – Heat transfer evolution for a $500W$ input with heated ram air disturbance, Valve1st control

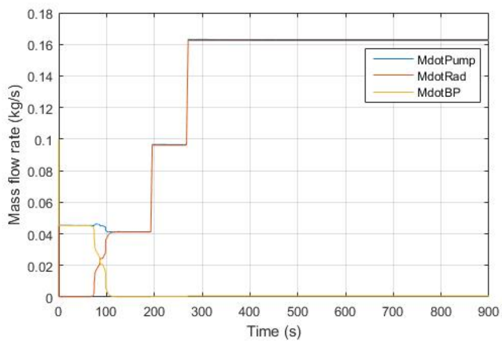

Figure 5.23 – Mass flow rate evolution for a $500W$ heat input with heated ram air disturbance, Valve1st control

The air heater increases the temperature of the air cooling down the system. At the beginning, as the water inside this component is colder than the felt outside air, the radiator absorbs some heat and in turn, the water warms up. This explains the negative heat power at the start of the simulation.

An effect of this preheating of the radiator, while there is not any water flow inside it, decreases the temperature stagnation time at the inlet of the pump, when it mixes with the water coming from the bypass.

Another interesting observation is done around $650s$. As $T_{w,o,CP}$ reaches $31°C$, the actuated fan speed intensifies, but the effect on the heat dissipation and in the radiator is absent. The increase of pressure produced is negligible on the existing airflow already applied by the front fans.

The stationary state is defined by an increased temperature in the system compared to the ram air disturbance alone.

The comparison with the Pump1st strategy doesn't give any new information and is not displayed.

Cabin heater - Valve1st

For this case, no ram air disturbance is applied, but the imaginary cabin requires some heating : $150W$. The results are shown on Figures 5.24, 5.25, 5.26 and 5.27, for the Valve1st control strategy.

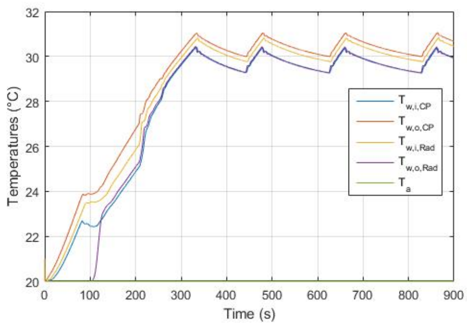

Figure 5.24 – Temperature evolution for a $500W$ input with cabin heating, Valve1st control

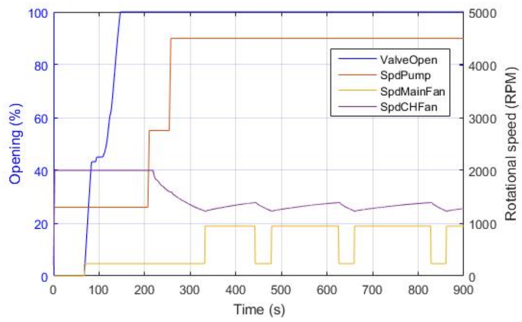

Figure 5.25 – Actuators state (+ cabin heater fan rotational speed) for a $500W$ input with cabin heating, Valve1st control

[*Author's illustrations*]

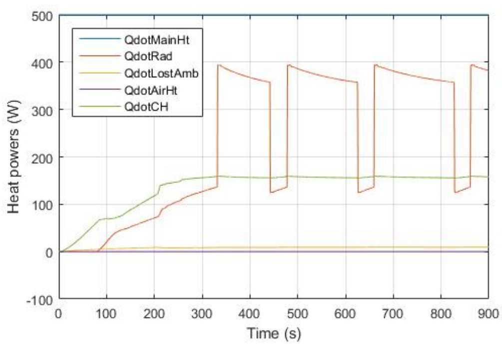

Figure 5.26 – Heat transfer evolution for a $500W$ input with cabin heating, Valve1st control

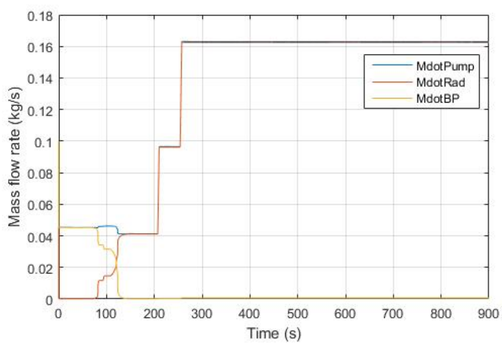

Figure 5.27 – Mass flow rate evolution for a $500W$ heat input with cabin heating, Valve1st control

To reach the set point value of heat dissipation in the cabin heater radiator ($150W$), the associated fan is first driven at full speed ($2000RPM$) to extract the maximum heat from the system.

Around 200s of simulation, once the fan is able to extract this heat, thanks to the sufficient temperature difference between the cold plate outlet $T_{w,o,CP}$ and the ambient air T_a, it decreases progressively its speed, to maintain a constant heat dissipation.

When the main fans are driven faster due to the stage of $T_{w,o,CP} = 31°C$ in application, the controlled temperature decreases : the heat extracted through both radiators is higher than the heat input. The cabin heating fan compensates this temperature drop by increasing its speed.

As $T_{w,o,CP}$ reaches the lower level of the hysteresis, the main fan speed goes back to its previous state, which makes $T_{w,o,CP}$ to increase again, and the cycle keeps going on indefinitely (*ceteris paribus*).

Two causes from this boosted heat dissipation can be noted :

- The temperature difference between $T_{w,o,CP}$ and $T_{w,i,Rad}$ is more marked, as there is not only the delay for the water to flow through the cabin heating radiator, but it looses some heat on the way as well.
- the warm-up time is a bit delayed compared to the case without any other input.

The comparison with the Pump1st strategy doesn't give any new information and is not displayed.

5.2 NEDC

A practical example of the control is done over the NEDC (see section 4.2).

Valve1st control strategy

The results with the Valve1st control strategy are visible on Figures 5.28, 5.29, 5.30, and 5.31.

Compared to the external input section in the previous chapter, the heat input is divided by 3 (for the heat transferred to the coolant, as before) and then by 20 (and not 40 any more). This is done to have a higher heat energy input over the full cycle, and more variations of the temperature. There is no other input than those related to the main heater and the vehicle speed.

The valve opens fully at the end of the cycle and the temperature $T_{w,o,CP}$ doesn't reach the higher stages of the control : the pump and the actuated fans stay at minimum speed.

The pump consumes 2,898kJ over the cycle and the fan 5,993kJ.

Pump1st control strategy

The results of the second strategy on the same cycle are displayed on Figures 5.32, 5.33, 5.34, and 5.35.

As the valve opens later, there is less heat extracted from the system in the first phase and the temperatures rise faster than with the Valve1st control. This strategy results in a higher level at the end of the simulation, and a faster warm-up of the system.

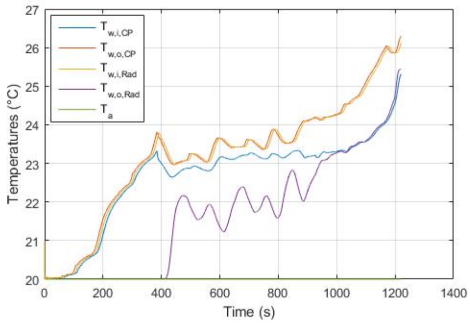

Figure 5.28 – Temperature evolution on the NEDC, Valve1st control

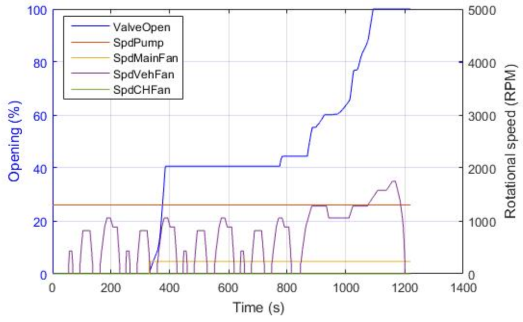

Figure 5.29 – Valve opening and fan speeds on the NEDC, Valve1st control

[*Author's illustrations*]

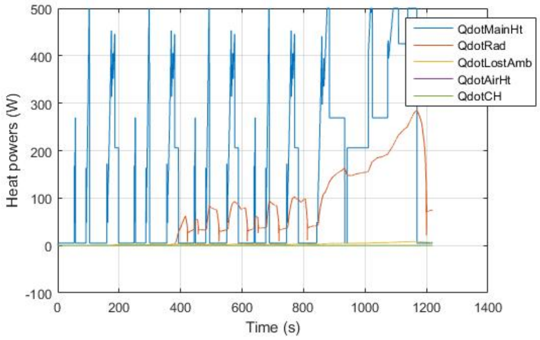

Figure 5.30 – Heat transfer evolution on the NEDC, Valve1st control

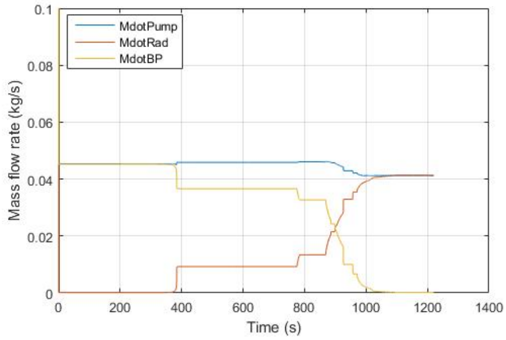

Figure 5.31 – Mass flow rate evolution on the NEDC, Valve1st control

Comparing the water mass flow rates between both cases, at the end of the simulation, the valve is not opened fully yet with Pump1st, but the mass flows in the radiator are almost equals due to the high speed of the pump. This, combined with a higher temperature, increases the heat dissipation in the radiator.

Concerning the energy required to activate the actuators, the pump consumes 80,41kJ (» 2,898kJ in the previous case) and the fan 5,336kJ.

5.3 Summary

These were only basic examples to show the behaviour of the demonstrator but it also allows to draw general conclusions.

A remark needs before to be done : the results were only obtained with the HiL simulator and they need to be checked on the real device. If the results are similar, the model allows to know and determine with only a small error the evolution of the system for a set of predefined inputs. A good advantage is also to determine the state of the fluid on relevant locations, even if there is not any sensor on the test rig on this specific place.

Each actuators have its own way of modifying the system :

The pump will allow to modify quickly the overall temperature of the system, while the fan actuation changes mainly the heat dissipation and the equilibrium point. The

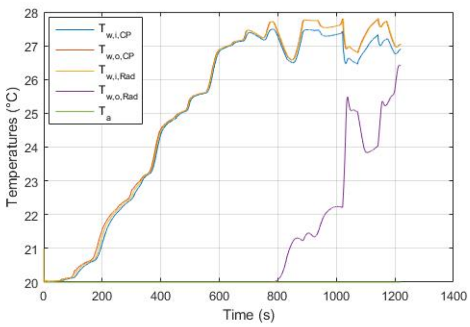

Figure 5.32 – Temperature evolution on the NEDC, Pump1st control

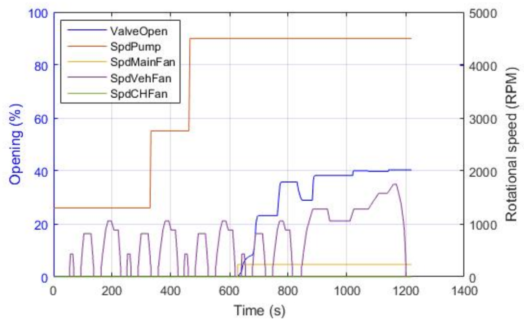

Figure 5.33 – Valve opening and fan speeds on the NEDC, Pump1st control

[*Author's illustrations*]

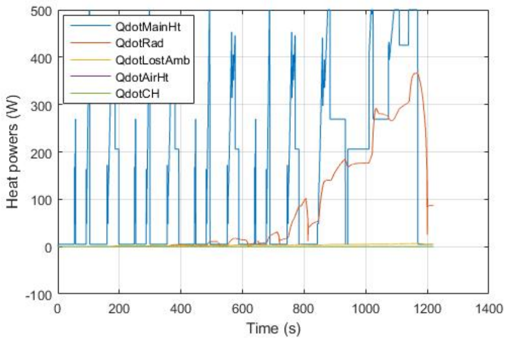

Figure 5.34 – Heat transfer evolution on the NEDC, Pump1st control

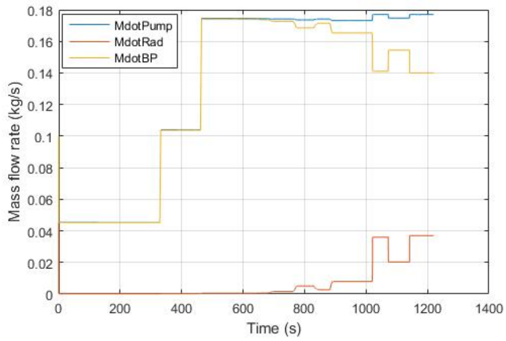

Figure 5.35 – Mass flow rate evolution on the NEDC, Pump1st control

opening (resp. closing) of the valve will slow down (resp. speed up) the evolution of the temperatures. Most of the time, opening this valve will cause a stagnation of temperature due to the mixing of cold water coming from the radiator with hot water from the bypass.

Each strategy has its own pros and cons, and the way of driving the actuators will obviously have a huge impact on the behaviour of the system and the final energy consumption.

As it was already mentioned in the literature survey and the previous studies, developing a good (and complex) strategy, with the right coordination between the bypass valve, the pump and the fan could decrease warm-up time, auxiliary consumptions, and maintain a good temperature range in the engine in operation mode.

Conclusion & perspectives

A vehicle thermal management demonstrator has been designed through this thesis. It allows a complex control in order to study and compare different strategies that could potentially decrease the energy consumption of the actuators. Therefore, it features a small scale version of each element that takes a part in the regulation of the temperature of an internal combustion engine :

A $500W$ electric heating unit (an assembly of cold plates, silicone heaters and an Aluminium plate) assumes the role of the engine, while a computer water cooling radiator serves to evacuate the resulting heat input.

PC water cooling pump and fans, plus a bypass valve, all electrically driven, are the actuators regulating the water flow and the heat dissipation of the radiator.

Moreover, the demonstrator can simulate various external inputs such as some front air speed, the heat dissipation of other low temperature radiators at the front of a vehicle or the cabin heating demand.

The overall device is controlled by an Arduino MEGA 2560 through adapted electrical connexions.

Elaborated in the context of a HiL simulation, a Simulink model reproducing the behaviour of the demonstrator has also been created. It can for example calculate the energy consumptions of the pump and the fans over a full driving cycle.

The plant and the model are both controlled with the same thermal management controller, which is also developed in Simulink. At this occasion, some basic control strategies have been implemented, and their results have been presented when applied to the model. Other future strategies are obviously to be added and compared.

At the end of the internship, a few work was still needed to add the last components and finish the build-up of the demonstrator. The test of every component, the validation of the results of the model and a potential better calibration of the parameters would be required. Finally, the integration of a mean of comparing the electrical consumption of the hardware pump and fans is still to be done.

Some improvements are also possible :

- Integration of an interface for the external inputs (CAN shields + HMI) ;
- Integration of a secondary heater to simulate an oil cooler ;
- Integration of more complex control strategies (purpose of the demonstrator).

In conclusion, this thesis is just the start of a future vehicle thermal management demonstrator, and a few steps and adjustments are still necessary to take it to the next level.

However, the main design has been realised and the first results are available and promising for a future continuation.

Appendix A

Literature survey

THERMAL MANAGEMENT CONTROL

LITERATURE SURVEY

Author(s):	Guillaume Feron, Trainee, Master's thesis
Co-Author(s):	
Approved by:	
Project Leader:	Armin Traußnig
Version:	1.3
Release date:	04.03.2016
Security level:	Confidential
Customer:	
Project:	P000000
Task ID:	7002
Department:	DAC

REVIEWED ARTICLES

- Aschemann, H., R. Prabel, C. Groß, and D. Schindele. "Flatness-Based Control for an Internal Combustion Engine Cooling System." In *2011 IEEE International Conference on Mechatronics (ICM)*, 140–45, 2011. doi:10.1109/ICMECH.2011.5971271.
- Butt, S. S., R. Prabel, and H. Aschemann. "Input-Output Linearisation with Input Constraints for an Innovative Engine Cooling System." In *Control Conference (ECC), 2014 European*, 2679–84, 2014. doi:10.1109/ECC.2014.6862392.
- Caresana, F., M. Bilancia, and C. M. Bartolini. "Numerical Method for Assessing the Potential of Smart Engine Thermal Management: Application to a Medium-Upper Segment Passenger Car." *Applied Thermal Engineering* 31, no. 16 (November 2011): 3559–68. doi:10.1016/j.applthermaleng.2011.07.017.
- Khodabakhshian, M., L. Feng, and J. Wikander. "Predictive Control of the Engine Cooling System for Fuel Efficiency Improvement." In *2014 IEEE International Conference on Automation Science and Engineering (CASE)*, 61–66, 2014. doi:10.1109/CoASE.2014.6899305.
- Khodabakhshian, Mohammad, Lei Feng, and Jan Wikander. "Fuel Saving Potential of Optimal Engine Cooling System." Society of Automotive Engineers, 2014. http://kth.diva-portal.org/smash/record.jsf?pid=diva2%3A828093&dswid=1316.
- Negandhi, V., D. Jung, and J. Shutty. "Active Thermal Management with a Dual Mode Coolant Pump." *SAE International Journal of Passenger Cars - Mechanical Systems* 6, no. 2 (2013). doi:10.4271/2013-01-0849.
- Salah, M. H., P. M. Frick, J. R. Wagner, and D. M. Dawson. "Hydraulic Actuated Automotive Cooling systems—Nonlinear Control and Test." *Control Engineering Practice* 17, no. 5 (Mai 2009): 609–21. doi:10.1016/j.conengprac.2008.10.016.
- Salah, M. H., T. H. Mitchell, J. R. Wagner, and D. M. Dawson. "A Smart Multiple-Loop Automotive Cooling System - Model, Control, and Experimental Study." *IEEE/ASME Transactions on Mechatronics* 15, no. 1 (February 2010): 117–24. doi:10.1109/TMECH.2009.2019723.
- Salah, M. H., T. H. Mitchell, J. R. Wagner, and D. M. Dawson. "Nonlinear-Control Strategy for Advanced Vehicle Thermal-Management Systems." *IEEE Transactions on Vehicular Technology* 57, no. 1 (January 2008): 127–37. doi:10.1109/TVT.2007.901892.

REVIEWED ARTICLES

- Setlur, P., J. R. Wagner, D. M. Dawson, and E. Marotta. "An Advanced Engine Thermal Management System: Nonlinear Control and Test." *IEEE/ASME Transactions on Mechatronics* 10, no. 2 (April 2005): 210–20. doi:10.1109/TMECH.2005.844707.
- Wang, Tianwei, and John Wagner. "Advanced Automotive Thermal Management – Nonlinear Radiator Fan Matrix Control." *Control Engineering Practice* 41 (August 2015): 113–23. doi:10.1016/j.conengprac.2015.04.004.
- Wang, T., A. Jagarwal, J. R. Wagner, and G. Fadel. "Optimization of an Automotive Radiator Fan Array Operation to Reduce Power Consumption." *IEEE/ASME Transactions on Mechatronics* 20, no. 5 (Oktober 2015): 2359–69. doi:10.1109/TMECH.2014.2377655.
- Zhou, Bing, XuDong Lan, XiangHua Xu, and XinGang Liang. "Numerical Model and Control Strategies for the Advanced Thermal Management System of Diesel Engine." *Applied Thermal Engineering* 82 (Mai 2015): 368–79. doi:10.1016/j.applthermaleng.2015.03.005.
- Hofer, Anton, and Filip Kitanoski. "Energy Efficient Model Predictive Control of a Cooling System." *International Journal Automation Austria*, 2011, 49–61.
- Kitanoski, F., and A. Hofer. "A Contribution to Energy Optimal Thermal Management for Vehicles." In *6th IFAC Symposium Advances in Automotive Control*, 87–92, 2010. doi:10.3182/20100712-3-DE-2013.00121.
- He, Fan, and Lin Ma. "Thermal Management of Batteries Employing Active Temperature Control and Reciprocating Cooling Flow." *International Journal of Heat and Mass Transfer* 83 (April 2015): 164–72. doi:10.1016/j.ijheatmasstransfer.2014.11.079.
- Park, Sungjin. "A Comprehensive Thermal Management System Model for Hybrid Electric Vehicles." University of Michigan, 2011. http://hdl.handle.net/2027.42/84563.
- Tao, X., K. Zhou, A. Ivanco, J.R. Wagner, H. Hofmann, and Z. Filipi. "A Hybrid Electric Vehicle Thermal Management System - Nonlinear Controller Design." *SAE Technical Papers* 2015-April, no. April (2015). doi:10.4271/2015-01-1710.

INTRODUCTION - QUESTIONS TO BE ANSWERED

AVL

- Cooling/Conditioning Application (Combustion Engine, E-motor, …)
- Cooling system Plant model
  - Number of States
  - Simplifications and assumptions (Fluid Properties, Heat transfer,)
- Controlled actuators
  - Fan, Pump, Valve,…
- Control Objective (Temperature, Energy consumption,…)
- Control laws
  - Linear, Nonlinear, Model based
- Validation/Verification
  - Measurement
  - Lab Test Rig
  - Nonlinear plant model
- Outcome, Result
  - Temperature tracking performance
  - Energy saving

ICE THERMAL MANAGEMENT

AVL

Setlur, P., J. R. Wagner, D. M. Dawson, and E. Marotta. "An Advanced Engine Thermal Management System: Nonlinear Control and Test." *IEEE/ASME Transactions on Mechatronics* 10, no. 2 (April 2005): 210–20. doi:10.1109/TMECH.2005.844707.

- Objective : Engine outlet coolant temperature tracking
- Model : Reduced order 2 node lumped parameter model
- Actuator(s) : Servo-motor driven smart thermostat valve
- Control : Lyapunov-based nonlinear control algorithm (vs PID ; linear opening)
- Experiment : Scale experimental cooling system test platform (heaters)
  Various heat loads XOR desired temperature
- Results : Low error signal + compensate disturbances

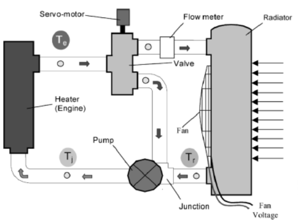

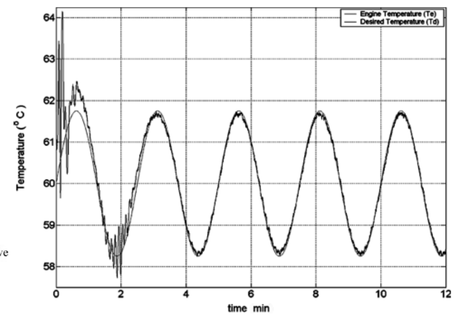

ICE TM

Salah, M. H., T. H. Mitchell, J. R. Wagner, and D. M. Dawson. “Nonlinear-Control Strategy for Advanced Vehicle Thermal-Management Systems.” *IEEE Transactions on Vehicular Technology* 57, no. 1 (January 2008): 127–37. doi:10.1109/TVT.2007.901892.

- Objective : Engine outlet coolant temperature tracking
- Model : Reduced order 2 node lumped parameter model
- Actuator(s) : Variable-speed electric water pump, variable-speed electric radiator fan
- Control : Lyapunov-based nonlinear control algorithm / backstepping robust control
- Experiment : Experimental test bench (steam heat exchanger + engine)
  Various heat loads / vehicle speed / desired temperature
- Results : Temperature tracking not as accurate (vs normal operation)
  Lower energy consumption

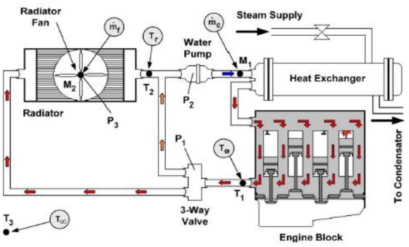

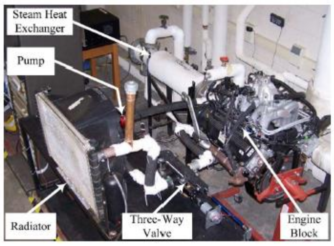

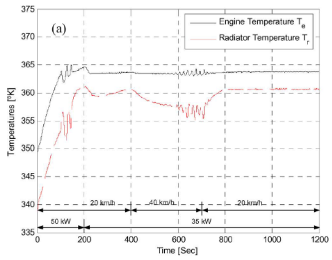

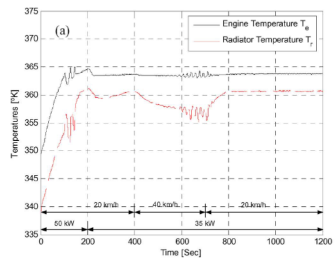

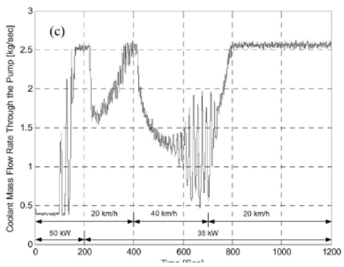

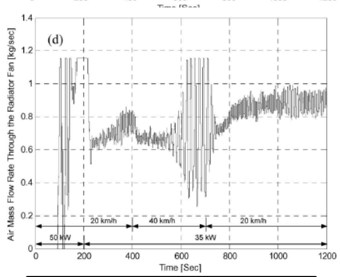

Various heat loads and speed

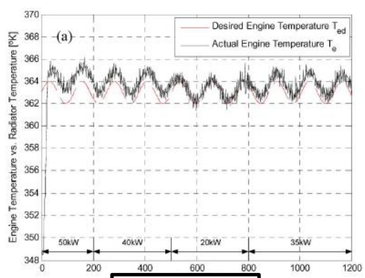

Sinusoidal T_{ed}

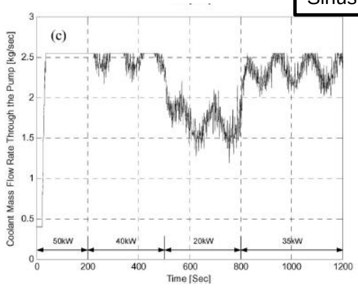

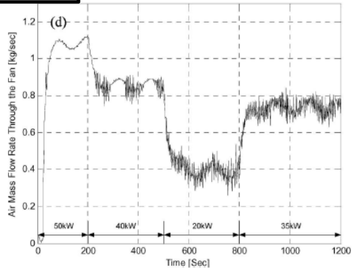

SIMULATION AND EXPERIMENTAL RESULTS SUMMARY FOR THE FOUR CONTROL STRATEGIES

Description	Error $\lvert e_{ss} \rvert$ [°K]		Power P_M [W]	
	Simulation	Experiment	Simulation	Experiment
Backstepping robust control	0.616	0.695	31.625	33.231
Normal radiator operation strategy	0.105	0.175	38.052	38.699
Adaptive control	1.003	1.075	37.497	37.968
Robust control	0.905	0.935	34.346	35.786

ICE TM

Salah, M. H., P. M. Frick, J. R. Wagner, and D. M. Dawson. "Hydraulic Actuated Automotive Cooling systems—Nonlinear Control and Test." *Control Engineering Practice* 17, no. 5 (Mai 2009): 609–21. doi:10.1016/j.conengprac.2008.10.016.

- Objective : Engine outlet coolant temperature tracking
- Model : Reduced order 2 node lumped parameter model
- Actuator(s) : Variable-speed hydraulic water pump, variable-speed hydraulic radiator fan
- Control : Lyapunov-based nonlinear control algorithm / backstepping robust control
- Experiment : Experimental test bench (heaters)
  Variable heat input / ram air disturbance / desired T°
- Results : Better temperature tracking error but consumes more energy (vs PID ; ON/OFF)

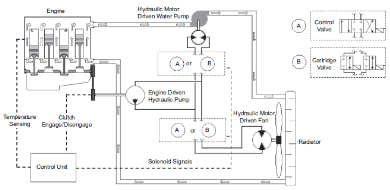

Table 3
Experimental summary for three cooling system control strategies with steady heat, no ram air disturbance, and sinusoidal temperature tracking (test two).

Case	Operation strategies description	Valve	$\|\eta_{ess}\|$ (K)	P_{sys} (W)
1	Backstepping robust controller	Servo-solenoid	0.7	165.2
2	PID controller	Servo-solenoid	1.2	160.5
3	PWM control method	Poppet	2.2	127.9

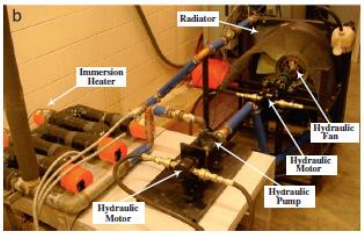

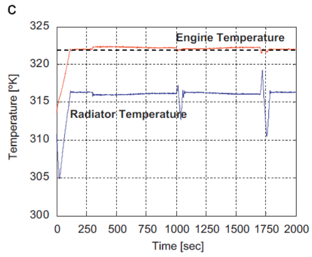

ICE TM

Salah, M. H., T. H. Mitchell, J. R. Wagner, and D. M. Dawson. "A Smart Multiple-Loop Automotive Cooling System - Model, Control, and Experimental Study." *IEEE/ASME Transactions on Mechatronics* 15, no. 1 (February 2010): 117–24. doi:10.1109/TMECH.2009.2019723.

- Objective : Engine + transmission outlet coolant temperature tracking
- Model : Reduced order 3 node lumped parameter model
- Actuator(s) : three-way smart valve, variable-speed electric water pump and fan
- Control : Lyapunov-based nonlinear control algorithm / backstepping robust control
- Experiment : Experimental test bench (steam heat exchanger + engine + transmission)
  Variable heat input / vehicle speed
- Results : Best temperature tracking error and consumes less energy (vs PID ; traditional)

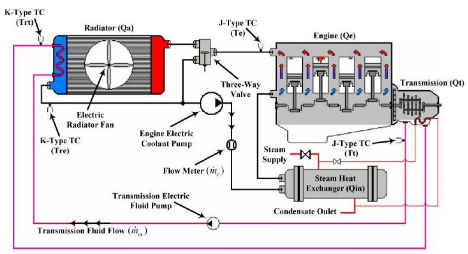

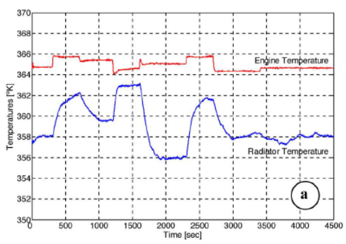

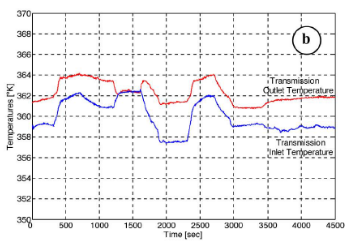

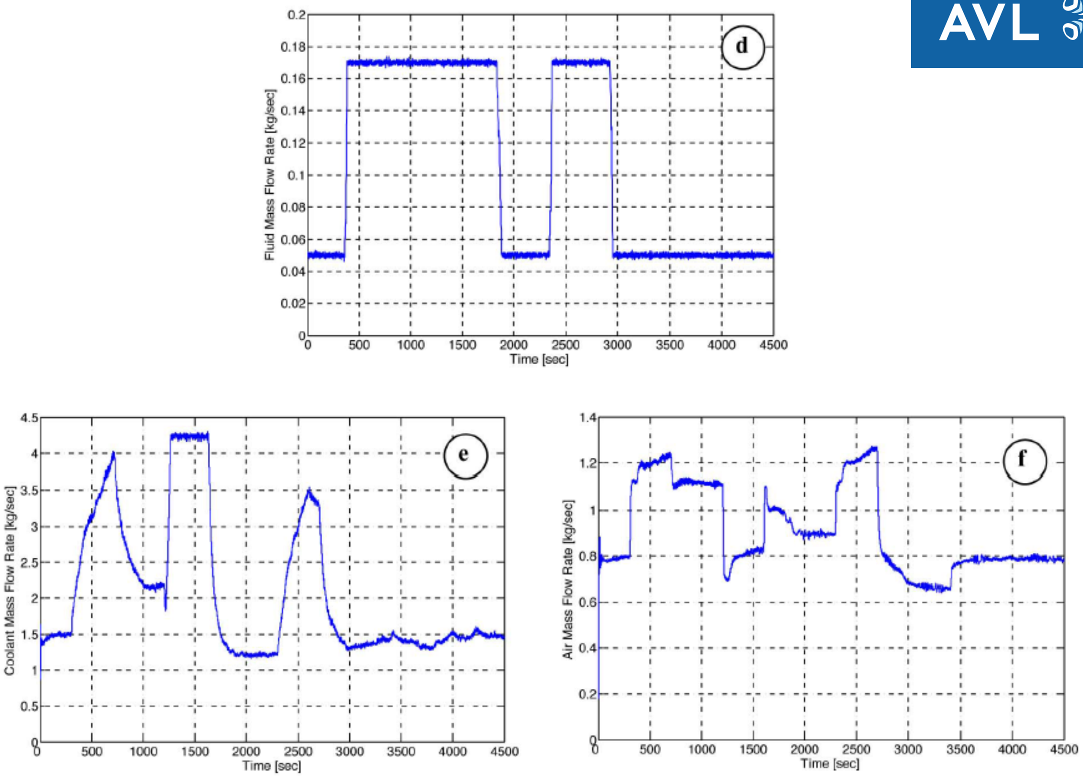

ICE TM

Caresana, F., M. Bilancia, and C. M. Bartolini. "Numerical Method for Assessing the Potential of Smart Engine Thermal Management: Application to a Medium-Upper Segment Passenger Car." *Applied Thermal Engineering* 31, no. 16 (November 2011): 3559–68. doi:10.1016/j.applthermaleng.2011.07.017.

- Objective : Definition of a perfect cooling system and evaluation on the fuel consumption
- Model : Fuel consumption and heat transfer rate maps of the engine, based on AVL's Boost program + detailed lumped parameter model for the internal cooling system
- Actuator(s) : Valve
- Control : Proportional temperature controller, with a non-linear static gain
- Experiment : Theoretical simulation on the NEDC
- Results : 14% fuel reduction consumption on the NEDC
  17% if instantaneous engine warm-up
  (respectively 12 and 28% on the EU CITY)

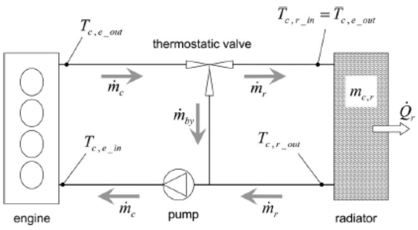

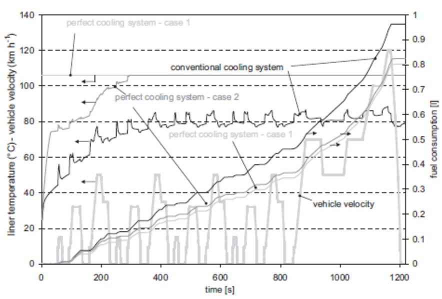

Fig. 12. Simulation results for the perfect cooling systems.

ICE TM

Aschemann, H., R. Prabel, C. Groß, and D. Schindele. "Flatness-Based Control for an Internal Combustion Engine Cooling System." In *2011 IEEE International Conference on Mechatronics (ICM)*, 140–45, 2011. doi:10.1109/ICMECH.2011.5971271.

- Objective : Engine outlet coolant temperature tracking
- Model : Control oriented mathematical model + optimization of certain parameters via a least-squares approach
- Actuator(s) : variable-speed electric pump and fan + bypass valve for the warm-up
- Control : Flatness-based control algorithm
- Experiment : Small-scale test rig build up
  Variable heat input XOR desired T°
- Results : Excellent temperature tracking and disturbance rejection.

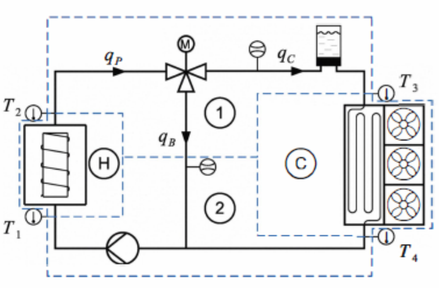

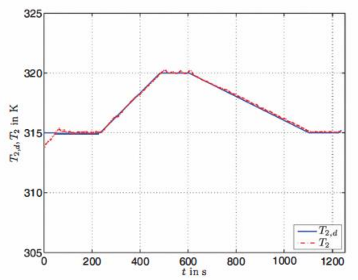

ICE TM

Negandhi, V., D. Jung, and J. Shutty. "Active Thermal Management with a Dual Mode Coolant Pump." *SAE International Journal of Passenger Cars - Mechanical Systems* 6, no. 2 (2013). doi:10.4271/2013-01-0849.

- Objective : Max Engine (90°C) or EGR (115°C) outlet temperature tracking
- Model : GT-suite 1D model
- Actuators : Dual mode coolant pump (electrical and mechanical)
- Control : PID + most efficient mode strategy (constraint : max speed limit of EM)
  + zero pump speed strategy.
- Experiment : Light duty commercial vehicle on a vehicle dynamometer - UDDS Drive Cycle
- Results : Reduction of energy required by 63.2% (fuel economy of 2.15%)

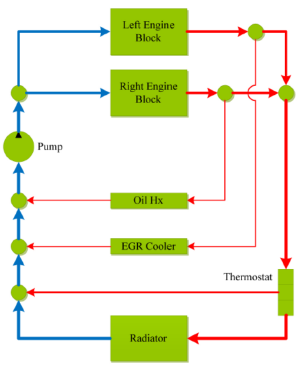

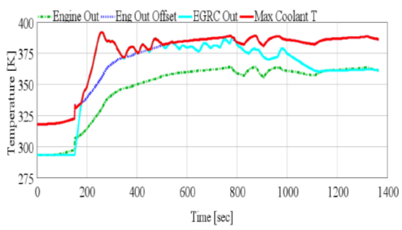

Figure 9. Maximum Coolant Temperature

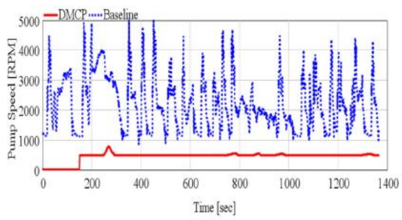

Figure 11. Comparison of Pump Speed

ICE TM

Khodabakhshian, Mohammad, Lei Feng, and Jan Wikander. "Fuel Saving Potential of Optimal Engine Cooling System." Society of Automotive Engineers, 2014. http://kth.diva-portal.org/smash/record.jsf?pid=diva2%3A828093&dswid=1316.

- Objective : Regulation of the engine temperature + minimization of the fuel consumption.
- Model : Reduced order 2 node lumped parameter model + longitudinal dynamics + engine map
- Actuator(s) : Pump + BP valve
- Control : Dynamic programming (vs state feedback controller)
- Experiment : Simulation on a simple and real driving cycle of a truck
- Results : fuel consumption improved by 1.6% (simple) and 1.2% (real)

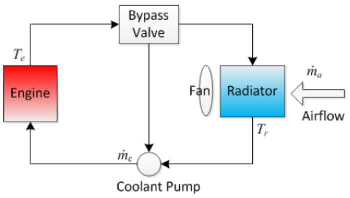

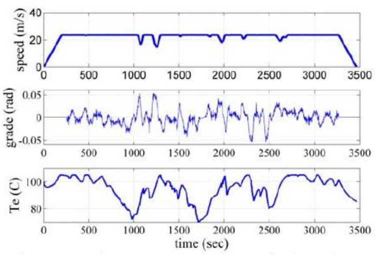

Figure 6. Engine temperature trajectory in the real driving cycle

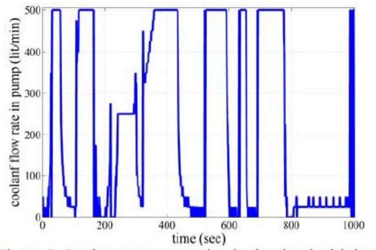

Figure 5. Coolant pump actuation in the simple driving cycle

ICE TM

Khodabakhshian, M., L. Feng, and J. Wikander. "Predictive Control of the Engine Cooling System for Fuel Efficiency Improvement." In *2014 IEEE International Conference on Automation Science and Engineering (CASE)*, 61–66, 2014. doi:10.1109/CoASE.2014.6899305.

- Objective : Regulation of the engine temperature + minimization of the fuel consumption.
- Model : Reduced order 2 node lumped parameter model + longitudinal dynamics + engine map
- Actuator(s) : Coolant mass flow rate + air mass flow rate
- Control : (30 sec) Model predictive controller (vs Dynamic programming ; state feedback)
- Experiment : Simulation on a simple and real driving cycle of a truck
- Results : fuel consumption improved by 1.6% (simple) and 1.2% (real)

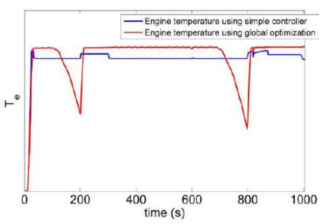

Figure 5. Engine temperature using global optimization and simple controller

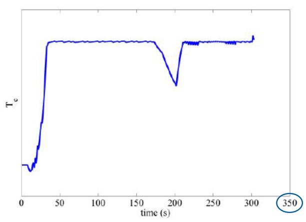

MPC

controller / Cycle	DP	*MPC (increase in fuel consumption)*	*Simple (increase in fuel consumption)*
simple	28.91	28.97 (0.2%)	29.12 (0.7%)
complex	41.92	42.1 (0.4%)	42.35 (~1%)

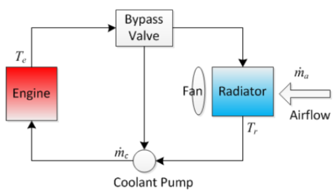

ICE TM

Butt, S. S., R. Prabel, and H. Aschemann. "Input-Output Linearisation with Input Constraints for an Innovative Engine Cooling System." In *Control Conference (ECC), 2014 European*, 2679–84, 2014. doi:10.1109/ECC.2014.6862392.

- Objective : Engine inlet + outlet temperature tracking
- Model : Control oriented mathematical model
- Actuator(s) : electrically driven coolant pump + servo-controlled bypass valve
- Control : Input-output linearization (actuators) + Discrete-time extended Kalman filter (estimation of the unknown heat flows : combustion + losses)
- Experiment : Prototype test-rig (heaters)
  Variable desired T°
- Results : Good tracking behaviour

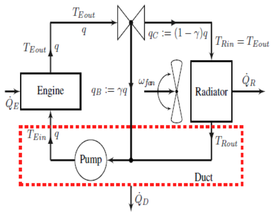

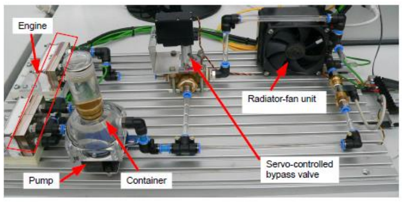

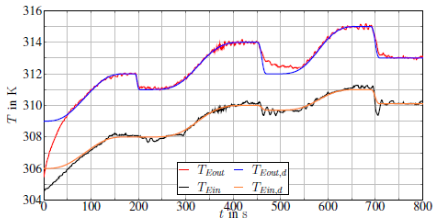

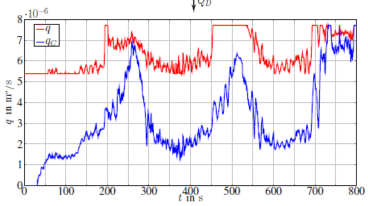

(a) Volume flow provided by the pump and through the radiator.

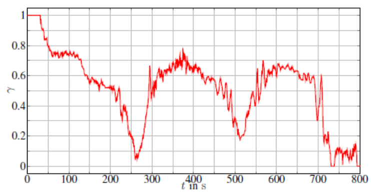

(b) Valve splitting ratio.

ICE TM

Wang, T., A. Jagarwal, J. R. Wagner, and G. Fadel. "Optimization of an Automotive Radiator Fan Array Operation to Reduce Power Consumption." *IEEE/ASME Transactions on Mechatronics* 20, no. 5 (Oktober 2015): 2359–69. doi:10.1109/TMECH.2014.2377655.

- Objective : Minimization of the fan power consumption – rule of thumb
- Model : lumped parameter system model
- Actuator(s) : Fan speed + number of operating fan
- Control : Mixed integer nonlinear programming - interior-point approach
- Experiment : Experimental test bench (steam supply + wind tunnel + 6 fan array)
  Variable heat input

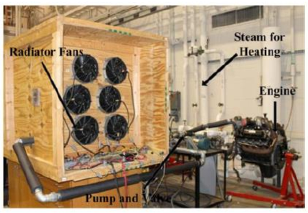

(a)

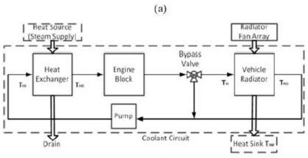

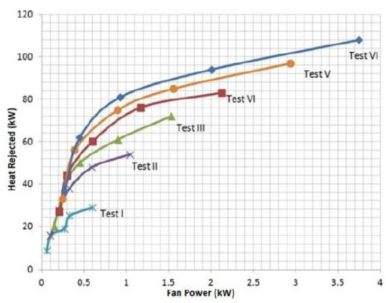

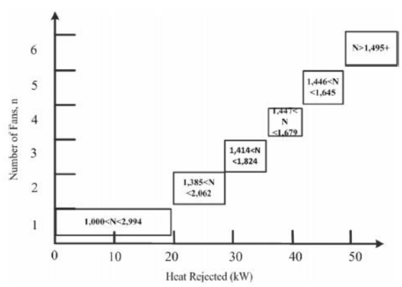

ICE TM

Wang, Tianwei, and John Wagner. "Advanced Automotive Thermal Management – Nonlinear Radiator Fan Matrix Control." *Control Engineering Practice* 41 (August 2015): 113–23. doi:10.1016/j.conengprac.2015.04.004.

- Objective : Engine outlet temperature tracking
- Model : Reduced order 2 node lumped parameter model
- Actuator(s) : Fan speed
- Control : Lyapunov-based backstepping adaptive controller (vs PI ; bang-bang)
- Experiment : Experimental bench (heat exchanger ; wind tunnel ; engine)
  Various heat loads XOR desired T°
- Results : Smaller errors ; fewer fluctuations ; faster response ; min power consumption

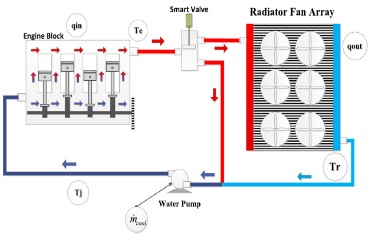

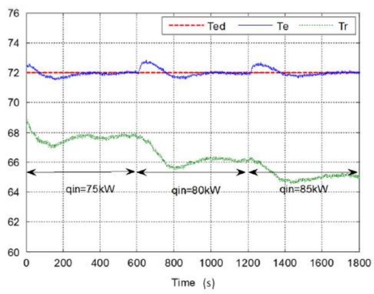

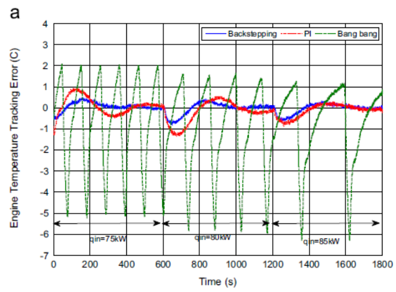

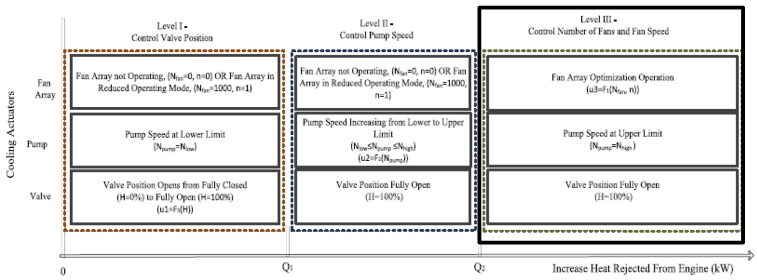

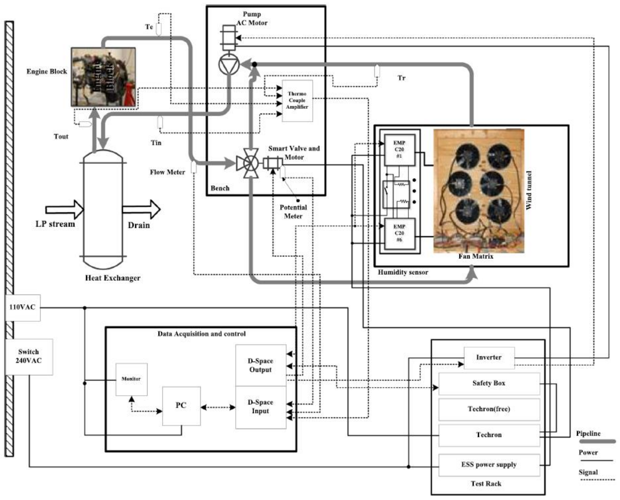

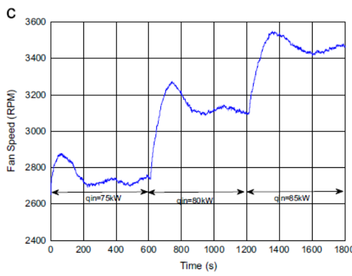

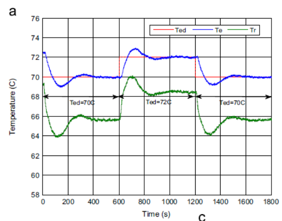

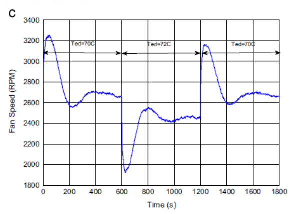

ICE TM

Zhou, Bing, XuDong Lan, XiangHua Xu, and XinGang Liang. "Numerical Model and Control Strategies for the Advanced Thermal Management System of Diesel Engine." *Applied Thermal Engineering* 82 (Mai 2015): 368–79. doi:10.1016/j.applthermaleng.2015.03.005.

- Objective : coolant and oil engine outlet T tracking + lowest fuel consumption
- Model : Reduced order multiple node lumped parameter model
- Actuator(s) : coolant / oil pump + air velocity + coolant/oil valve
- Control : - Feedforward (from engine conditions)
  - Feedback (for flow rates + air velocity)
  - Proportional (linear) T° controller + hysteresis (for the valves, warm-up)
- Experiment : Numerical simulation on the ETC
- Results : 57% power reduction on the ETC (up to 72.1% on the expressway)

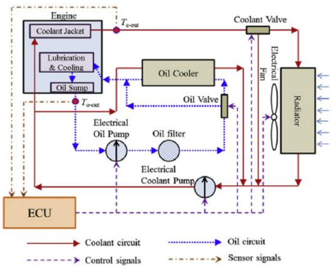

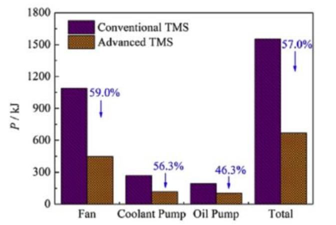

Fig. 12. Comparison of the power consumptions between the advanced TMS and the conventional one.

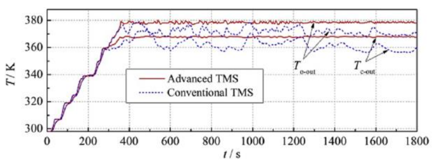

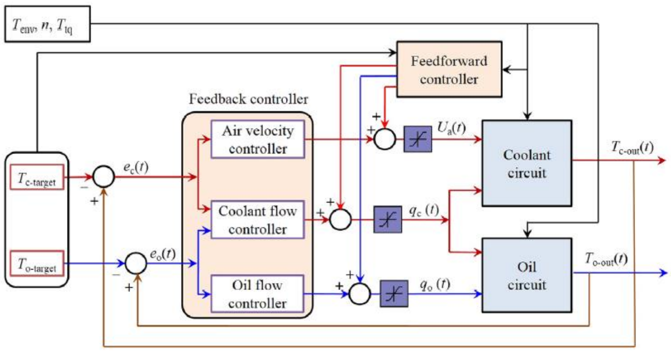

Fig. 4. Feedforward and feedback control strategy for the coolant flow rate, oil flow rate and air velocity.

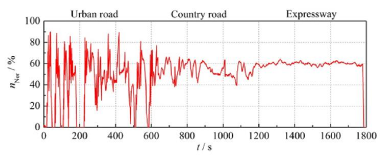

Fig. 9. Variation of the normalized speed of the engine with time during the ETC [40].

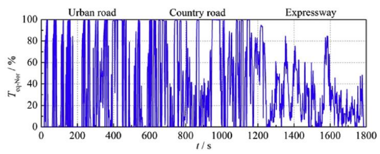

Fig. 10. Variation of the normalized torque with time during the ETC [40].

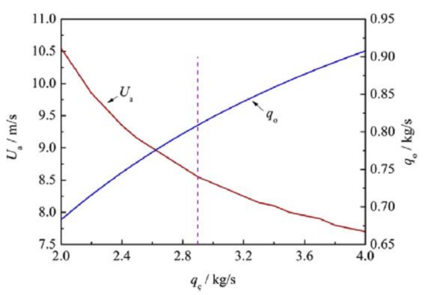

Fig. 5. Variations of the oil flow rate and the air velocity that can satisfy the engine working requirements with the coolant flow rate.

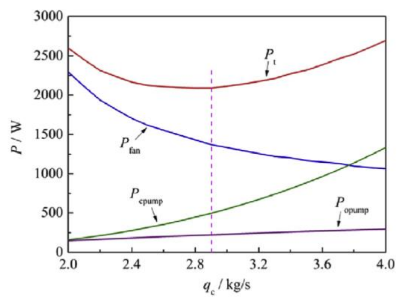

Fig. 6. Power consumptions of components in the TMS.

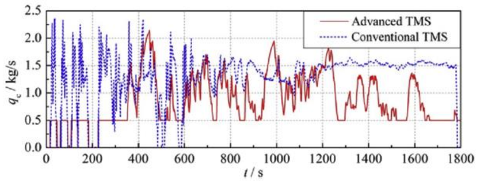

Fig. 13. Variations of the coolant flow rates of the advanced TMS and the conventional one with time during the ETC.

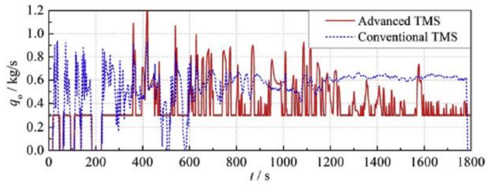

Fig. 15. Variations of the oil flow rates of the advanced TMS and the conventional one with time during the ETC.

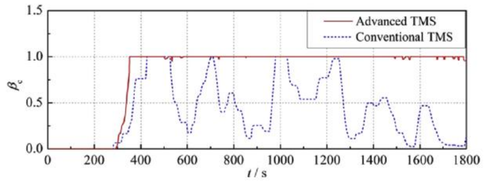

Fig. 14. Variations of the coolant flow distribution coefficients of the advanced TMS and the conventional one during the ETC.

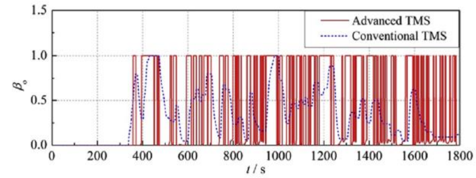

Fig. 16. Variations of the oil flow distribution coefficients of the advanced TMS and the conventional one with time during the ETC.

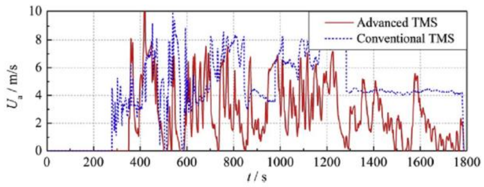

Fig. 17. Variations of the air velocities of the advanced TMS and the conventional one with time during the ETC.

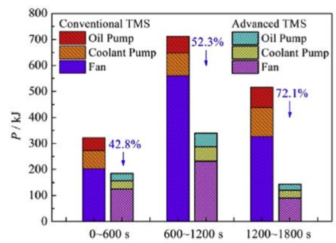

Fig. 18. Power consumptions of the advanced TMS and the conventional one under different periods of time.

EM TM

Kitanoski, F., and A. Hofer. "A Contribution to Energy Optimal Thermal Management for Vehicles." In *6th IFAC Symposium Advances in Automotive Control*, 87–92, 2010. doi:10.3182/20100712-3-DE-2013.00121.

- Objective : Min energy consumption
- Constraints : Max motor temperature (50°C) + max ΔT through radiator (10°C)
- Model : 5 node lumped thermal mass model
- Actuator(s) : Discrete (3) water pump and fan stages
- Control : Mixed integer linear program (MILP - global optimal solution)
- Experiment : Numerical simulation on the NEDC
- Results : Energy consumption : 420 kJ (always ON) -> 148.84 kJ

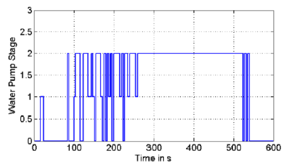

Fig. 4. Optimal water pump stage selection

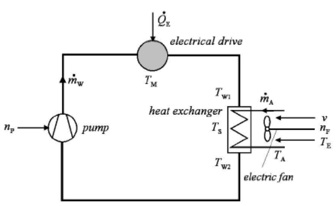

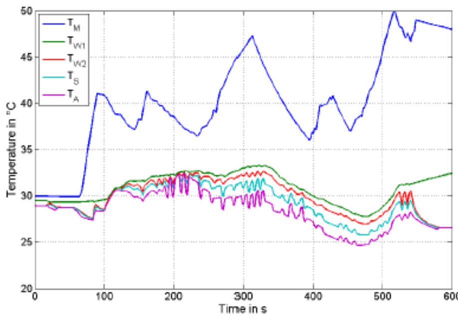

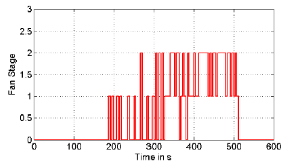

Fig. 5. Optimal fan stage selection

EM TM

AVL

Hofer, Anton, and Filip Kitanoski. "Energy Efficient Model Predictive Control of a Cooling System." *International Journal Automation Austria*, 2011, 49–61.

- Objective : Min energy consumption
- Constraints : (Dynamic) max motor temperature + max ΔT through radiator (10°C)
- Model : 5 node lumped thermal mass model
- Actuator(s) : Discrete (3) water pump and fan stages
- Control : Model predictive cooling control strategy (MILP solution required)
- Experiment : Numerical simulation on the NEDC
- Results : Energy consumption : 185.12 kJ

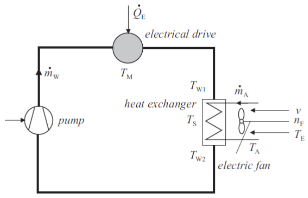

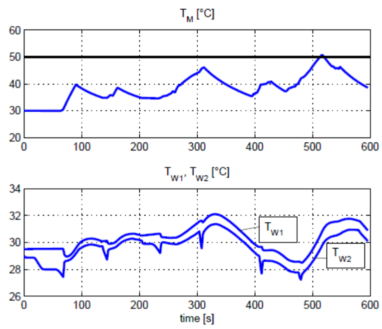

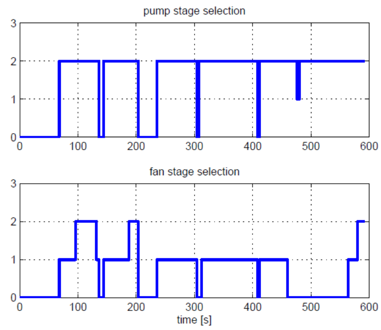

Confidential P000000-7002-12 Guillaume Feron | DAC | 4 March 2016 | 23

BATTERY TM

AVL

He, Fan, and Lin Ma. "Thermal Management of Batteries Employing Active Temperature Control and Reciprocating Cooling Flow." *International Journal of Heat and Mass Transfer* 83 (April 2015): 164–72. doi:10.1016/j.ijheatmasstransfer.2014.11.079.

- Objective : Battery core temperature tracking (of 3 cells /8)
- Model : Reduced order multiple node lumped parameter model
- Actuator(s) : Valves (flow directions) + Fan speed (air flow rate)
- Control : Luenberger observer + (hysteresis) ON/OFF fan + alternative flow direction
- Experiment : real battery module (8Px4S config) ; measurements on 1 row, cells 1-4-8
- Results : Reduction of temperature non-uniformity
  Improved temperature tracking
  Reduction of air flow consumed

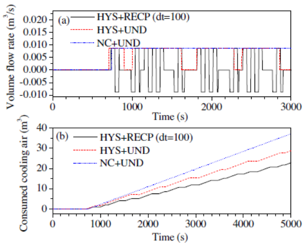

Fig. 11. Instantaneous flow rate and total cooling flow consumption for three different schemes.

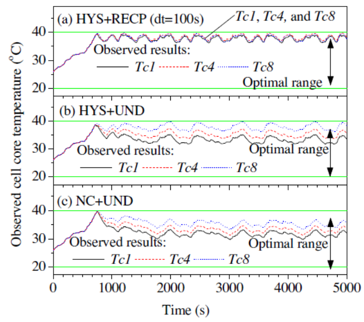

Fig. 12. Temperature variation of cell 1, 4 and 8 for three different schemes.

Confidential P000000-7002-12 Guillaume Feron | DAC | 4 March 2016 | 24

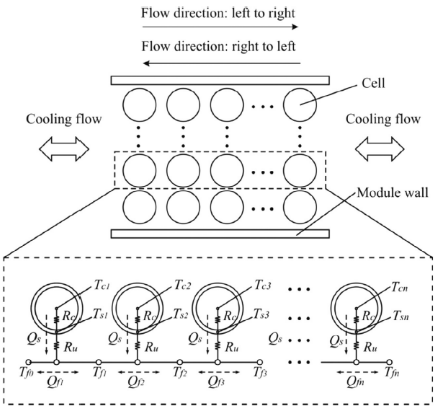

Fig. 1. Schematic of the ROM for a battery module and the notation used in its development.

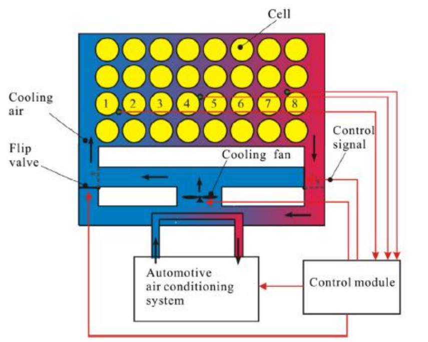

Fig. 8. Diagram of a battery thermal management system with active temperature control and reciprocating cooling flow.

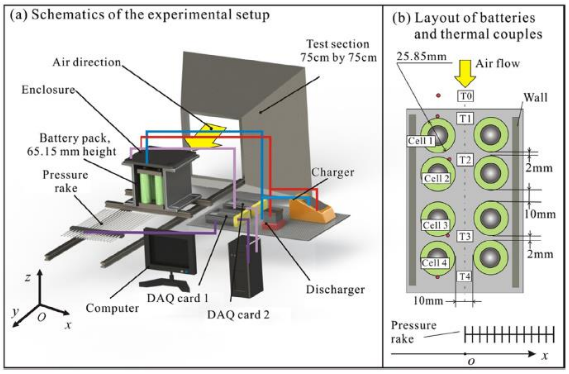

Fig. 2. Panel (a) Schematics of the experimental setup. Panel (b) Layout of cells and thermal couples in the battery pack.

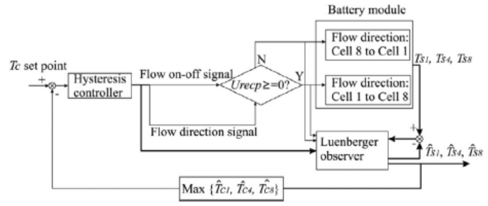

Fig. 9. Block diagram of an observer-based control system.

HYBRID TM

Park, Sungjin. "A Comprehensive Thermal Management System Model for Hybrid Electric Vehicles." University of Michigan, 2011. http://hdl.handle.net/2027.42/84563.

- Objective : Develop guidelines to improve the efficiency and performance of the VTMS for HEVs – study of 3 architectures - control target T° – energy management
- Model : Lumped thermal mass model
- Control : - Electric coolant pump (for EM) : PI controller with anti wind-up
  - Mechanical coolant and oil pump (for ICE) : linked to the engine speed
  - BP Valve (for ICE) - proportional (nonlinear) T° controller + hysteresis
  - T° cabin : A/C - ON/OFF
  - T° battery : electric oil pump speed – linked to CCS (climate control system)
  - Fan : ON/OFF
- Experiment : Simulation on 3 driving cycles (grade load, max speed, urban+cross country)

VTMS Architecture Design	Grade Load		Maximum Speed		Urban + Cross Country Driving Cycle	
	Fuel Economy (MPG)	Improve-ment of Fuel Economy	Fuel Economy (MPG)	Improve-ment of Fuel Economy	Fuel Economy (MPG)	Improve-ment of Fuel Economy
Architecture A	1.782	--	7.415	--	7.776	--
Architecture B	1.779	-0.1%	7.378	-0.5%	7.443	-4.3%
Architecture C	1.798	+0.9%	7.453	+0.5%	8.212	+6.1%

HYBRID TM

Tao, X., K. Zhou, A. Ivanco, J.R. Wagner, H. Hofmann, and Z. Filipi. "A Hybrid Electric Vehicle Thermal Management System - Nonlinear Controller Design." *SAE Technical Papers* 2015-April, no. April (2015). doi:10.4271/2015-01-1710.

- Objective : battery core, electric motor internal hotspots and engine outlet T

Cooling subject	Thermal model	Controller design	Controller outputs
Battery pack	Lumped parameter: Eqns. (1)~(3)	Linear Optimal Eqns. (15)~(21)	Compressor speed: Eqns. (20),(21)
Engine	Lumped parameter: Eqns. (4)~(7)	Nonlinear Backstepping Eqns. (22)~(34)	Coolant mass flow rate: Eqns. (26) Cooling air mass flow rate: Eqns. (32)
Electric motor	Reduced order FEA: Eqn. (8)~(14)	Linear Optimal+ Nonlinear Backstepping Eqns. (34)~(49)	Coolant mass flow rate: Eqns. (49) Cooling air mass flow rate: Eqns. (48)

- Experiment : Numerical simulation on Urban Assault and Convoy Escort Driving Cycles

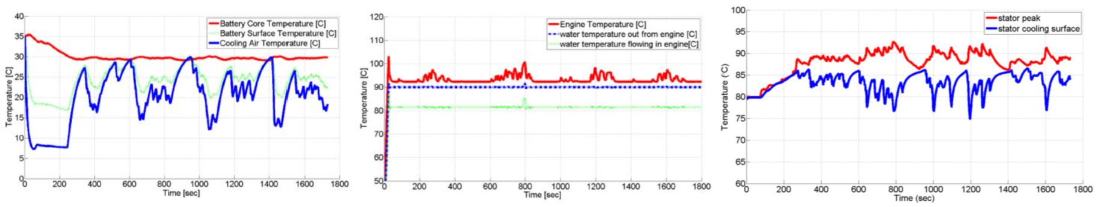

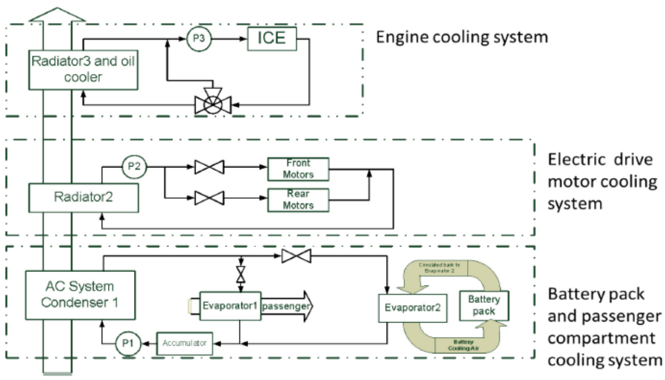

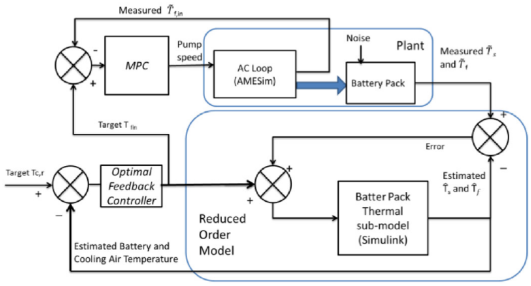

Figure 5. Controller Design for Battery Cooling System

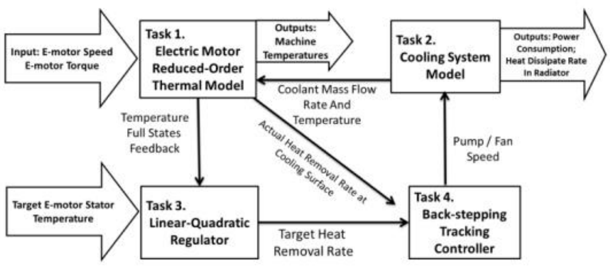

Figure 6. Controller Design for E-Motor Cooling System

Appendix B

25kHz PWM S-function

This function go over the different parts of code inside the *S-function builder* Simulink block to obtain a PWM signal of $25kHz$.

Basically, it modifies the timer 3 (which controls the pins 2, 3 and 5) of the ATmega2560 (the chip driving the Arduino MEGA 2560) and adapts the duty cycle for a correct PWM signal output of the Arduino.

Only the function for the timer 3 is displayed. The function for the timer 4, driving the pins 6, 7 and 8, is very similar.

With this code, the pins 5 and 6 (OC3A and OC4A) are not able to provide a PWM signal anymore.

PWM_25kHzT3_wrapper.cpp

```
/*
 * Include Files
 *
 */
#if defined(MATLAB_MEX_FILE)
#include "tmwtypes.h"
#include "simstruc_types.h"
#else
#include "rtwtypes.h"
#endif

/* %%%-SFUNWIZ_wrapper_includes_Changes_BEGIN --- EDIT HERE TO _END */
#ifndef MATLAB_MEX_FILE
#include <Arduino.h>
int pinA3 = 5 ;
int pinB3 = 2 ;
int pinC3 = 3 ;
#endif
/* %%%-SFUNWIZ_wrapper_includes_Changes_END --- EDIT HERE TO _BEGIN */
#define u_width 1
/*
 * Create external references here.
 *
 */
/* %%%-SFUNWIZ_wrapper_externs_Changes_BEGIN --- EDIT HERE TO _END */
/* extern double func(double a); */
/* %%%-SFUNWIZ_wrapper_externs_Changes_END --- EDIT HERE TO _BEGIN */

/*
```

```
 * Output functions
 *
 */
extern "C" void PWM_25kHzT3_Outputs_wrapper(const uint16_T *PWM_2,
                                const uint16_T *PWM_3,
                                const real_T *xD)
{
/* %%%-SFUNWIZ_wrapper_Outputs_Changes_BEGIN --- EDIT HERE TO _END */
/* wait until after initialization is done */
if (xD[0]==1) {

    /* don't do anything for mex file generation */
    # ifndef MATLAB_MEX_FILE

    OCR3B = PWM_2[0];
    OCR3C = PWM_3[0];

    # endif
}
/* %%%-SFUNWIZ_wrapper_Outputs_Changes_END --- EDIT HERE TO _BEGIN */
}

/*
  * Updates function
  *
  */
extern "C" void PWM_25kHzT3_Update_wrapper(const uint16_T *PWM_2,
                                const uint16_T *PWM_3,
                                real_T *xD)
{
  /* %%%-SFUNWIZ_wrapper_Update_Changes_BEGIN --- EDIT HERE TO _END */
if (xD[0]!=1) {

    /* don't do anything for MEX-file generation */
    # ifndef MATLAB_MEX_FILE

    //pinMode(pinA,OUTPUT); // output pin
    pinMode(pinB3,OUTPUT);
    pinMode(pinC3,OUTPUT);

    //noInterrupts();

    TCCR3A = _BV(COM3A0) | _BV(COM3B1) | _BV(COM3C1) | _BV(WGM31) | _BV(WGM30);
    TCCR3B = _BV(WGM33) | _BV(WGM32) | _BV(CS30);
    // CSn  = 0 0 1 =  no prescalering
    // WGMn = 1 1 1 1 = Fast PWM ; OCRnA = TOP
    OCR3A = 639; //count to 639 (16MHz/(640-1)=25 kHz)

    //interrupts();
    # endif

    /* initialization done */
    xD[0]=1;
}
/* %%%-SFUNWIZ_wrapper_Update_Changes_END --- EDIT HERE TO _BEGIN */
}
```

List of Figures

Bibliography

[1] Groupe Renault. Renault powertrain. www.powertrain.renault.com.

[2] P. Ngendakumana. *Moteur à combustion interne.* ULg, Liège, Belgium, 2014-2015.

[3] V. Lemort. *Thermal and electrical management of vehicles.* ULg, Liège, Belgium, 2015-2016.

[4] M. Khodabakhshian, L. Feng, and J. Wikander. Predictive control of the engine cooling system for fuel efficiency improvement. pages 61–66. IEEE conference proceedings, 2014.

[5] Royal Air Force Air Cadets. www.sandy-aircadets.org.uk/.

[6] HELLA Automotive. Thermostats, thermoswitches & temperature sender units - product / technical information. www.hella.com/hella-za/en/index.html.

[7] AGCO Automotive. www.agcoauto.com.

[8] Viva-Lancia. www.viva-lancia.com.

[9] How a car works. www.howacarworks.com.

[10] Tianwei Wang and John Wagner. Advanced automotive thermal management – Nonlinear radiator fan matrix control. *Control Engineering Practice*, 41:113–123, August 2015.

[11] Tianwei Thomas Wang, Amit Jagarwal, John R. Wagner, and Georges Fadel. Optimization of an Automotive Radiator Fan Array Operation to Reduce Power Consumption. *IEEE/ASME Transactions on Mechatronics*, 20(5):2359–2369, October 2015.

[12] Armin Traussnig, Bernd Klima, Andreas Ennemoser, and Michael Waltenberger. Konzeptbewertung und auslegung der thermischen betriebsstrategie in einem hev. In *Thermomanagement für elektromotorisch angetriebene PKW*. VDI Wissensforum, December 2013.

[13] Bing Zhou, XuDong Lan, XiangHua Xu, and XinGang Liang. Numerical model and control strategies for the advanced thermal management system of diesel engine. *Applied Thermal Engineering*, 82:368–379, May 2015.

[14] M.H. Salah, T.H. Mitchell, J.R. Wagner, and D.M. Dawson. A smart multiple-loop automotive cooling system - model, control, and experimental study. *IEEE/ASME Transactions on Mechatronics*, 15(1):117–124, February 2010.

[15] Harald Aschemann, Robert Prabel, Christian Gross, and Dominik Schindele. Flatness-based control for an internal combustion engine cooling system. pages 140–145. IEEE, April 2011.

[16] Saif Siddique Butt, Robert Prabel, and Harald Aschemann. Input-output linearisation with input constraints for an innovative engine cooling system. pages 2679–2684. IEEE, June 2014.

[17] Saif Siddique Butt, Robert Prabel, Robert Grimmecke, and Harald Aschemann. Nonlinear model-predictive control for an engine cooling system with smart valve and pump. pages 520–525. IEEE, September 2014.

[18] Wikipedia. www.wikipedia.org.

[19] O. Leonard. *Turbomachines*. ULg, Liège, Belgium, 2010.

[20] Lytron. www.lytron.com.

[21] HORN GmbH. *Flexible silicone heaters*. Gottmadingen, Germany.

[22] Yu-Juei Chang and Chi-Chuan Wang. A generalized heat transfer correlation for Iouver fin geometry. *International Journal of Heat and Mass Transfer*, 40(3):533–544, February 1997.

[23] Heat Exchanger Design Handbook. hedhme.com.

[24] H. Huisseune, C. T'Joen, P. De Jaeger, B. Ameel, J. Demuynck, and M. De Paepe. Numerical Study of Flow Deflection and Horseshoe Vortices in a Louvered Fin Round Tube Heat Exchanger. *Journal of Heat Transfer*, 134(9):091801, 2012.

[25] MUT MECCANICA TOVO. *Electrical Shunt Gate Valves. Serie VDE - Datasheet.* www.mutmeccanica.com.

[26] STEGO. *SPACE-SAVING FAN HEATER - HV 031 - technical Datasheet.* www.stego.de.

[27] Swiftech. www.swiftech.com.

[28] ifm. *SM6004 - Datasheet.* www.ifm.com.

[29] Arduino. www.arduino.cc.

[30] RS Components. www.rs-components.com.

[31] Intel. 4-Wire Pulse Width Modulation (PWM) Controlled Fans. Technical report, September 2005.

[32] bildr.org. High-power control: Arduino + n-channel mosfet. bildr.org.

[33] MUT MECCANICA TOVO. *VDE/ML SOC 24V Passo/Passo - Datasheet.* www.mutmeccanica.com.

[34] Velleman. *VMA03 - Datasheet + manual.* www.velleman.co.uk.

[35] Circuitar Eletrônicos. www.circuitar.com.

[36] *Transducer LKM 211 - Datasheet.* www.LKMelectronic.de.

[37] L. Guzzemma and A. Amstutz. *The QSS Toolbox Manual*, June 2005. https://fr.scribd.com/doc/300855613/QSS-TB-Manual.

[38] www.thermalbench.com.

[39] Tianwei Thomas Wang and John R. Wagner. A Smart Engine Cooling System-Experimental Study of Integrated Actuator Transient Behavior. Technical report, SAE Technical Paper, 2015.

[40] Power control with thyristors and triacs. In Philips Semiconductors, editor, *Power Semiconductor Applications*. 1994.

[41] https://gist.github.com/Epsilon99/2757e52e06a7d2d50221.

[42] P. Setlur, J.R. Wagner, D.M. Dawson, and E. Marotta. An Advanced Engine Thermal Management System: Nonlinear Control and Test. *IEEE/ASME Transactions on Mechatronics*, 10(2):210–220, April 2005.

[43] C. Klejn. Introduction to hardware-in-the-loop simulation. www.hil-simulation.com.